PHYSICAL AND PHOTO PROPERTIES OF 4,4′- METHYLENEBIS(PHENYLISOCYANATE) AND POLYTETRAHYDROFURAN BASED POLYURETHANES

By

Madagammana Arachchillage Sandhya Rani Senevirathna

Thesis submitted to the University of Sri Jayewardenepura for the award of the Degree of Doctor of Philosophy in Chemistry on 2016

Certification of the supervisors

We certify that the candidate has incorporated all corrections, additions and amendments recommended by the examiners to the final version of the Ph.D thesis.

Signature

Prof. Laleen Karunanayake

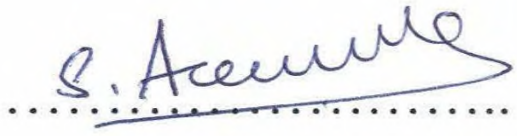

Signature

Dr. Shantha Amarasinghe

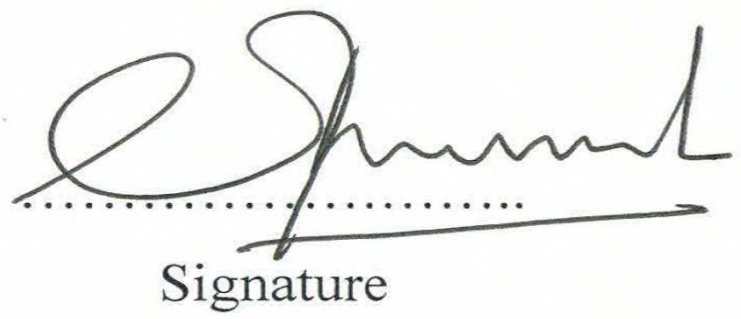

Signature

Prof. Veranja Karunaratne

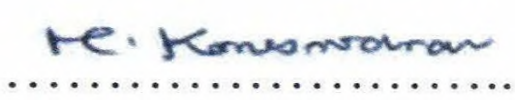

Signature

Dr. Masilamani Koneshwaran

DECLARATION

The work described in this thesis was carried out by me under the supervision of Prof. Laleen Karunanayake, Dr. Shantha Amarasinghe, Prof. Veranja Karunaratne and Dr. Masilamani Koneshwaran and a report on this has not been submitted in whole or in part to any University or any other institution for another Degree /Diploma.

.....Sandhya.....

Signature

We certify that the above statement made by the candidate is true and that this thesis is suitable for submission to the University for the purpose of evaluation.

.....

Signature

Prof. Laleen Karunanayake

.....

Signature

Dr. Shantha Amarasinghe

.....

Signature

Prof. Veranja Karunaratne

.....

Signature

Dr. Masilamani Koneshwaran

Table of Contents

List of Tables

List of Figures

ACKNOWLEDGEMENTS

This dissertation would not have been possible without the help of so many people in so many ways. I would like to extend my sincere thanks to all of them. First and foremost, I wish to convey my heartfelt thanks to my principal supervisor Prof. Laleen Karunanayake for his continuous support throughout my study period. I am wordless to convey my gratitude towards his guidance, advices, comments, suggestions and specially the kindness and the patience. The valuable time spent on me is highly appreciated. Next, I would like to convey my deep sense of gratitude to my co-supervisor Dr. Shantha Amarasinghe who guided me throughout the period spending his valuable time to fulfill my research work successfully. I wish to express my gratitude towards the two other co-supervisors; Prof. Veranja Karunaratne and Dr. Masilamani Koneswaran who gave their kind support to complete my Ph.D work successfully. All of them always encouraged me and improved my knowledge and showed me how to build up a productive research.

I acknowledge the financial support provided by the National Science Foundation of Sri Lanka (RG/2011/NANO/01). Without their financial support I would be unable to start my post graduate career.

I am thankful to Faculty of Graduate Studies in University of Sri Jayewardenepura for accepting me as a Ph.D student in their faculty.

Sri Lanka Institute of Nano Technology (SLINTEC) was the place where I carried out my Ph.D research work in the past three years. Without the help of the management and staff members of the SLINTEC I would be unable to complete my work. I wish to thank all the staff members at SLINTEC for the support given during my study.

I would like to thank the staff members of the department of material science in University of Moratuwa for facilitating sample preparations of some parts of my research work.

Further, I would like to extend my thanks to all my colleagues who helped me in various ways during my study. I must mention some of them specially Nadeesha Rathuwadu, Muditha dias, Ravithree Senanayake, Chaturi Silva, Geethika Liyanage, Asanka Yapa, Sashya Meedeniya, Malini Damayanthi, Nuwanthi Katuwavila, Veromi Kalpana and Madhubhashini Lakdhusinghe who was with me to help and encourage.

Last but not least, I wish to thank my family: my parents, brothers and sisters in law for their endless love and unconditional support during the years of my study.

PHYSICAL AND PHOTO PROPERTIES OF 4,4′- METHYLENEBIS(PHENYLISOCYANATE) AND POLYTETRAHYDROFURAN BASED POLYURETHANES

Madagammana Arachchillage Sandhya Rani Senevirathna

ABSTRACT

Polyurethane is a versatile industrial polymer which can be modified in various methods to achieve different properties depending on their particular application. In the field of polymer based research, polyurethanes have achieved a higher rank in the priority list due to their utility in diverse applications. In the work described, attention was paid to the fluorescence properties of 4,4′- methylenebis(phenylisocyanate) (MDI) based polyurethanes to open up a new path to develop different applications. As volatile organic compounds is a huge problem in the polymer industry, through the introduction of hydrophilic group to the polyurethane backbone, the highly hydrophobic polyurethanes were made hydrophilic in such a way that they can be dissolved in water based medium. Dispersion and film properties of those hydrophilic polyurethanes were optimized.

The polyurethanes which are synthesized using MDI and long chain hydrophobic PTHF are highly hydrophobic. In order to achieve the hydrophilic nature to the polyurethane chains, a monomer having a hydrophilic pendant carboxylic group; dimethylolpropionic acid (DMPA) was introduced. That additional monomer was acted as a chain extender and distributed over the polymer chain uniformly. By varying the DMPA/PTHF molar

ratio, five different polyurethane dispersions were prepared in a 30% DMF-WATER mixture. Dispersion properties of those polyurethane dispersions were analyzed. Particle size and Zeta potential data suggested that all the five dispersions which were prepared are stable. Absence of phase separations or sedimentations over long period of time proves the stability of the dispersions. With higher DMPA/PTHF molar ratios, it was able to achieve a higher stability as proven by zeta potential data in such a way that zeta potential was increased gradually from -44.9 mV to 54.9 mV with the increase of molar ratio from 1:1.5 to 1:0.38. The increased stability was attributed to the increased hydrophilicity in the higher DMPA/PTHF systems.

In addition to the films obtained from above dispersions, polyurethane prepolymer films also used to investigate the fluorescence properties of MDI based polyurethanes. Polyurethane prepolymers were prepared by reacting long chain polytetrahydrofuran (PTHF) which has 2000 molar mass and MDI.

As there were two peaks around 356 nm and 423 nm in the emission spectra of polyurethane films, it was able to identify that, there is an internal fluorophore in the MDI based polyurethanes. The detailed analysis confirmed that the peak around 356 nm was due to isolated hard segments and peak around 423 nm was due to crystalline hard segment bundles. Understanding of the microstructural arrangements of polyurethanes was necessary to explain the fluorescence behavior. XRD, DSC and FT-IR results were used to understand the microstructure of polyurethanes.

As explained by XRD, DSC and FT-IR results, polyurethane prepolymers have a crystalline soft segment matrix where hard segments are available only as isolated hard segments while films from polyurethane dispersions have crystalline hard segment bundles.

By comparing the XRD, DSC and FT-IR results of films of five dispersions, it was able to show that the hard segment crystallinity was increased with increasing DMPA/PTHF molar ratios which results in higher hard segment contents.

The extended analysis showed that in addition to the excitation of fluorophores, the localized melting was taken place in polyurethane films with the exposure to 293 nm wavelength. This melting allowed the available isolated hard segments to come close to each other to form crystalline hard segment bundles via hydrogen bonds. Subsequently, the 423 nm peak intensity was increased while reducing the 356 nm peak with the exposure time to the 293 nm peak. Even though during the UV exposure hard segments come closure, when UV exposure was ceased, some of the hard segments separate apart due to the tensile forces. As a result of this re-increase in 356 nm peak intensity and re-decrease in 423 nm peak intensity was observed after the UV cease. These tensile forces are retarded by residual solvent molecules when solvent molecules are small enough to embed in to the matrix retarding reversibility.

Correlation of microstructure, microstructural rearrangements during the UV exposure and UV cease with the observed fluorescence behavior has explained the complete picture of the fluorescence behavior.

CHAPTER 1 - INTRODUCTION

1.1 Polyurethane

1.1.1 Polyurethane structure

Polyurethane is one of the most versatile polymers in the world was first described by Bayer in 1937. (1) It is a co-polymer consisting of a soft segment domain and a hard segment domain. (2) Polyurethanes are formed via a poly-addition reaction (3) by forming urethane linkages (4). Urethane linkage is formed between a hydroxyl group and an isocyanate group. (5) Often the hydroxyl group comes from a long chain polyether polyol or polyester polyol and isocyanate group is from an aliphatic or aromatic diisocyanate. In addition to polyol and diisocyanate, a chain extender is also involved in the polyurethane synthesis. It is a simple organic molecule which has two hydroxyl or amine groups in the two terminals. Compared to diisocyanate compound and the chain extender, polyol group is very long, hence it is more flexible compared to others. Because of this higher flexibility polyol is known as the soft segment and the comparatively rigid diisocyanate compound and chain extender together is known as the hard segment. (6)

1.1.2 Polyurethane applications

Due to the versatile nature of the chemistry of polyurethanes, products developed can be found in various forms of thermoplastics, fibers, soft and hard elastomers, foams, skins, adhesives, binders, coatings and highly cross-linked plastics. (7) Polyurethanes are applied in lacquers, paints, foam mattresses, cushions, floor finishing, medical implants, sealants, in engineering components, in the maritime industry, electrical encapsulations,

wide range of rollers from soft printing rollers to hard rollers used in steel industry, in nuclear industry and in the mining industry. (5)

1.1.3 Chemical components for polyurethane synthesis

Polyurethane synthesis is carried out by reacting a polyol and a diisocyanate in the presence of a catalyst under a nitrogen environment in order to reduce the side reactions. In order to control the chain length chain extenders and chain terminators are also used during the synthesis.

1.1.3.1 Diisocyanates

Diisocyanate is one of the main two precursors of the polyurethane synthetic process. In order to form a urethane linkage, the isocyanate group is reacted with a hydroxyl group. For polymerization to continue, it is essential to have at least two isocyanate groups within the molecule. The usage of aromatic isocyanates in the polyurethane industry is more prevalent compared to aliphatics as the former is more reactive towards hydroxyl groups. (8) Toluene diisocyanate (TDI) and methylenebis(phenyl isocyanate) (MDI) are the most frequently used aromatic isocyanates. From their isomeric structures 2,4-TDI and 4,4`-MDI are commonly applied in the industry. In addition to them 1,5-naphthalene diisocyanate (NDI), *p*-phenylene diisocyanate (PPDI) are also categorized under aromatic isocyanates. Even though aromatic isocyanates are more reactive they are less stable in the presence of light. Therefore, aliphatic isocyanates are utilized during the synthesis of polyurethanes for outside uses. Among them, [5-isocyanato-1-(isocyanatomethyl)-1,3,3-trimethylcyclo-hexane] (IPDI); isophorone diisocyanate, hexamethylene diisocyanate (HDI), 4,4'-methylenebis(cyclohexyl isocyanate) (HMDI) are leading.

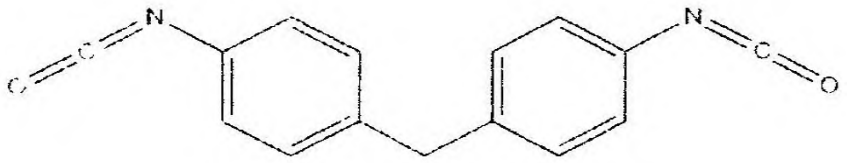

4,4' methylenebis(phenyl isocyanate)

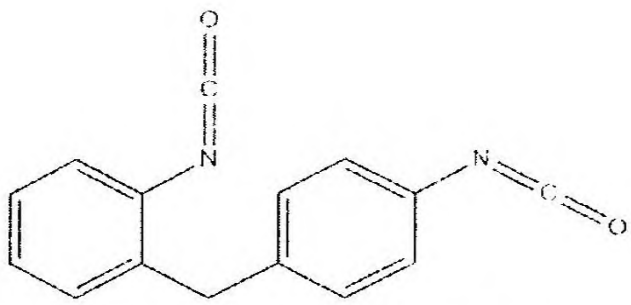

2, 4-methylenebis(phenyl isocyanate)

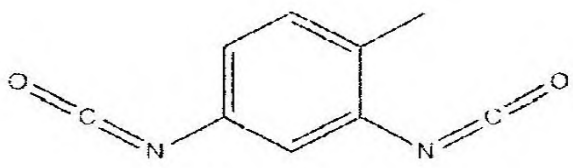

2,4-toluene diisocyanate

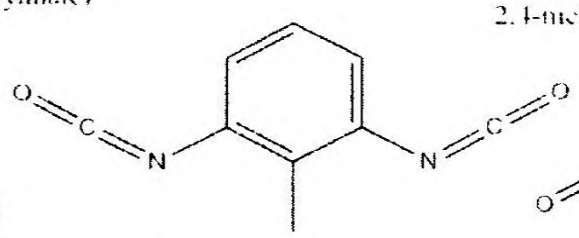

2,6-toluene diisocyanate

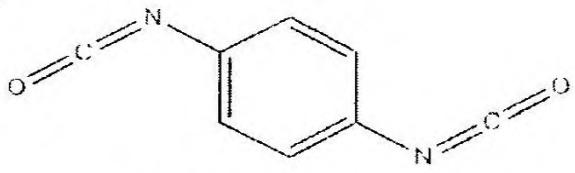

p-phenylene diisocyanate

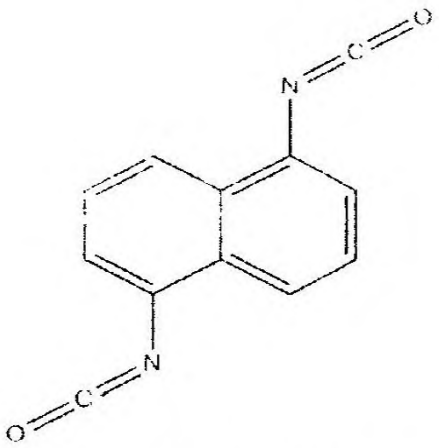

1,5-naphthalene diisocyanate

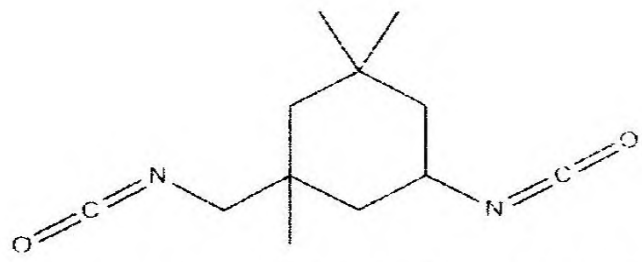

[5-isocyanato-1-(isocyanatomethyl)-1,3,3-trimethylcyclohexane]

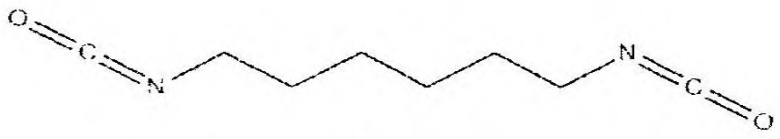

hexamethylene diisocyanate

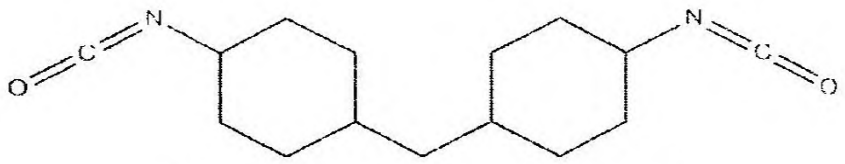

4,4' methylenebis(cyclohexyl isocyanate)

Figure 1: Commonly used diisocyanate compounds

The predominant commercial method for isocyanate production is the Hetschel method which is basically the phosgenation of amines. (8,9)

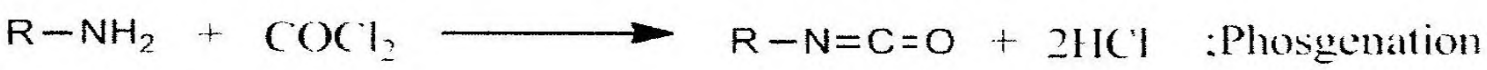

1.1.3.2 Polyols

Polyols are responsible for the flexibility and some other properties of polyurethanes. The polyurethane properties can be changed widely by varying the polyol chain length

and the chemical composition of the polyol. Polyols can be divided into two categories. Those are polyether polyols and polyester polyols.

There are two main ways to obtain polyether polyols. They are (a) ring opening polymerization of cyclic ethers and (b) anionic polymerization of alkylene oxides with di- or poly- functional alcohol initiators. The later polyols are known as polyoxyalkylene polyols. Commonly used polyether polyol, polytetramethylene ether glycol is obtained through method (a), ring opening. (8) Using the second method functionality and equivalent weight of polyol can be easily varied. For linear polyurethanes via polyether polyols, di-functional polyols or in other words polyether diols are utilized. Polyether polyols have several advantages over polyester polyols such as possibility to obtain polyols with different functionalities and equivalent weights, lower viscosity, cost effectiveness, higher hydrolytic stability. (8)

Polyester polyol based polyurethanes have lesser hydrolytic stability (9) than polyether polyols but higher oxidation resistance. (8) Polyester polyols can be subdivided into aliphatics and aromatics. Common preparation techniques for aliphatic polyesters are poly-condensation of dibasic acids with glycols and ring opening polymerization of lactones. Trans-esterification of recycled polyethylene terephthalate is the method for aromatic polyester polyols. (8)

In addition to these two types there are polyols in the form of polycarbonate polyols, hydrogenated polyols, polyolefinic polyols and hydantoin-containing polyols. (8)

1.1.3.3 Chain extenders

Chain extenders are compounds with low molecular weights and having two hydroxyl groups or two amine groups. They are used to bond the polyurethane prepolymers

together to obtain the long chain polyurethanes with desired properties. In the case of amines instead of polyurethane links polyurethane-urea links are formed. (9) Commonly used extenders are ethylene glycol, diethylene glycol, 1,4-butanediol, 1,6-hexanediol, 1,2-ethylenediamine 1,6-hexamethylene diamine (Figure 2). (9) In the waterborne polyurethane synthesis processes hydrophilicity is achieved by using ionic chain extenders. Anionic extenders have a carboxylic group while cationic chain extenders have an amine group.2,2-bis(hydroxymethyl)propionic acid (DMPA) and N,N.'-bis(2-hydroxyethyl)isonicotinamide are examples for an anionic and cationic extenders respectively (Figure 2). (9)

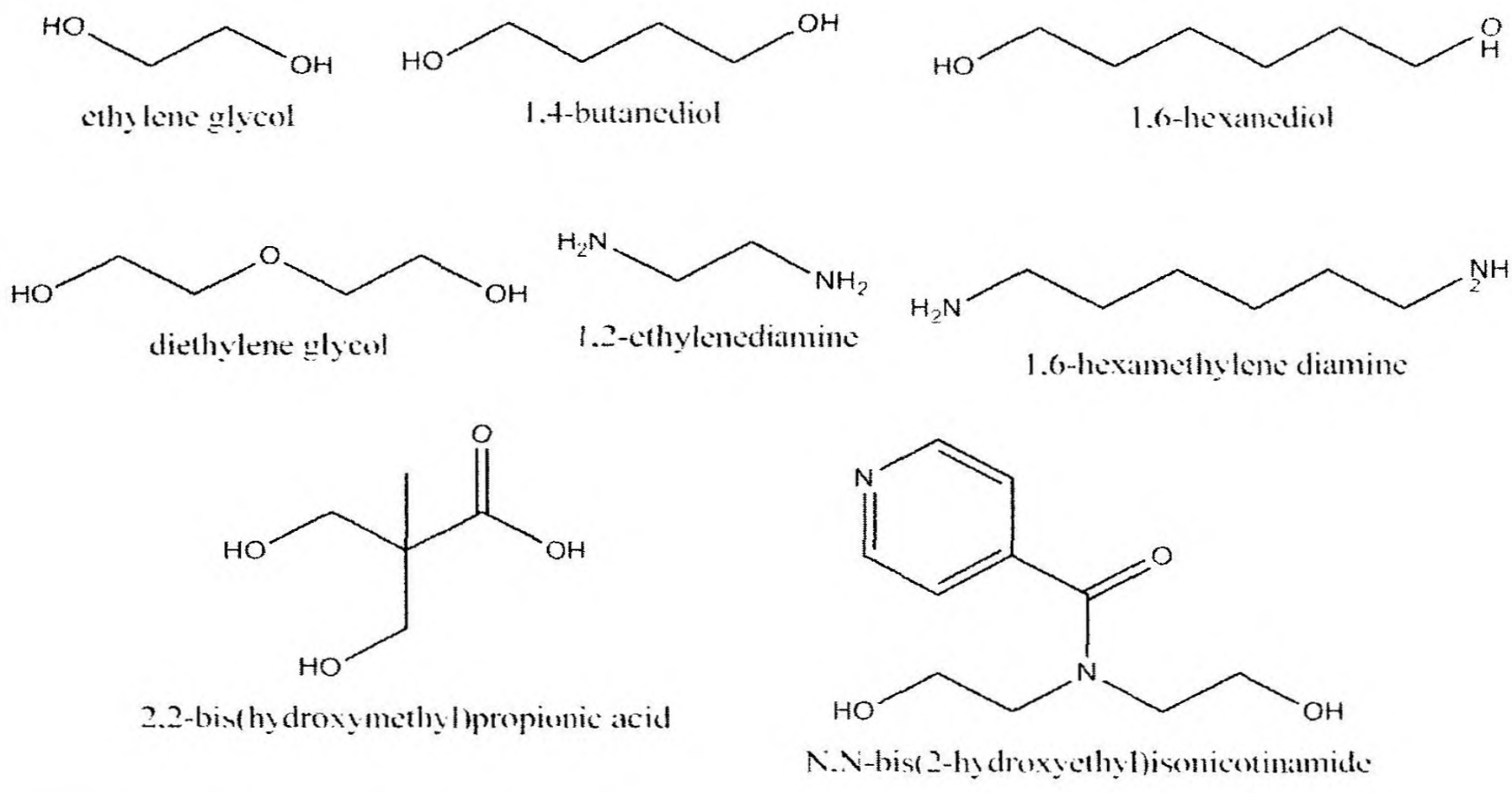

Figure 2: *Commonly applied chain extenders*

1.1.3.4 Chain terminators

Polyurethane formation is a step growth polymerization (10,11) which involves two different monomers each having the functionality of two. In order to terminate this kind of polymerization, a mono-functional compound having a functional group similar to one of the monomers has to be introduced. (11) These compounds can behave as chain

terminators. Simply mono-alcohols are used for polyurethane termination. (12) As more selective chain terminators, mono-functional organic molecules containing secondary hydroxyl groups such as 2,6,8-trimethylnonanol-4 and 2,4,8-trimethyl-2,4,8-trichloro-6-nonanol have been introduced to the industry. (12)

1.1.3.5 Catalysts

Catalysts are used during the polyurethane synthesis in order to catalyze the reaction between isocyanate and hydroxyl. Generally amines and Lewis acids such as organometallic compounds are employed as catalysts. (13) N,N-dimethylcyclohexylamine, tryethylenediamine, 1,4-diazabicyclo-[2,2,2]-octane, 2,2-bis-(dimethylaminoethylether), N-ethylmorpholine, N,N-dimethylpiperazine are some of the catalysts under the amine category while dibutyltindilaurate, dibutyltindioctanoate stannous octoate, zirconium chelates are widely utilized under organometallic catalysts (Figure 3). (14)

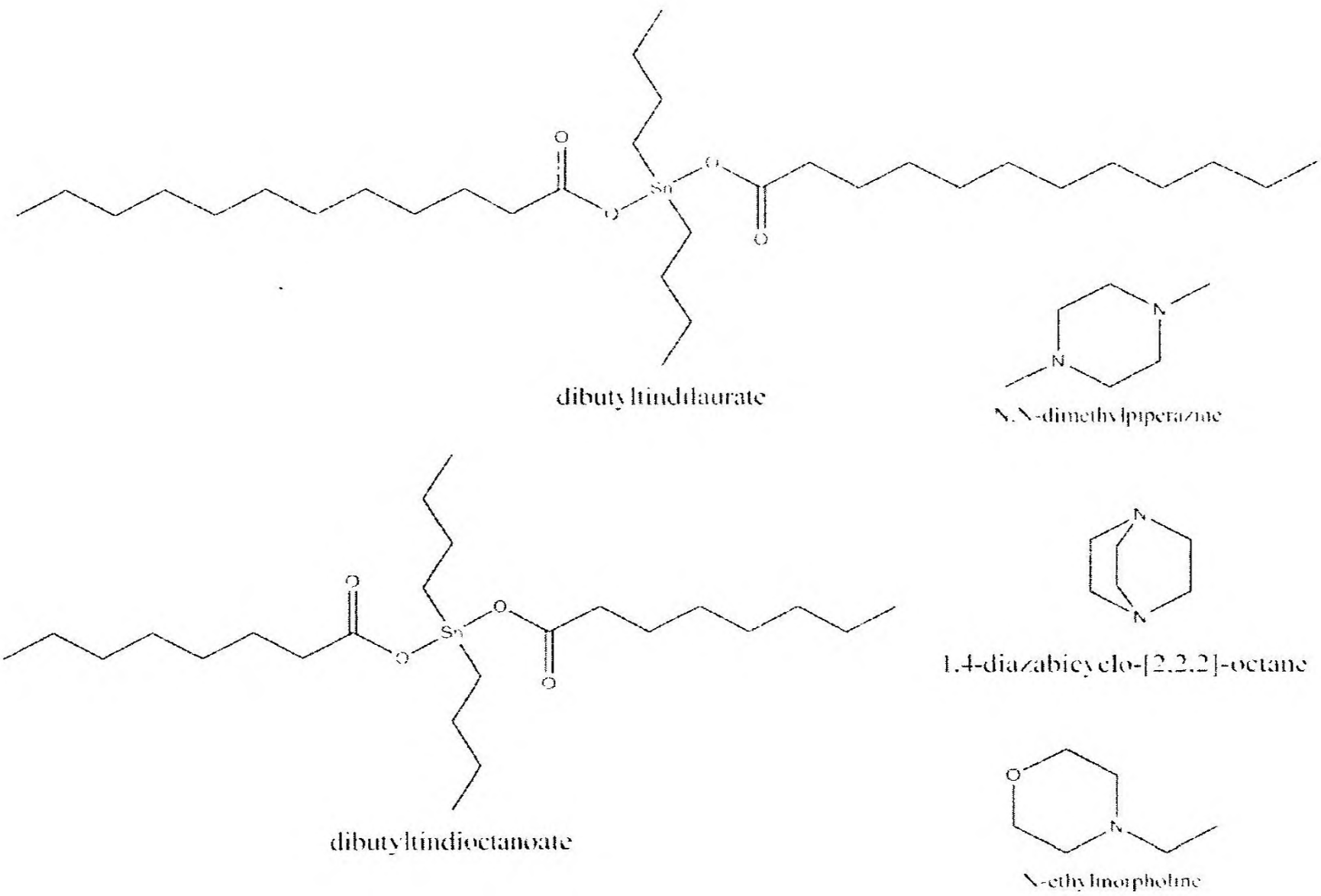

Figure 3: Catalysts used for polyurethane synthesis

Two mechanisms have been proposed for the amine catalysis of the polyurethane reaction. (14) According to one mechanism, the isocyanate forms a complex with the tertiary amine and then nucleophilic reagent forms a hydrogen bonded complex with that complex through the tertiary amine and subsequently through a second step, the nucleophile attacks to the isocyanate. (14) The other mechanism also involves two steps, in the first step protonation of the catalyst and complex formation via nucleophilic addition of alcohol adduct to the isocyanate take place and in the next step proton transfer from protonated catalyst to the complex occurs. (14)

For organo-tin catalysts also two possible paths are used to explain the catalytic activity. (14)First one proposes an activation of isocyanate via coordination of tin through oxygen or nitrogen in the isocyanate group prior to the nucleophilic attack of the

hydroxyl group. (14) The other path is the opposite of the first one where initial activation of alcohol by the tin catalyst happens followed by complex formation with isocyanate. (14)

1.1.4 Polyurethane chemistry

Polyurethane is a result of a poly-addition reaction between a polyol and a diisocyanate. (8) Addition reaction takes place between the nucleophilic hydroxyl group and the electrophilic isocyanate group in order to form the urethane linkage. The isocyanate group is highly reactive towards nucleophiles due to the high electrophilicity developed on to the C atom on isocyanate group by the cumulative double bond sequence of nitrogen, carbon, and oxygen (Figure 4). (1) High electronegativity of the SP^2 hybridized oxygen and nitrogen leads to this pronounced electrophilicity of the C atom on isocyanate group. (1) When R_1 is aromatic, it can delocalize the resulting negative charge when a nucleophile reacts with the isocyanate carbonyl. (15)

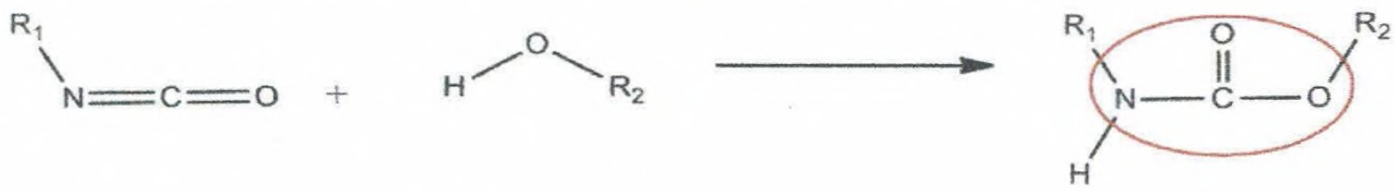

Figure 4: Urethane linkage formation

In order to obtain the linear polyurethane chains diisocyanates and polyols with a functionality of two are reacted. (9) Polyurethane chain formation via poly-addition from polytetrahydrofuran (PTHF) and 4,4'-methylenebis(phenyl isocyanate) (MDI) is shown below (Figure 5).

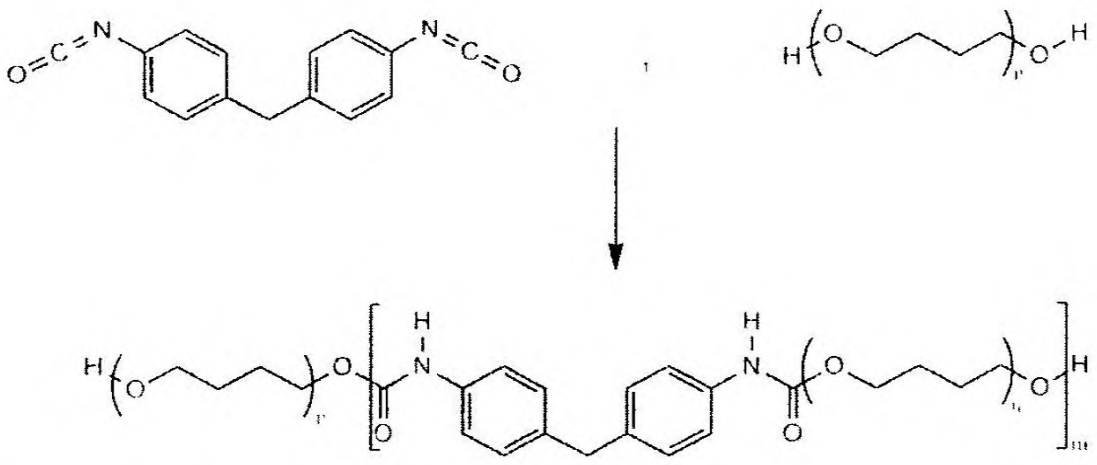

Figure 5: Polyurethane formation from MDI and PTHF

As isocyanate groups are highly reactive, there are many side reactions possible during the polyurethane synthesis. Similar to the urethane linkage formation, isocyanates can give different addition products by reacting with compounds containing any active hydrogen. (8) Hence, in the presence of water isocyanates react with water to give unstable carbamic acid which readily decomposes into an amine and carbon dioxide (Figure 6). (5) As those amines also contain active hydrogens, they can react with more isocyanate groups to give substituted urea molecules. (5) Therefore, reaction of isocyanates with water leads to a substituted urea compounds with the evolution of carbon dioxide. During the polyurethane synthesis, it is advisable to keep the reactants dry and to use a moisture free environment such as a nitrogen atmosphere.

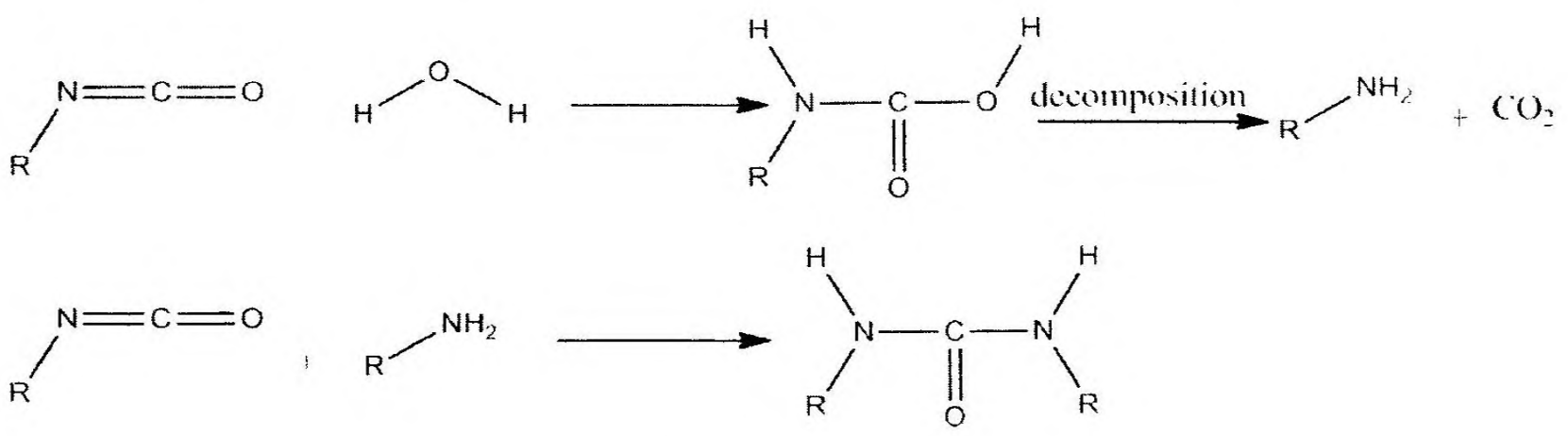

Figure 6: Reaction between isocyanate and water

Highly reactive isocyanate groups can reacts with pre-formed urethane group to give allophanate groups which can also interfere with the polyurethane formation (Figure 7). (8)

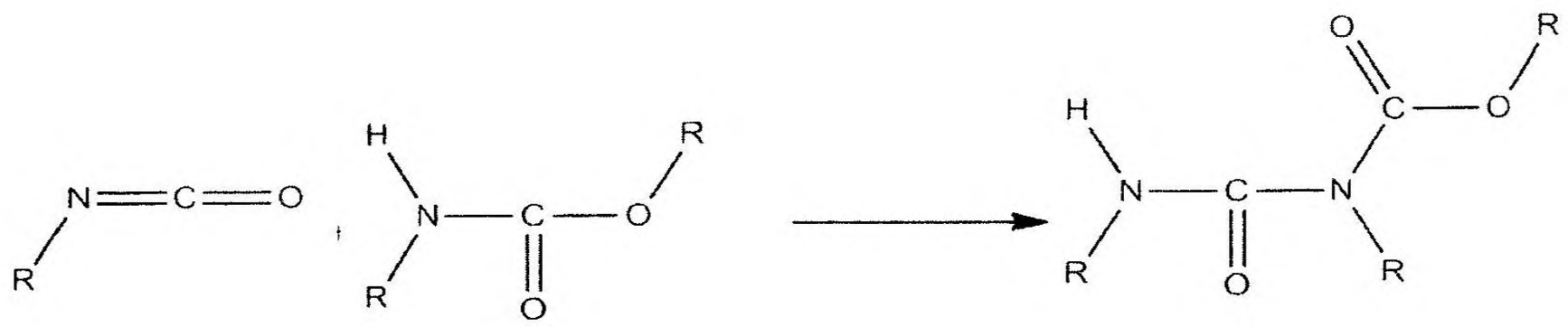

Figure 7: Allophanate group formation

Similarly pre-formed urea groups leads to biuret compounds by reacting with isocyanates (Figure 8). (8)

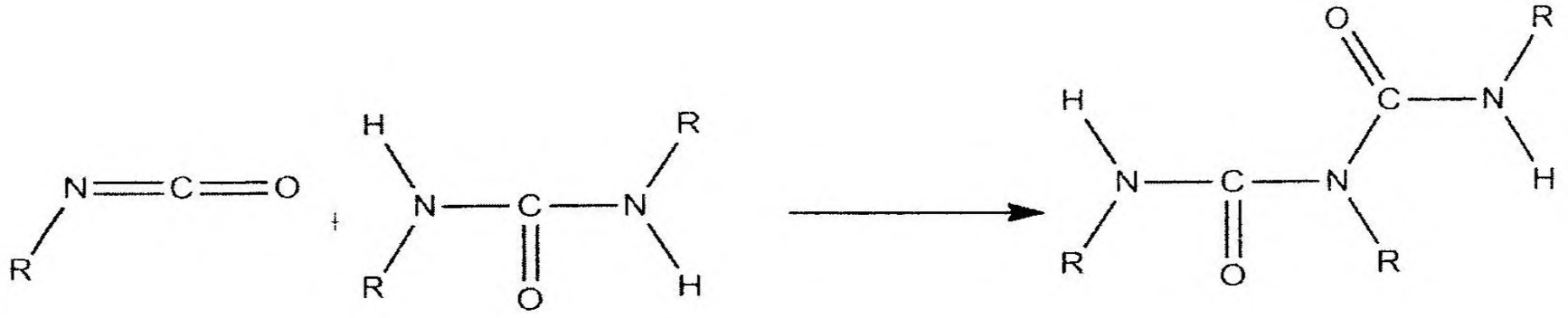

Figure 8: Biuret group formation

In addition to addition reactions there are several side reactions which are possible in the polyurethane reaction medium. Isocyanate dimerization and trimerization lead to form uretidione and isocyanurate structures respectively (Figure 9). (8,9)

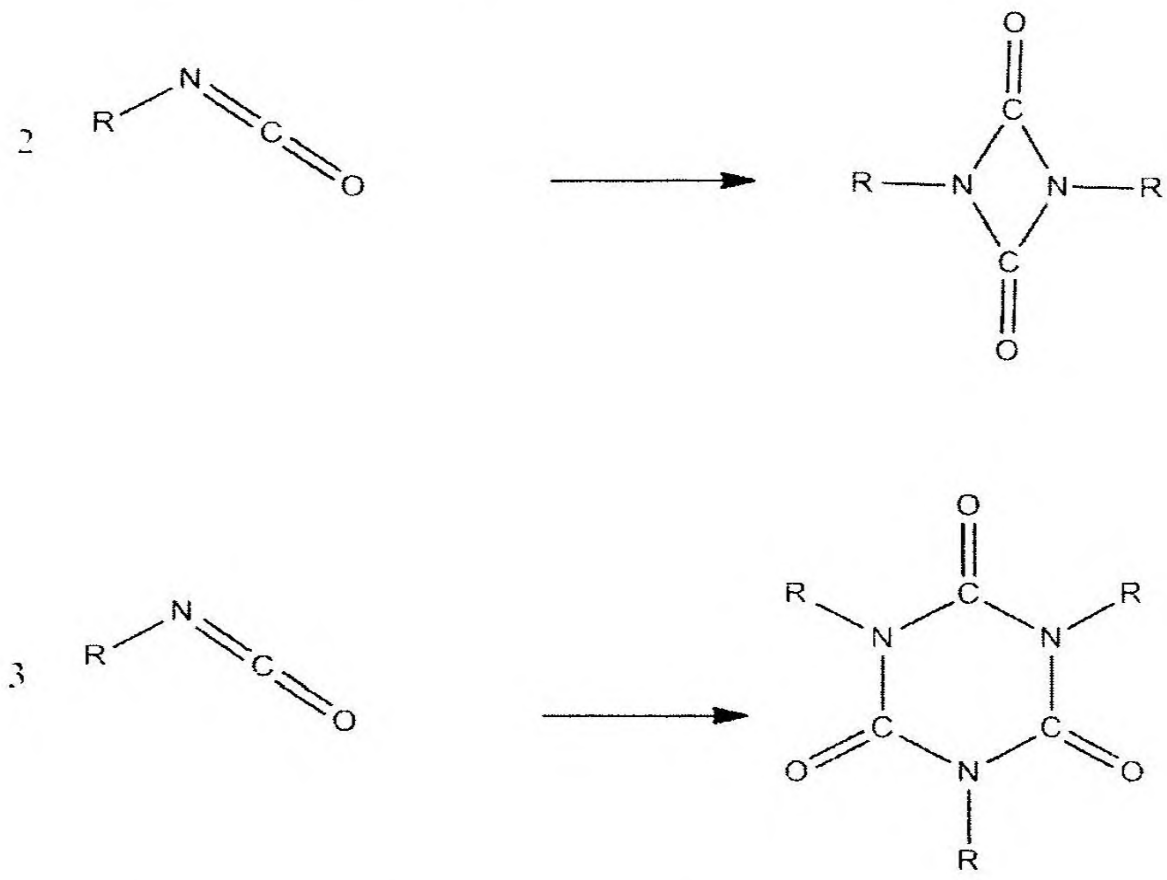

Figure 9: Uretidione and isocyanurate formation

Radical polymerization of isocyanate compounds is also possible under low temperatures and an alkaline environment (Figure 10). (8,9)

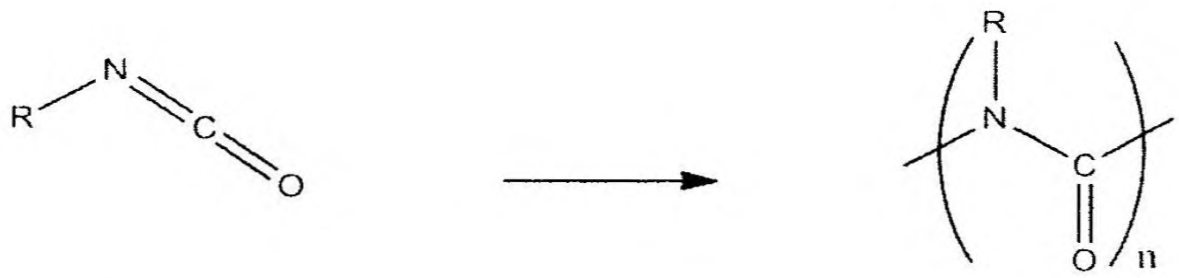

Figure 10: Poly-condensation of isocyanates

Condensation polymerization of isocyanates is also observable some times. Condensation leads to carbodiimide structures (Figure 11). (8,9)

Figure 11: Carbodiimide formation

To promote the required reaction and avoid the possible side reactions, correct monomers and catalysts have to be selected. The reaction conditions such as temperature, time, molar ratio of monomers, method of feeding, amount of catalyst, the reaction environment (eg: under nitrogen environment) also play a major role. (9)

1.2 Characterization techniques

During and after the polyurethane synthesis there are lot of characterization techniques which can be applied to study the polyurethane synthetic processes and polyurethane properties.

1.2.1 FT-IR

During the polyurethane synthesis polymerization process is monitored by the variation in the intensity of the IR peak corresponding to isocyanate group which is located around 2270 cm^{-1}. (16) It is reduced with the urethane linkage formation as isocyanate is consumed to form urethane during the polymerization.

Chemical changes to the polyurethane structure can also be monitored using the FT-IR technique. It is well known that polyurethanes undergo photo-degradation and photo-oxidation in the presence of UV light. These photo induced effects can be monitored using FT-IR spectroscopy. (17) Conversion of urethane into *ortho* aromatic amine ester via photo-Fries rearrangement, decomposition of aliphatic ester via Norrish type reaction, oxidation of aromatic structure to quinone products and formation of peroxides via photo-oxidation are such photo induced effects are taking place simultaneously in the presence of UV light which can be monitored by FT-IR. (17) The conversion of polyurethane into photo-induced products has been explained by recording the FT-IR spectra before and after the UV irradiation and interpreting the changes in the spectra. (17)

Hydrogen bonding plays a major role in determining the overall properties of polyurethane. It is important to monitor the hydrogen bonding in the polyurethane. It can be carried out using FT-IR. There appears frequency shifts in peaks corresponding to N-H and C=O stretching to a lower frequency due to the formation of hydrogen bonding. (18,19) Free N-H stretching at around 3445–3450 cm^{-1} shift down towards the 3260-3290 cm^{-1} range for H bonded N-H while free urethane C=O stretching at around 1730-1740 cm^{-1} shifts down towards the 1703-1710 cm^{-1} range for H bonded C=O stretching. (18,20) This provides a strong evidence for the H bond formation in polyurethanes.

Since UV curing is increasingly used in the formation of polyurethanes, it is essential to monitor the UV curing process. To obtain UV curability to polyurethanes, "ene" groups are incorporated at the chain ends. (21,22) During UV curing, they are cross-linked to give improved physical and chemical properties. (21) Such changes can be monitored

using FT-IR via the changes in peaks for "ene" groups at around 1638 cm^{-1} (C=C), 1410 cm^{-1} (=CH_2) and 810 cm^{-1} (=CH). (21,22)

1.2.2 DSC

The differential scanning calorimetry (DSC) is a good analytical technique that can be used to monitor the thermal transitions and reactions which can occur in a material. (23) It is widely used in industries related to semiconductors, batteries, food, explosives, metallurgy, cosmetics, textile, petroleum, coal and polymers. (23)

In the polyurethane industry, the DSC technique has been applied for several aspects. It is commonly applied to determine the thermal properties of polyurethanes. (24,25,26,27,28) Murakami and coworkers have used DSC to monitor the influence of the molecule rotaxane on thermal properties of polyurethane and revealed that it exerts no influence on glass transition temperature of polyurethane in another instance, it was revealed a retardation effect of the re-crystallization of polycaprolactone (PCL) in polyurethane. (24) The effect of aromatic polyamide sulfone (APAS) on the glass transition temperature has been discussed by Mohamed and his team and increase in glass transition temperature with APAS is related to the increase in polymer rigidity. (25) Jueyu Pan et al have obtained the thermogram of polyethyleneglycol (PEG) based polyurethane and the melting peak observed around 30-50 ^{0}C which has been assigned to melting of PEG moiety and percentage crystallinity has been calculated using melting enthalpy obtained from the thermogram. (26) In addition to thermal properties, to monitor the reaction between isocyanate and hydroxyl group DSC has been applied. (29) Here, they have used data obtained from DSC to fit with a kinetic model for the bulk reaction of isophorone diisocyanate and castor oil. (29)

1.2.3 UV-VIS Spectrophotometry

In polyurethane industry UV-visible spectroscopy has been applied in the determination of the naphthalene content in polyurethanes using a calibration curve. (30) To monitor the structural changes in polyurethanes modified with stilbene chromophores upon the UV irradiation, variation in UV visible spectra of polyurethanes with irradiation time has been recorded. (31)

1.2.4 Fluorescence

Fluorescence technology has been applied in the field of polyurethane to achieve different aspects. Fluorescence has been used to monitor the photo induced changes in polyurethanes such as photo-isomerization (32,31), photo-oxidation (33,34) and photo-degradation (35,36,37). Further, fluorescence properties have been used to develop polyurethanes as different kinds of sensors such as humidity sensors (38), vapor-based chemical sensors (39) , anion sensors (40) and metal ion sensors (41).

1.2.5 Particle size analysis

It is important to control the particle size of aqueous polyurethanes depending on their applications. Large particles are required in surface coatings requiring rapid drying while small particles are required to achieve a deep penetration of the dispersion in to a substrate. (42) Particle sizes of grafted polyurethanes which were synthesized using Poly(ethylene glycol monomethyl ether) (PEGMME) as the grafting agent has been studied by Mohaghegh *et al* and they were able to correlate the particle size of polyurethanes and the molecular weights of PEGMME. (42) They have observed that particle size decreases with the increase of the molecular weight of PEGMME. This is because of the increase of hydrophilicity of PEGMME and also the increase in chain flexibility with the increase in molecular weight. (42) This technique has been used to

evaluate the effect of the amount of ionic groups on the polyurethane properties. (43) Liminana and coworkers have observed that particle size of polyurethane particles obtained from number distribution method had increased with the decrease in the amount of dimethylolpropionic acid due to two reasons namely, the decrease in hydrophilicity of the polyurethane ionomer and decrease in electrolytic stability of the dispersion. (43) There is literature precedent explaining that there is an effect from the type of the ionic group on the polyurethane particle size. (44) Thus, sulphonated polyurethanes have small particle sizes compared to carboxylated polyurethanes due to the dispersion formation efficiency of sulphonate ions. (44) The hard segment content also had an effect on the particle size of polyurethanes in such a way that increase in the solid content leads to a decrease in particle size. (45) This is probably because the increase of solid content leads to decrease in particle mobility subsequently to a reduction in probability of particle-particle interactions. (45) Thus, large numbers of small particles are formed when solid content is high. (45)

1.2.6 Zeta potential

Zeta potential has also been applied in polyurethane study especially waterborne polyurethanes to check the dispersion stability. (46,47,48) The effect of surfactant on polyurethane dispersions have been established and accordingly ionic surfactants lead to a higher stability compared to non-ionic surfactants and stability of dispersions increase as surfactant concentration increases. (46) The effect of the position of ionic groups in the polyurethane chain, the weight percentage of ionic group, and chain flexibility of polyurethane chain on the polyurethane dispersion stability has been measured using the zeta potential values. (47) The position of ionic groups has an effect in such a way that when an ionic group is at the chain end, it gives the highest stability while when the

ionic group is at the hard segment, it gives the least stability and stability of the ionomers when ionic groups in the soft segment is in between. (47) As ionic content increases dispersion stability increases due to increase hydrophilicity and increase in chain flexibility leads to a higher stability. (47) To monitor the influence of different ingredients on water based polyurethanes zeta potential measurements has been applied as a strong tool. (48) The influence of lot of factors such as the type of the surfactant, percentage content of acrylic polymerization initiator azobisisobutyronitrile (AIBN), molecular weight of polypropylene oxide, the weight percentage of the ionomer DMPA, the weight percentage of acrylic monomer cross-linker, and polyurethane to acrylate mass ratio on the dispersion stability has been discussed using the zeta potential data. (48)

1.3 Focus of this study

Even though vast variety of studies has been carried out on polyurethanes still there are unexplored areas. Among those sub areas our attention was directed towards the fluorescence behavior of waterborne MDI based polyurethanes. There were two major objectives to achieve at the end of the project.

* Design a new MDI based waterborne polyurethanes system with high stability.
* Develop an optical technique to monitor the microstructural changes of MDI based polyurethane matrixes.

CHAPTER 2 - LITERATURE REVIEW

2.1 Polyurethane fluorescence

In addition to common techniques such as DSC, TGA, GPC, FT-IR (7,26,27,28) which are applied in the field of polyurethane, fluorescence is an additional technique which can be used as a method to monitor the photo induced changes in polyurethanes such as photo-isomerization (32,31), photo-oxidation (33,34) and photo-degradation (35,36,37). In addition, fluorescence techniques can be used as a way to develop new applications of polyurethanes such as humidity sensors (38), vapor-based chemical sensors (39) , anion sensors (40) and metal ion sensors (41). Using the difference in fluorescence behavior of *cis* and *trans* isomers of stilbene chromophores, the photo-isomerization of polyurethanes with stilbene pendants was studied by E.C Buruiana and his team. (32,31) *Trans* stilbene gives fluorescence while conversion to cis isomer leads to a loss of fluorescence. This *cis-trans* isomerization of the pendant stibene can be used to control the chain conformation of the polymer backbone. (31) Photo-oxidation of polyurethanes leads to form peroxides which are liable to easy decomposition to alkoxy and hydroxyl radicals. (33,34) Quenching of the excited states of fluorophores by those photo-oxidation products creates a path to monitor the photo-oxidation of polyurethanes via fluorescence. (33,34) The main advantage of fluorescence as a technique to detect the photo-oxidation is its ability to detect the initial stages of the oxidation. (33) The main disadvantage of aromatic diisocyanate based polyurethane is the discoloration with the exposure to UV light. (35) This discoloration is a consequence of photo-degradation. (35) Two different ways of aromatic diisocyanate based polyurethane photo degradation have been explained in the literature. (35,36,37) One path leads quinone-imide products which are colored while the other leads to aryl amine cleavage type products and photo-

Fries rearrangement type products (*ortho-* and *para-* photo-Fries products). (35,36) Photo-Fries products yield colored azo compounds up on further photolysis. (36) Hence, both the degradation schemes lead to discoloration. The differences shown in fluorescence spectra before and after photo-degradation, such as emission maxima and intensity variations, are useful to explain the photo-degradation of polyurethanes. (35,36,37)

In order to apply fluorescence in the field of polyurethanes, it is necessary to incorporate a fluorophore to the polymer system, which may be extrinsic or intrinsic. When extrinsic, a fluorescent probe is externally introduced to the surrounding environment of the polymer. Peinado and co-workers have used two extrinsic fluorescent probes *p*-dimethylamino salicylic acid and 2',7'-difluorfluorescein to monitor the photo-oxidation of polyurethanes. (33) To develop a humidity sensor, Bosch and co-workers have used several extrinsic fluorophores. (38) They have obtained a homogeneous mixture of polyurethane adhesive and fluorescent probe and then casted on to glass slides to obtain polyurethane films which can be used as humidity sensors. (38) Hydrophilic polyurethanes have been used as a matrix to embed 2,3-di(pyrrole-2yl)quinoxaline(DPQ) based fluorescence sensors which are developed as anion sensors to increase their water compatibility. (40) Increase in water compatibility is very important as water is the natural solvent for most anions. (40) When intrinsic, the fluorophore is attached to the polymer chain. It may be in the polymer backbone or it may be attached to polymer backbone as a pendant. If the isocyanate group consists of a highly conjugated aromatic system which can produce fluorescence, it can be used as the intrinsic fluorophore, which is in the backbone, to study the fluorescence properties of the polyurethane. For example, fluorescence

properties of naphthalene diisocyanate based polyurethanes have been studied widely. (30,49) Some fluorescence properties of naphthalene diisocyanate based polyurethanes have been attributed to excimer formation. (49) It has been reported that naphthalene diisocyanate based polyurethane forms solvent dependent intra-molecular excimers between carbamate groups on the same polymer at low concentrations and that the critical concentration required for intermolecular excimer formation is dependent on the compatibility of the solvent to the polymer. (49) It has also been suggested that the excimer formation in polyurethane is enhanced by the hydrogen bonds which are formed between a hydrogen atom connected to the central nitrogen atom of a urethane linkage and the carbonyl of another urethane group. (49) Similarly, in MDI based polyurethanes, MDI has been used as the intrinsic fluorophore in the backbone, to study the photo-degradation behavior of MDI based polyurethanes. (35,36,37) Another possibility for the incorporation of a fluorophore to the backbone is the use of a new monomer having a fluorophore to combine the two conventional prepolymers. Such efforts were used in the synthesis a polyurethane containing the fluorescent brightening agent, disodium 4,4'-bis[(4-anilino-6hydroxyethylamino-1,3,5-triazin-2-yl)amino] stilbene-2,2-disulphonate (VBL). (50,51) It was proved that VBL-based polyurethane shows a very stable fluorescence. In another effort to incorporate a fluorophore to the polymer backbone, an aqueous polyurethane emulsion containing the fluorescent moiety 1,4-diamino-2,3-diphenoxyanthraquinone (DDAQ) has been developed by incorporating DDAQ into the polyurethane chain made using 2,4-tolylenediisocyanate (TDI), poly(propyleneglycol) and 2,2-dimethylolpropionic acid to produce a polyurethane with very stable fluorescence properties. (52) Fluorophore can be attached to polymer backbone as a pendant to the polymer chain as well. It can be easily carried

out during the quaternisation step of polyurethane ionomers using a neutralizer which contains the fluorophore. Polyurethane cationomers with the anthracene chromophores attached on the quaternary ammonium units have been used as metal ion sensors since they show fluorescence quenching in the presence of different metal ions (UO_2^{2+}, Fe^{3+}, Cu^{2+}). (41) Another study where the incorporation of pendant fluorophores during the quaternisation is the work carried out by Buruiana to study the photo-isomerization of stilbene. (32) Pyrene is also an interesting fluorophore which can be incorporated to polyurethane chain as a pendant. There are studies carried out to develop vapor based chemical sensors by incorporating pyrene during the quaternisation of polyurethane ionomers. (39,53,54) Quenching of excited pyrene by nitrobenzene vapour has been applied to develop the sensors. (39,53,54) In addition to during the quaternisation step, a pendant fluorophore can be attached to the chain by reacting an active region of the polymer chain (eg: urethane linkage) with a suitable compound containing the fluorophore. Stilbene fluorophores have been located on to the urethane nitrogen atoms of the polyurethane chain as a pendant and photo-isomerization of stilbene has been discussed by the same team who incorporated the stilbene to the quaternisation center. (31)

2.2 Waterborne Polyurethanes

Volatile organic compounds (VOCs) are a huge problem faced by industries such as paints, inks, and coatings. (55) As a solution for this problem, it has focused on replacing the reaction mediums from organic solvents to the environmental friendly solvents such as water. (55) With this revolution, attention was paid towards the aqueous polyurethanes (polyurethane dispersions). Basically there are two main methods for making polyurethane dispersions, namely the prepolymer mixing process

and the acetone process. (55) In the prepolymer mixing process, a medium molecular weight polymer known as prepolymer is synthesized by reacting a polyol and a diisocyanate. In order to disperse the polymer in water, an internal emulsifier is also added to the reaction. A small amount of organic solvent is used to dissolve the emulsifier and reduce the viscosity. After the neutralization of the emulsifier, dispersion in water is carried out. Finally, chain extension is carried out using a water soluble chain extender. (55) This prepolymer process leads to a product with the least amount of organic solvents. However, the acetone process leads to a product with no organic solvent. In that process also a prepolymer is obtained and an emulsifier is introduced followed by the neutralization and chain extension while acetone is used as the solvent in a comparatively higher amount. Then the mixture is dispersed in water after which no further chain extension can proceed. After the dispersion the low boiling acetone is removed from the system to obtain a product with no organic solvent. (55)

Researchers have focused on either the prepolymer method (56,43,57,58) or the acetone process (59,60,61,62). One of the main differences in the prepolymer mixing method and the acetone process is the stage where the chain extension step is carried out. In prepolymer mixing method chain extension is carried out after the water addition. Jhon and coworkers have studied the chain extension of polyurethane dispersions, particularly the degree of chain extension. (56) Lei and co-workers have also studied the chain extension by changing the chain extender. (58) They have used three different chain extenders, namely ethylenediamine (EDA), diethylenetriamine (DETA), and triethylenetetramine (TETA). The effect of the amount of ionic groups on the polyurethane dispersion properties such as particle size, electrolyte stability and film properties such as crystallinity, thermal stability was investigated by the Luminana and

coworkers. (43) The NCO/OH ratio is also an important parameter in the polyurethane field. The effect of NCO/OH ratio on dispersion, film and coating properties has been discussed by Pacios *et al.* (59) When the acetone process is applied, there are several factors which can affect the dispersion properties such as initial PU content in acetone, phase-inversion temperature, evaporation conditions, and the nature of the solvent. (61) Nanda and co-workers have used both the prepolymer mixing process (63) and the acetone process (55) to obtain polyurethane dispersions using poly(hexyleneadipate-isophthalate)diol, IPDI, DMPA, triethylamine (TEA) as the neutralizer, and hexamethylenediamine (HMDA) as the chain extender. For the prepolymer mixing process N-methylpyrrolidinone was used as the organic solvent. (63) They have focused on the effect of DMPA concentration, concentration of the polymer, degree of pre/post-neutralization of the carboxylic acids and chain extension on the dispersion properties. (55,63)

When considering polyurethane dispersions, it is important to discuss about emulsifier or the ionomer which is introduced to the polymer backbone to make the polymer dispersible in water. Often the ionomer is a diol compound with ionic groups. (55) It can be categorized as anionic and cationic. Dimethylol propionic acid (55,63,64,43) is the most commonly used ionomer which is anionic. Dimethylol butanoic acid is also used as anionomer. (65) In addition to carboxylate pendants there are some situations where the sulfonate pendants impart the hydrophilicity of polyurethanes in dispersions. (57) Instead of DMPA, a compound which comprise a long side chain with 23–24 repeat units of ethylene oxide and/or propylene oxide and end-capped with a sulfonate group which is designated as PESS has been applied by Lee *et al.* (57) Cationic ionomers were used during the preparation of polyurethane dispersions. (66,67,68) N-

methyldiethanolamine has been used as cationomer by those researchers to achieve a polyurethane dispersion. (66,67,68) In addition to incorporation of diol compound with ionic groups to polymer backbone there are techniques of introducing pendent ionic groups to the polymer chain. In literature, it is explained that 2-acrylamido-2-methylpropanesulphonic acid (ATBS) anionomer has been introduced to the polyurethane chain by graft polymerization of ATBS to the unsaturated polyester polyol before the reaction with diisocyanate. (69) Athawale and his team were able to achieve a PU dispersion with high viscosity compared to DMPA based polyurethane dispersions due to crosslinking ability of the new anionomer and also improved thermal stability and enhancement in mechanical and chemical properties. (69)

After the incorporation of ionomer to the polymer backbone it is a must to neutralize those ionomer groups to achieve the hydrophilicity. If it is an anionomer most of the time a carboxylic acid group is present. In such cases an amine is used to neutralize the carboxylic acid group by converting into carboxylate ion. Triethylamine is the neutralizing agent which is commonly concomitant with the anionomer DMPA. (55,63,64) With the cationomers an amine group is neutralized by a carboxylic acid to give a quaternary ammonium salt. Acetic acid (66,67) and formic acid (68) were used to neutralize the N-methyldiethanolamine.

In literature, there are lot of works carried out which are related to aqueous polyurethane dispersions. Among the studies on aqueous polyurethanes a considerable attention is paid towards the UV curable waterborne polyurethanes due to their excellent mechanical properties. UV curable waterborne polyurethanes have been developed by incorporating different functional groups to the polyurethane chain. In general UV curable waterborne coatings are prepared by capping the isocyanate terminated

polyurethane chains with a single hydroxyl acrylate. Hwang and coworkers have introduced acrylate groups to the polyurethane chain ends by reacting the isocyanate terminated polyurethane chains with three different capping agents, namely 2-hydroxyethylmethacrylate, 2-hydroxyethylacrylate and pentaerythritoltri-acrylate. (21)

Zhang and coworkers have modified the conventional aqueous anionic polyurethane synthesis process to increase the UV curing ability. (22) They have introduced 'ene' groups via the pendent side chains attached to the polyurethane backbone, in addition to the 'ene' groups which are present in the chain terminators. Here, the isocyanate terminated anionic polyurethane prepolymer was reacted with 2,2-bis(hydroxymethyl)propane-1,3-diyl diacrylate to incorporate the 'ene' group containing pendent side chains before chain termination with 2-hydroxyethyl acrylate. (22) The effect of the amount of 'ene' groups on various film properties has been studied by them.

Yang and coworkers have introduced the thiol- 'ene' chemistry to UV curable polyurethanes to achieve a higher degree of crosslinking. (70,71) They have prepared UV curable polyurethane coatings by mixing multifunctional thiol terminated aqueous polyurethane dispersion and a multifunctional 'ene' terminated aqueous polyurethane dispersion together. 2,2-Bis(3-sulfanylpropanoyloxymethyl)butyl-3-sulfanylpropanoate (TriSH), 2,2-bis(prop-2-enoxymethyl)butan-1-ol (DiAE) were the thiol terminator and ene terminator, respectively. (70) They were able to achieve excellent physical properties compared to the conventional UV curable urethane–acrylate based systems.

CHAPTER 3 - Methodology

3.1 Materials and Analytical instruments

3.1.1 Materials

The three main monomers which were used during this research work, polyether polyol; polytetrahydrofuran with average molar mass of 2000, 98% 4,4′-methylenebis(phenylisocyanate), and 98% 2,2-bis(hydroxymethyl)propionic acid were from Sigma Aldrich and was used without further purification. The catalyst 98% 1,4-diazabicyclo[2,2,2]octane, a photo initiator 98% 2-hydroxy-4'-(2-hydroxyethoxy)-2-methylpropiophenon, a chain terminator 98% trimethylolpropanediallyl ether and a quaternizing agent ≥99.5% diethylamine were also from Sigma Aldrich and was used without further purification. N,N-dimethylacetamide(≥99.5%), N,N-dimethylformamide (≥99.8) and acetone (≥99.5%) were used as solvents which were also obtained from Sigma Aldrich and were dried and stored over molecular sieves.

3.1.2 Analytical instruments

FT-IR data were obtained using ATR mode of Bruker VERTEX 80 FT-IR spectrophotometer (Germany). The related software was OPUS spectroscopy software version 6. UV-vis absorption spectra were recorded by SHIMADZU UV 3600 UV-VIS-NIR spectrophotometer (Japan). The applied software was UVProbe 2.33. Fluorescence analysis was carried out using HORIBA Fluorolog spectrofluorometer (Japan) with the help of FluorEssence V3.5 software. DSC and TGA data were obtained from TA Instruments (USA) Q200 DSC and Q600 TGA, respectively, while TA instrument explorer software was applied in both. Zetasizer nano series particle size analyzer from MALVERN Instruments (UK) was used to monitor the zeta potentials and particle sizes

of the dispersions. In that case Zetasizer software was used. To obtain the XRD patterns, Bruker D8 FOCUS XRD (Germany) was used and Eva software was used for XRD analysis.

3.2 Polyurethane synthesis

3.2.1 Polyurethane prepolymer synthesis

Polyurethane prepolymer having the degree of polymerization of three was synthesized. From here onwards it will be called as PUP-3. Several precautions were taken to avoid the isocyanate water side reaction. Polytetrahydrofuran (PTHF) was dried in vacuum oven for 24 h at 105 ^{0}C prior to use, solvents were dried over the molecular sieves, and reactions were carried out under a nitrogen atmosphere. A 2.5025 g of 4,4′-methelenebis(phenyl isocyanate) (MDI) was dissolved in 30 ml of dimethylacetamide (DMAc). When MDI was completely dissolved, 40.0000 g of PTHF was added. The catalyst 1,4-diazabicyclo[2,2,2]octane (DABCO) was added to the reaction mixture and DMAc was added to bring the total volume up to 100 ml. The reaction mixture was stirred at 300 rpm at 80 °C for 5 hrs. MDI and polytetrahydrofuran were reacted to form the polyurethanes as shown in Figure 5.

3.2.2 Hydrophilic polyurethane synthesis and preparation of the aqueous dispersions

Via the introduction of the ionic groups to the polyurethane backbone, hydrophilicity of the polyurethane has been achieved. Five different kinds of polyurethane dispersions were obtained by varying the ionomer to polyol molar ratio while maintaining a constant ratio of total OH to total NCO at 1. The compositions used for the synthesis is given in Table 1. Reactions were carried under nitrogen atmosphere. The solvent N,N-dimethylformamide (DMF) was dried over molecular sieves. The ionomer, 2,2-

bis(hydroxymethyl)propionic acid commonly known as Dimethylolpropionic acid (DMPA) and PTHF were pre-dried in vacuum oven at 105 ^{0}C for 24 hours prior to use. The required amount of DMPA was dissolved in minimum amount of DMF and was added to the measured PTHF. The mixture was stirred properly to obtain a homogenized mixture. MDI was dissolved in DMF. The DMF volume was kept at 30 ml. After the complete dissolution of MDI, the DMPA-PTHF mixture was added to it and stirred for 5 hours at 350 rpm. The temperature was maintained at 80 ^{0}C. The temperature was reduced to 30 ^{0}C and the chain terminator, trimethylolpropanediallyl ether (DiAE) was added and stirring was continued for 30 min. Ionomers were neutralized by adding diethylamine (DEA). After the addition of DEA, stirring was continued for another 30 min. To obtain the dispersion, 70 ml of distilled water was added drop wise while maintaining vigorous stirring at 1000 rpm. After the completion of water addition, the dispersion was stirred for another 30 min. A polyurethane dispersion in a DMF-water mixture having 70% of water was obtained as shown in Figure 12.

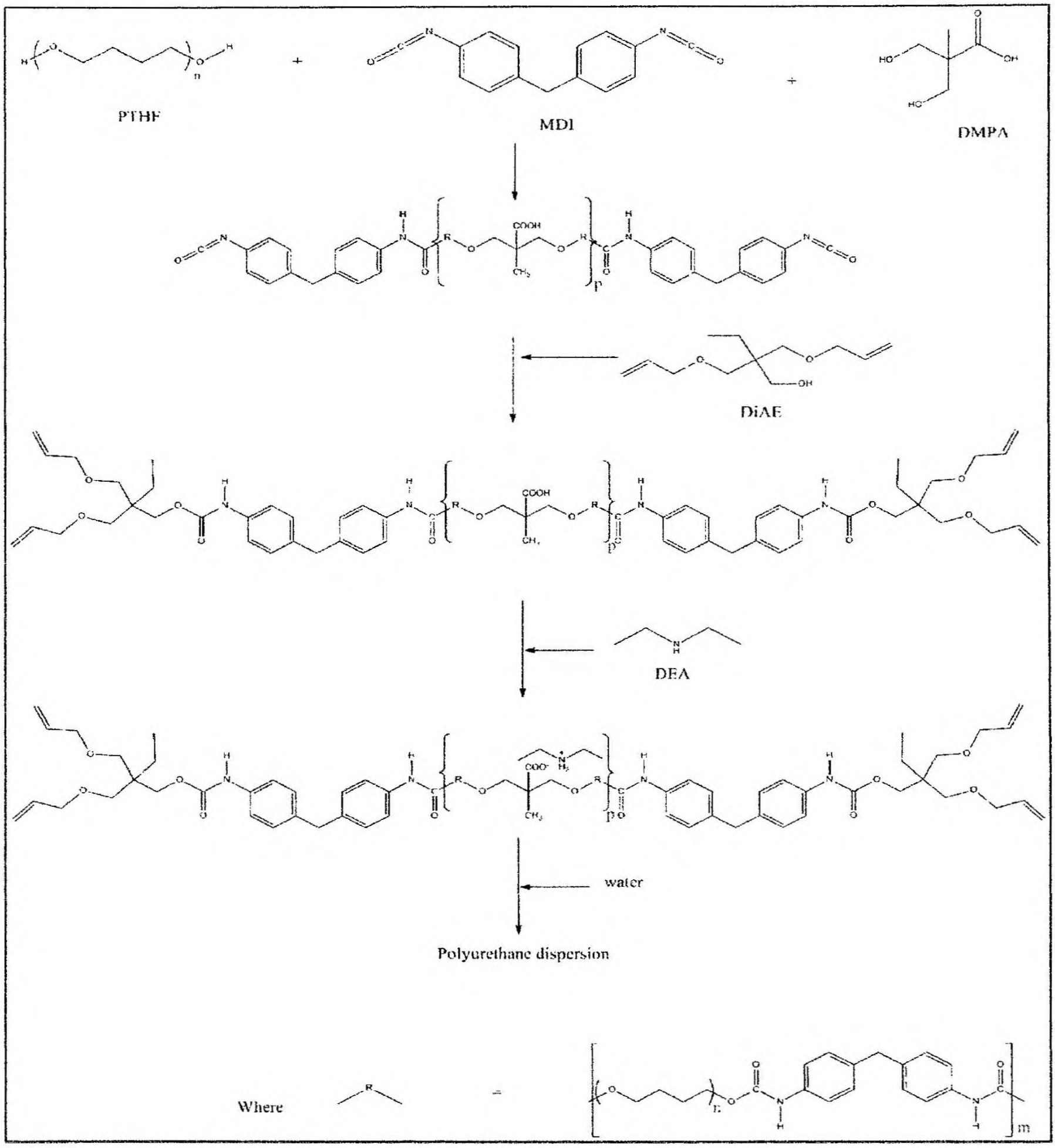

Figure 12: Synthesis of polyurethane dispersion

Table 1: Compositions used to prepare the polyurethane dispersions

Polyurethane dispersion	Amount of MDI (mol)	Amount of PTHF (mol)	Amount of DMPA (mol)	Amount of DiAE (mol)	Amount of DEA (mol)	Hard segment content (w%)
PUD-1	0.01	0.00175	0.00450	0.00750	0.00450	47.0
PUD-2	0.01	0.00225	0.00400	0.00750	0.00400	40.3
PUD-3	0.01	0.00275	0.00350	0.00750	0.00350	35.1
PUD-4	0.01	0.00325	0.00300	0.00750	0.00300	30.9
PUD-5	0.01	0.00375	0.00250	0.00750	0.00250	27.4

3.3 Dispersion Properties

The two dispersion properties, the average particle size and the zeta potential were measured using the particle size analyzer. The average size of the particles was measured via the intensity based distribution and the particle size was measured over a two month of time period to determine the stability of the dispersion. The zeta potential of the dispersion was also used to prove the dispersion stability which was continued for over two months.

3.4 Polyurethane film preparation

The films from PUP-3 solution and PU dispersions were obtained to analyze their film properties. The polyurethane solutions were cast onto dried glass slides which had been cleaned by tap water and then with distilled water. The solvent was then allowed to evaporate at 100 °C in a vacuum oven yielding smooth films.

3.5 Analysis of the film properties

3.5.1 Crystalline structure of polyurethane films; XRD

XRD patterns of all the five PUD films and the film obtained from the PUP-3 were obtained by scanning at diffraction angle 2θ from 10° to 60°.

3.5.2 Crystalline structure of polyurethanes; FT-IR

Urethane N-H region and urethane C=O (carbonyl) region of the PUD films and PUP-3 film was scanned. For each sample 64 scans were carried out at 4 cm^{-1} resolution.

3.5.3 Thermal properties of polyurethane films; DSC

The DSC thermograms of each polyurethane film (PUD films and PUP-3 film) were recorded. The sample was first cooled to -30 ^{0}C and then heated at 5 ^{0}C /min up to a maximum temperature of 300 ^{0}C. The sample was cooled to -30 ^{0}C again and reheated to 300 ^{0}C at 5 ^{0}C min^{-1} cooling/heating rate.

3.5.3.1 Microstructural changes during DSC profiling; FT-IR

In order to monitor the micro-structural changes in polyurethane films, FTIR spectra of the films were recorded again just after the completion of the following DSC cycles. The sample was first cooled to -30 ^{0}C and then heated to a maximum temperature of 220 ^{0}C at 5 ^{0}C /min. Then sample was cooled to -30 ^{0}C and reheated to 10 ^{0}C at 5 ^{0}C min^{-1} cooling/heating rate.

3.5.4 UV absorbance of polyurethane films

Absorption spectra of the polyurethane films (PUD films and PUP-3 film) were recorded in the range of 200 nm – 650 nm.

3.5.5 Fluorescence study

Fluorescence properties of the prepared films were studied by recording emission spectra. Excitation and emission slit widths were maintained at 3 nm for all the experiments. All the emission intensities presented in this study were normalized to excitation intensity. For each type of polyurethane film, fluorescence analysis was carried out as follows.

The fluorescence spectrum of the prepared polyurethane film was recorded using 293 nm as the excitation wavelength. The fluorescence spectrum of the film was recorded repeatedly (30 times). Each scan amounted to 30 s of UV irradiation at 293 nm wavelength. Then, the UV irradiated film was kept out of radiation for three days and spectrum was recorded again, after which the recording of the spectra was repeated 30 times. The above process was repeated for three complete cycles.

The following two factors were observed; the variations in the fluorescence spectra with extended UV exposure and the reversibility in those variations after UV ceasing. This lead to an extended analysis to determine the factors affecting this behavior, reasons for this nature and finally to propose a possible mechanism.

3.5.5.1 Effect of relaxation time on fluorescence

The PUP-3 system was used to examine the effect of relaxation time on the reversibility. In this case, the number of continuous repeats per cycle was maintained at 30. Relaxation time was varied from 1 day to 1 month as 1 day, 3 days, 7 days and 1 month. The extent of reversibility was calculated using the collected data.

3.5.5.2 Effect of exposure time on fluorescence

Using the PUP-3, the effect of exposure time on the reversibility was examined by varying the number of continuous repeats per cycle in such a way 20, 30, 40, 50, and 60

repeats per cycle while retaining a constant relaxation time of three days for each. Variations in fluorescence peak intensities were analyzed.

3.5.5.3 *Effect of degree of polymerization*

By varying the NCO:OH molar ratio while following the procedure explained in the 3.2.1 section, two other polyurethane prepolymers having different degree of polymerizations were prepared. Their labels and formulations are shown in Table 2.

Table 2: Formulations used to synthesis polyurethane prepolymers

Polyurethane system	Amount of MDI	Amount of PTHF	Degree of polymerization
PUP-3	0.01 mol (2.5025 g)	0.02 mol (40.0000 g)	3
PUP-10	0.0083 mol (2.0853 g)	0.01 mol (20.0000 g)	10
PUP-∞	0.01 mol (2.5025 g)	0.01 mol (20.0000 g)	∞

The results obtained related to the fluorescence behavior of three different polyurethane systems were compared to understand the effect of degree of polymerization.

3.5.5.4 Effect of solvent

In order to investigate the solvent effect, a new polyurethane system was prepared according to the formulations of PUP-3 given in Table 2 and the procedure explained in the 3.2.1, changing the solvent from DMAc to DMF. The system was labeled as PUP-$3_{\_DMF}$. The effect was discussed by comparing PUP-3 and PUP-$3_{\_DMF}$.

3.5.5.5 FT-IR

To monitor the chemical changes during the UV exposure, IR spectra of polyurethane films before and after UV irradiation were obtained. For each sample 64 scans were carried out at 4 cm^{-1} resolution.

CHAPTER 4 - RESULTS AND DISCUSSION

4.1 Polyurethane synthesis

4.1.1 Polyurethane prepolymer

To exclude the polyurea formation during the polyurethane synthesis, it is necessary to avoid the contact of moisture with the reactants. So precautions such as carrying out the reaction in a nitrogen environment, drying the PTHF and DMPA above 100 ^{0}C prior to use, and use of solvents which were dried over molecular sieves were employed.

According to the Carothers' equation (10), a polyurethane prepolymer having the degree of polymerization 3 was prepared using stoichiometric molar ratio of two reactants in 2:1. PTHF was used in excess in such a way that the polyol: diisocyanate molar ratio is 2:1. The Carothers' equation which is used to calculate the degree of polymerization is given below in Equation 1. The number average degree of polymerization $\bar{X}_n$ can be calculated using r and p where r and p represent the stoichiometric ratio and extent of reaction, respectively. Stoichiometric ratio (r) is always defined to have a value equal to or less than one. (10)

$$\overline{X}_n = \frac{(1+r)}{(1+r-2rp)}$$

Equation 1: Carothers' equation

It was assumed that the reaction approaches completion with in the period and extent of reaction was considered as 0.999.

When MDI:PTHF = 1:2

$$r = {}^1/_2 = 0.5$$

$$\overline{X}_n = \frac{(1+0.5)}{(1+0.5-2(0.5)(0.999))} \approx 3$$

MDI was dissolved in DMAc prior to react with PTHF as it is useful to confirm that there is no unreacted residual MDI. The reaction mixture was further diluted to reduce the viscosity of the final polymer solution.

4.1.2 Hydrophilic polyurethane synthesis and preparation of their aqueous dispersions

A common problem in the polyurethane synthesis is the formation of polyurea via the side reaction of the isocyanate group with water instead of the hydroxyl group. Hence, it is necessary to avoid the water - isocyanate side reaction by removing the moisture from the reaction environment. Thus, PTHF and DMPA were dried in vacuum oven at 105 ^{0}C prior to use and the DMF was dried over molecular sieves in order to remove the moisture. An inert reaction environment was maintained by carrying out the reaction in a nitrogen atmosphere.

As polyurethane chain does not contain ionic centers, it is highly hydrophobic. Due to this hydrophobicity, organic solvents have to be used during the polyurethane synthesis processes. With the use of large amount of organic solvents, significant environmental pollution was created due to the evaporation of volatile organic compounds (VOC) in the polyurethane industry. Now, the industry is focused on reducing the use of volatile organic solvents and shifting to water based formulations. In this study, we focused on the minimization of the amount of dimethylformamide (DMF) consumed and to introduce water to the reaction medium in order to develop a DMF-water mixture as the solvent.

We were able to develop a DMF-water mixture as the solvent because DMF is miscible with water. DMF and water are miscible in such a way that they can be mixed in all proportions to give a homogenized mixture. (72)

In this research work MDI and PTHF are used as the diisocyanate and the polyol, respectively. As both are non polar compounds the poyurethanes obtained from these monomers are highly hydrophobic. It is neccessary to maintain a hydrophilic nature in order to use a water based medium. It has been achieved by introducing a monomer containing a hydrophilic group. Dimethylolpropionic acid (DMPA) which was used as the ionomer has a pendant carboxylic acid group. It is important to attain a uniform distribution of the ionic monomer inside the polyurethane chain in order to avoid phase seperations of the polymer. It has been achieved by obtaining a homogenized mixture of PTHF and DMPA via a proper mixing of PTHF and DMPA which is dissolved in DMF through magentic stirring prior to the addition of MDI. The need of obtaining a homogenized mixture of polyol and ionomer prior to the addition of diisocyanate is emphasised by SM Cakic and co-workers. (73) The introduced ionic groups; the carboxylic acid groups were neutralized using diethyamine which is capable of forming a carboxylate ion and quarternary ammonium moiety. These pendant carboxylate ions which are uniformely distributed in the polurethane backbone have the ability to convert the polyurethanes from hydrophobic to hydrophilic.

The step growth polymerization was stopped using the chain terminator DiAE. It consists of a single hydroxyl group which can reacts with a isocyanate group and avoid further polymerization. DiAE also contains two terminal 'ene' groups which are useful in crosslinking via UV curing.

Through dropwise addition of the water to the polyurethanes prepared in DMF, it was possible to obtain a poyurethane dispersion in DMF-water mixture. In order to disperse properly, it was necessary to stir the reaction mixture vigouruosly 1000 rpm.

4.2 Dispersion properties

When discussing polyurethane dispersions it is mandatory to discuss the stability of the dispersion. All the five dispersions which were prepared here are highly stable. There was no phase separation or sedimentation during a period of two months. The dispersion stability can be verified using the zeta potential. Dispersions having zeta potentials more positive than +30 mV or more negative than -30 mV are generally considered as stable. (74) Also higher the absolute value of the zeta potential higher the dispersion stability. (46) Particle size measurements taken over a long period of time is also an indirect evidence for the dispersion stability. In other words, absence of significant changes in particle size indicates that dispersion is stable or no considerable agglomerations have occured.

Particle size and zeta potential were measured using a Malvern Zetasizer nano series particle size analyzer at 30 ^{0}C. The material was selected as polyurethane and refractive index of the material was given as 1.50 according to the sample dispersion and refractive index guide of Malvern instruments. (75) Dispersant was given as 30% DMF-water. Dispersant properties were supplied using literature values of the refractive index, viscosity and dielectric constant of a 30% DMF-water mixture. As the measured values were not given, refractive index was back calculated as 1.368 using the given data and equations in the relevant article. (76) According to the literature, the viscosity was provided as 1.478 (77) while dielectric constant was 69.9 (78).

The average particle sizes and zeta potentials of the five dispersants over two months are given below.

Table 3: Particle sizes (diameter) and zeta potentials of polyurethane dispersions

Dispersion	PUD-1		PUD-2		PUD-3		PUD-4		PUD-5	
DMPA:POLYOL	72:28		64:36		56:44		48:52		40:60	
Number of days	Average particle size (nm)	Zeta potential (mV)	Average particle size (nm)	Zeta potential (mV)	Average particle size (nm)	Zeta potential (mV)	Average particle size (nm)	Zeta potential (mV)	Average particle size (nm)	Zeta potential (mV)
1	63.4	-54.9	98.9	-51.2	156.6	-48.9	171.1	-45.9	205.2	-44.9
2	62.8	-57.6	99.3	-51.6	157.2	-47.8	171.5	-47.1	204.3	-45.2
3	63.5	-59.4	100.8	-54.4	159.0	-48.6	171.5	-48.5	206.9	-47.3
6	63.1	-58.4	97.4	-54.2	161.0	-47.6	172.2	-45.6	204.9	-45.0
7	63.4	-61.0	100.5	-56.1	163.7	-47.9	170.9	-48.1	205.0	-44.7
8	64.1	-59.8	101.7	-57.0	166.4	-48.6	168.5	-48.8	206.2	-45.0
9	63.0	-60.4	101.5	-59.5	166.9	-50.1	170.3	-49.8	205.8	-49.0
13	61.4	-58.2	102.5	-57.7	173.3	-46.2	170.5	-45.8	200.9	-44.8
14	64.2	-57.0	102.0	-53.6	173.6	-47.5	169.6	-47.5	204.5	-45.5
21	64.0	-50.6	102.6	-50.6	161.8	-46.9	170.8	-46.2	205.6	-43.2
28	63.1	-51.4	101.8	-51.0	173.1	-46.4	171.8	-45.1	208.7	-42.4
35	61.0	-52.9	101.9	-52.1	172.7	-46.7	176.5	-45.4	206.4	-45.1
42	62.0	-50.2	101.7	-49.6	171.5	-44.6	172.0	-44.7	205.4	-44.1
49	61.1	-52.8	101.2	-49.0	170.8	-46.9	173.5	-46.0	204.5	-44.7
56	60.6	-53.7	100.0	-51.8	173.6	-46.2	173.0	-44.0	206.0	-42.7
63	60.9	-54.1	100.1	-52.0	173.0	-48.7	173.7	-47.1	207.1	-46.8

It is clearly seen that the higher the ionomer: Dimethylolpropionic acid ratio, the lower the particle size. Inevitably, an increase in the DMPA percentage results in a subsequent increase in the hydrophilicity of the polyurethane due to the increase in the number of ionic groups per polyurethane chain. As a result, a reduction in particle size can be predicted. The relationship between hydrophilicity and particle size has been discussed in literature. This inverse correlation has been attributed to the stabilization mechanism of dispersed particles which involves diffusing electrical double layer formation. (79,80,81) Also with the increase in DMPA percentage, the PTHF percentage is decreased simultaneously. The molar mass of PTHF used is 2000 and hence it is a long chain polymer. It is obvious that a decrease in the amount of these long chain monomers per polymer chain leads to a reduction in the length of the resulting polymer and subsequently leading to smaller polymer particles. Due to the increase in hydrophilicity and decrease in chain length, particle size is small in the polymers with higher percentage of DMPA.

Dispersion stability is a key feature in the field of polyurethane ionomers. Absolute zeta potentials of all the dispersions were greater than 30 mV indicating that they are highly stable. With the increase in DMPA percentage, there is an increase in the absolute value of the zeta potential which indicates an increase in dispersion stability. The stability of aqueous dispersions is governed by the density of ionic groups in a particle. The polyurethane particles in aqueous dispersions are formed as tiny spheres having a core formed by hydrophobic segments and a boundary layer which consists of ionic groups which are in general hydrophilic. (43) These tiny spheres of polyurethane particles form remarkably stable dispersions. (43) Hence, higher amount of ionic groups leads to higher dispersion stability. There was an indirect evidence to prove this dispersion

stability; the average particle sizes of these dispersions were measured over a two months of period and it was clearly shown that variations in particle sizes with time were negligible. It indicates that agglomerations of particles are low, indirectly showing that the dispersions are stable.

4.3 Obtaining the polyurethane films

Both polyurethane prepolymers which were in DMAc medium and polyurethane dispersions prepared in DMF-Water mixture were casted on to a clean glass slides which were kept on petri dishes. The solvent was allowed to evoporate. Smooth polyurethane films were obtained by evaporating the solvent via overnight drying in a vacuum oven at 100 ^{0}C.

4.4 Analysis of film properties

4.4.1 Crystalline structure of polyurethane films; XRD

4.4.1.1 Films from polyurethane dispersions (PUD films)

The XRD patterns of five PUD systems are shown in Figure 13.

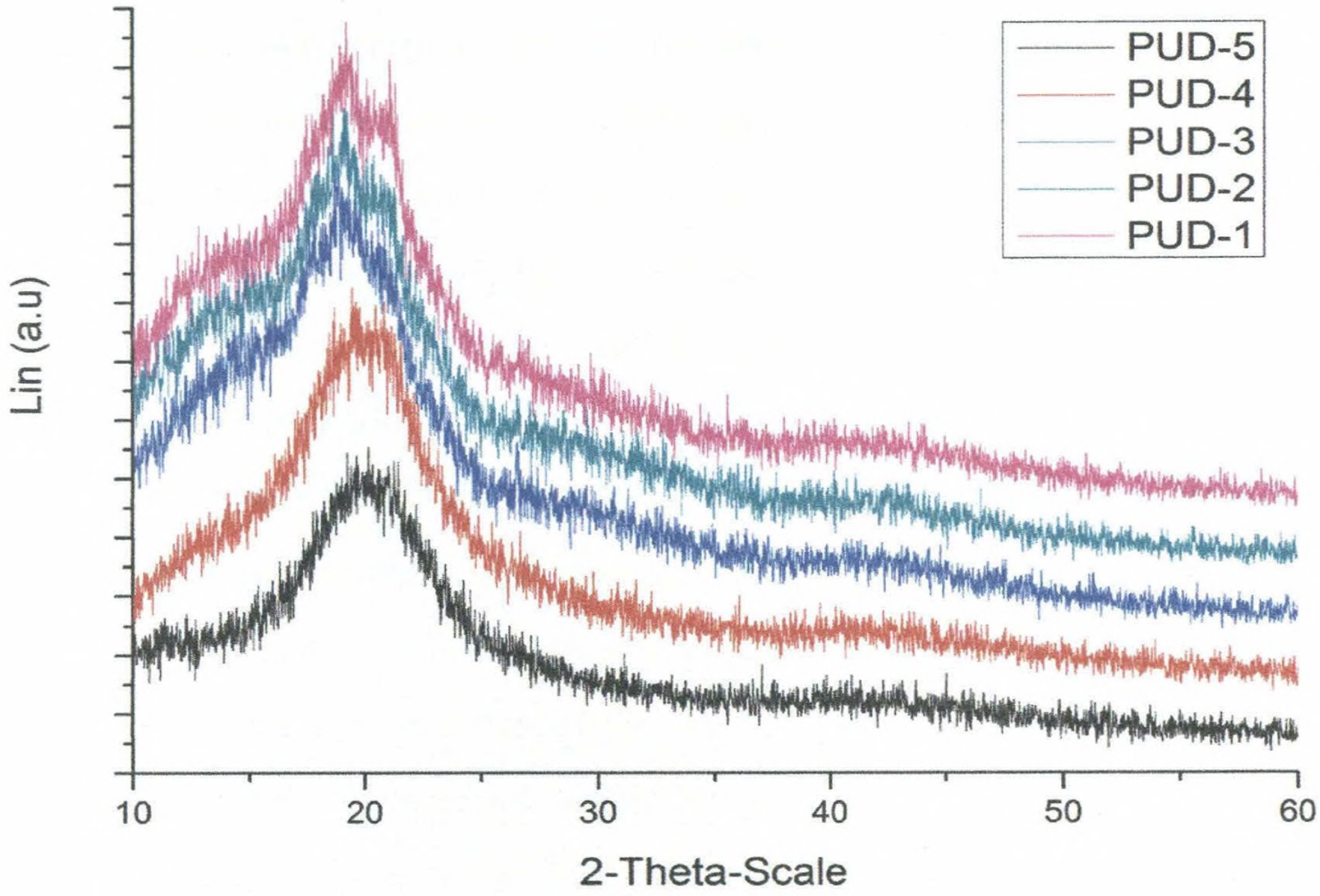

Figure 13: The XRD patterns of five PUD systems

All the five PUD systems have a broad XRD peak at 2θ around 20°. This peak is corresponding to the MDI based hard segment crystallinity. (82,83,84) When closely observed, in the five patterns there is an increase in the sharpness of the peak from PUD5 to PUD1 which is the order of increase of the hard segment content. It indicates that hard segment crystallinity becomes higher with the increase in hard segment content.

It is well established that crystalline hard segment bundles exists due to hydrogen bonds which are formed between the urethane linkages. With the increase of hard segment content, even though the degree of polymerization is same, the chain length becomes shorter. Hence, number of chains per unit volume becomes higher which increases the probability of finding two hard segments which are close enough to form hydrogen bonds. Therefore, with the increase of the hard segment content, the extent of hydrogen

bonding is increased and subsequently the amount of bundled hard segments. This will lead to an increase in the crystallinity of the system. In our systems, the increase in the hard segment content has been achieved by increasing the DMPA/PTHF molar ratio which leads to an increase in the ionic centers. The coulombic interactions between the ionic centers make physical cross-links between polymer chains. (43,85) As the number of ionic centers increases, the inter-chain interactions become higher: polymer chains are attracted to each other strongly. (85) Due to the increased interactions, crystallinity becomes stronger. In addition, inter-chain coulombic interactions increase the attraction between the polymer chains and reduce the distance between chains. As a result, the strength of hydrogen bonds is increased eventually results in higher crystallinity. This kind of influence from coulombic interactions on the hydrogen bonding has been discussed in the field of molecular docking. An influence of the coulombic interactions between the anionic subsite of the acetylcholinesterase enzyme and the cationic ligand of the tail group of the acetylcholine substrate on the catalytic activity aroused from the hydrogen bond formation between esteratic subsite (catalytic subsite) of enzyme and head group of acetylcholine has been discussed by Kua and co-werkers. (86)

4.4.1.2 Film from polyurethane prepolymer (PUP-3 film)

The XRD pattern of the PUP-3 prepolymer film is shown in Figure 14.

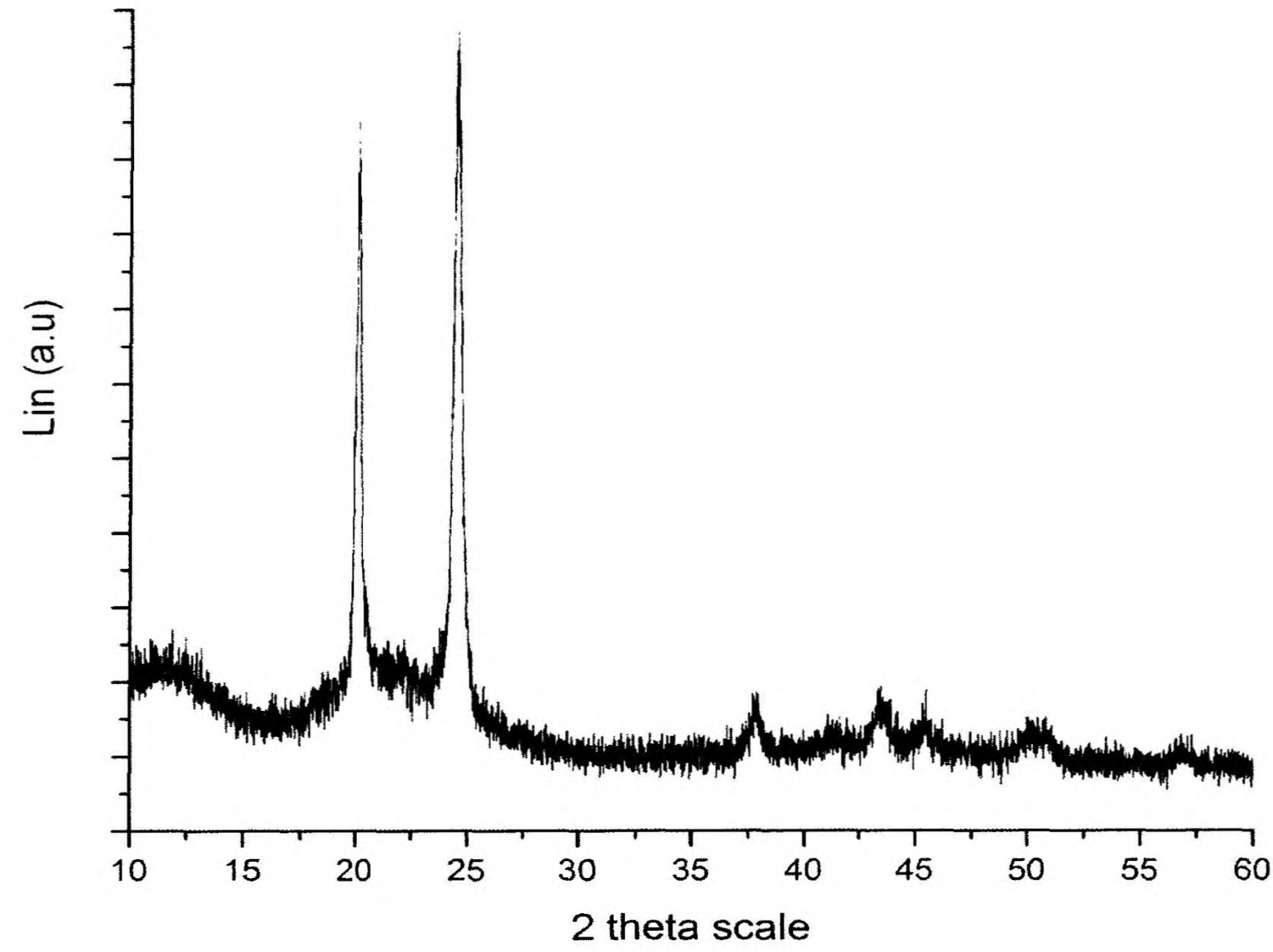

Figure 14 : The XRD pattern of the polyurethane prepolymer PUP-3

The diffraction pattern which is obtained from prepolymer is similar to the pattern corresponding to the crystalline PTHF. (87,88) This shows that the prepolymer PUP-3 has a microstructure consisting of crystallized soft segment matrix. Hence, it is clear that PUP-3 film does not have crystalline hard segment bundles in contrast to PUD films.

4.4.2 Crystalline structure; FT-IR

4.4.2.1 Films from polyurethane dispersions (PUD films)

Generally, polyurethanes have a microstructure consisting of crystalline hard segment bundles and isolated hard segments trapped in the soft segment matrix. (89,90) These crystalline hard segment bundles are produced due to the hydrogen bonds which are

formed between the N-H group and C=O groups of the urethane linkages of neighboring molecules. Hence, polyurethanes having the microstructure of hard segment crystallinity show H bonded peaks due to crystalline bundles while peaks of free bonds due to isolated hard segments which are trapped in the soft segment domain. (90)

The characteristic absorption frequencies for free urethane carbonyl and urethane carbonyl which is H bonded to NH should appear in the ranges of 1730-1740 cm^{-1} and 1703-1710 cm^{-1} , respectively. (91) Characteristic IR frequencies corresponding to free NH appear in the range of 3445-3450 cm^{-1} and that of NH which is hydrogen bonded to oxygen appears in the range 3260-3290 cm^{-1}. (91)

The presence of crystalline hard segment bundles in PUD films is confirmed by the presence of IR absorption peaks corresponding to hydrogen bonded urethane NH groups and hydrogen bonded urethane carbonyl groups. The Figure 15 and Figure 16 show the C=O region and N-H region of the five polyurethane films obtained from five dispersions respectively.

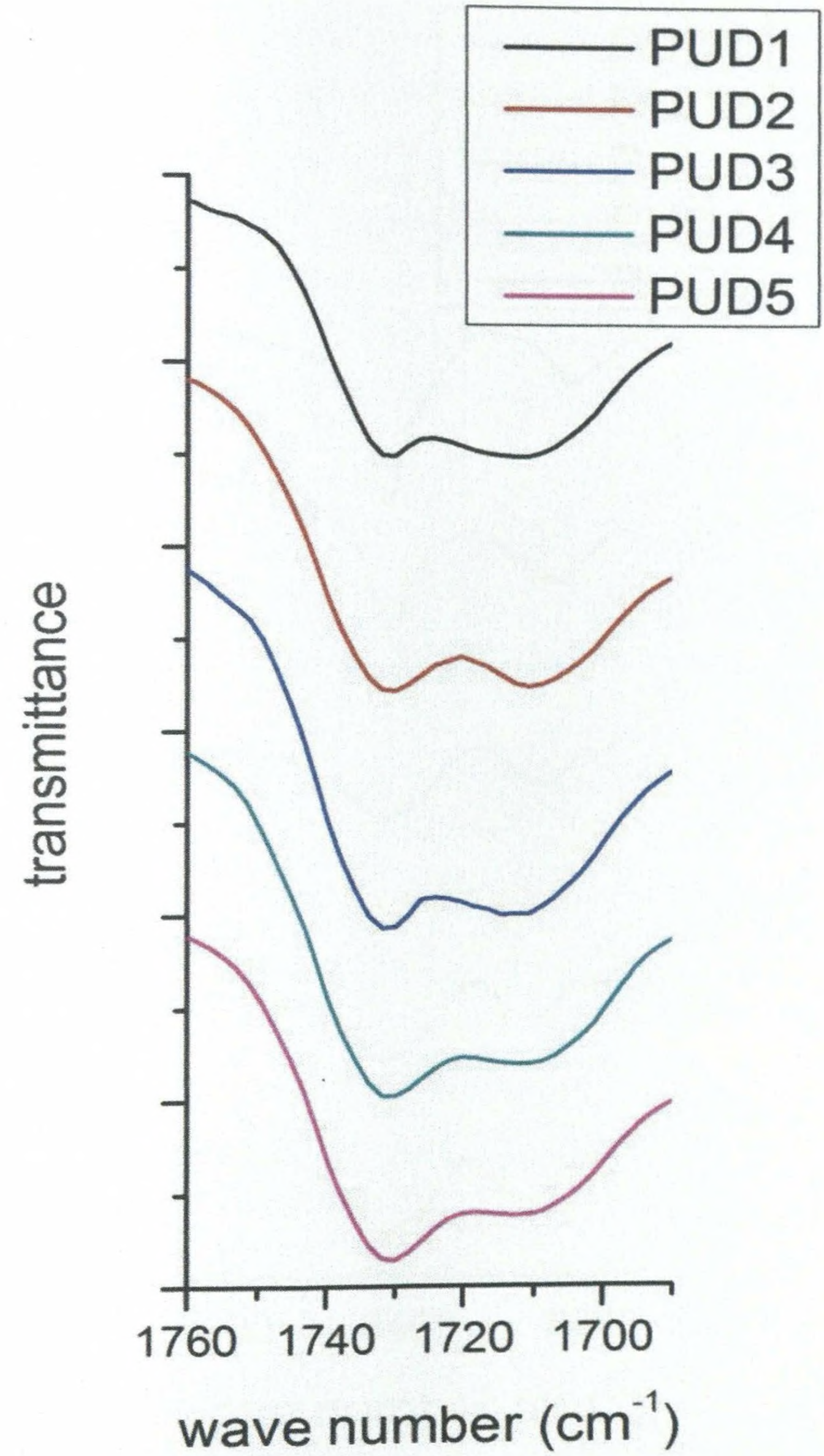

Figure 15: The C=O region of the FT-IR spectra of PUD films

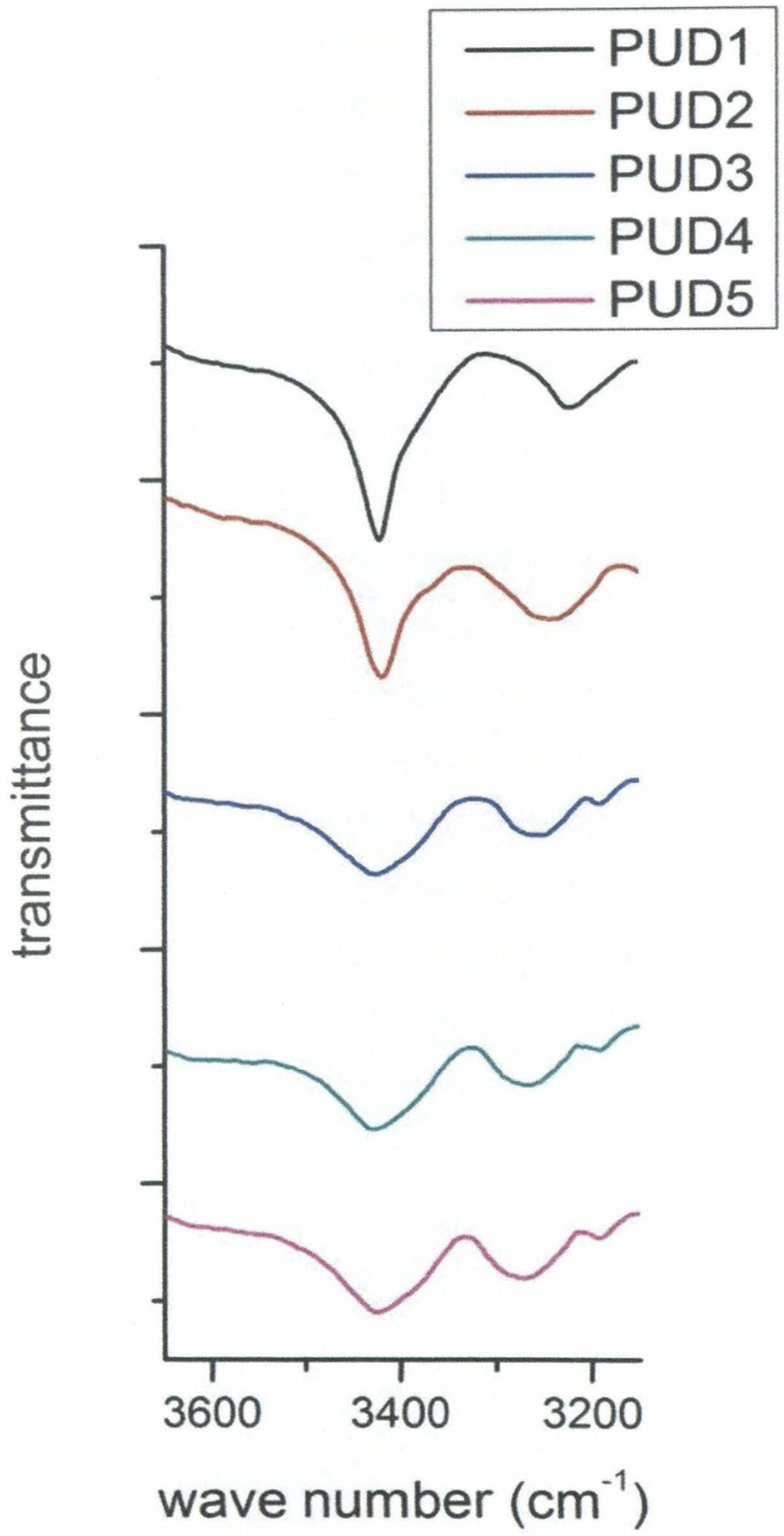

Figure 16: The N-H region of the FT-IR spectra of PUD films

In all five films, there are two peaks in the carbonyl region around 1730 cm^{-1} and 1710 cm^{-1} , which can be assigned to the free carbonyl and carbonyl which is hydrogen bonded to NH, respectively. Similarly there are two peaks in the NH region, one is around 3425 cm^{-1} and the second peak varying in the range between 3280-3220 cm^{-1} which can be assigned to free NH and H bonded NH, respectively. The presence of hydrogen bonded NH and CO peaks in addition to free NH and CO peaks in all five films obtained from five dispersions proves the presence of crystalline hard segment bundles in all the films.

The increase in extent of hydrogen bonding and the increase in the strength of hydrogen bonding with respect to hard segment content can be explained using the FT-IR spectroscopy. According to the Figure 15, it can be identified that relative intensity of the hydrogen bonded carbonyl peak is increased from PUD-5 to PUD-1 as the hard segment content get increased. The parameter "hydrogen bond index" clearly depicts this variation. The hydrogen bond index (HBI) is measured as the intensity ratio of hydrogen bonded carbonyl peak and free carbonyl peak which implies the relative absorbance of hydrogen bonded carbonyl peak to that of free carbonyl peak. (92)

Once the HBI is calculated, there was a trend of increase in HBI with respect to hard segment content.

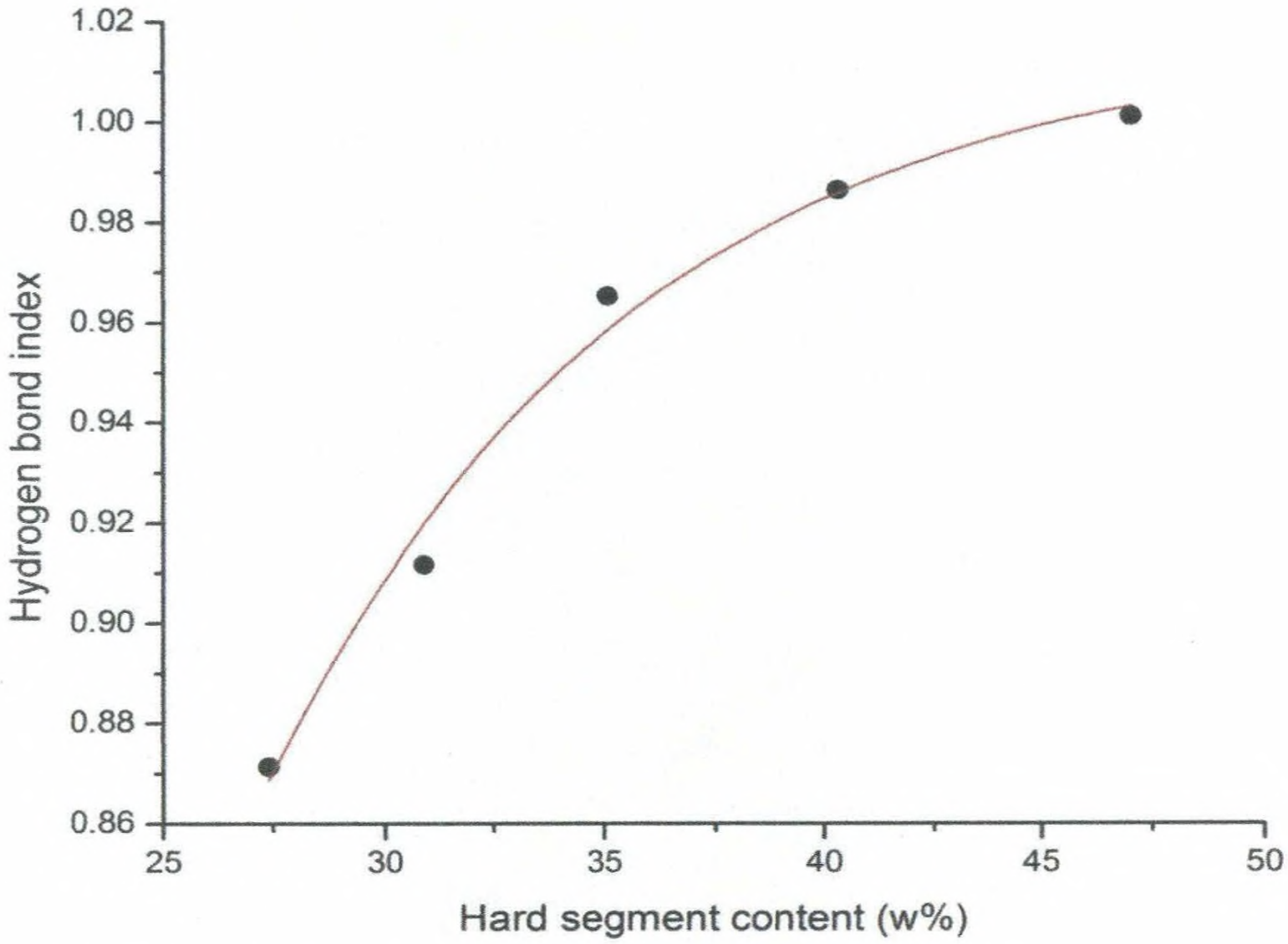

Figure 17: The relationship between hard segment content and hydrogen bond index

As shown in Figure 17, HBI data were fitted very well to an exponential curve having the following equation with a significantly high R-square value of 0.9879.

$$y = A_1 e^{-x/t_1} + Y_0$$

Where A_1= -4.06829, t_1 = 8.27185 and y_0 =1.01687.Data implies that the extent of hydrogen bonding is increased with increased hard segment content (DMPA/polyol molar ratio). As explained earlier this increase in the extent of hydrogen bonding leads to an increase in crystallinity.

The shift in the NH peak position is a signal of the strength of hydrogen bonds. When NH bond is involved in H bond formation, the NH bond strength becomes less and this will lead to a red shift in absorption frequency. (93) The magnitude of shifts in the NH peak position is a measure of Hydrogen bond strength. (91,94)

As shown in Figure 18, with the increase of hard segment content (DMPA/polyol molar ratio) the NH peak shift was increased.

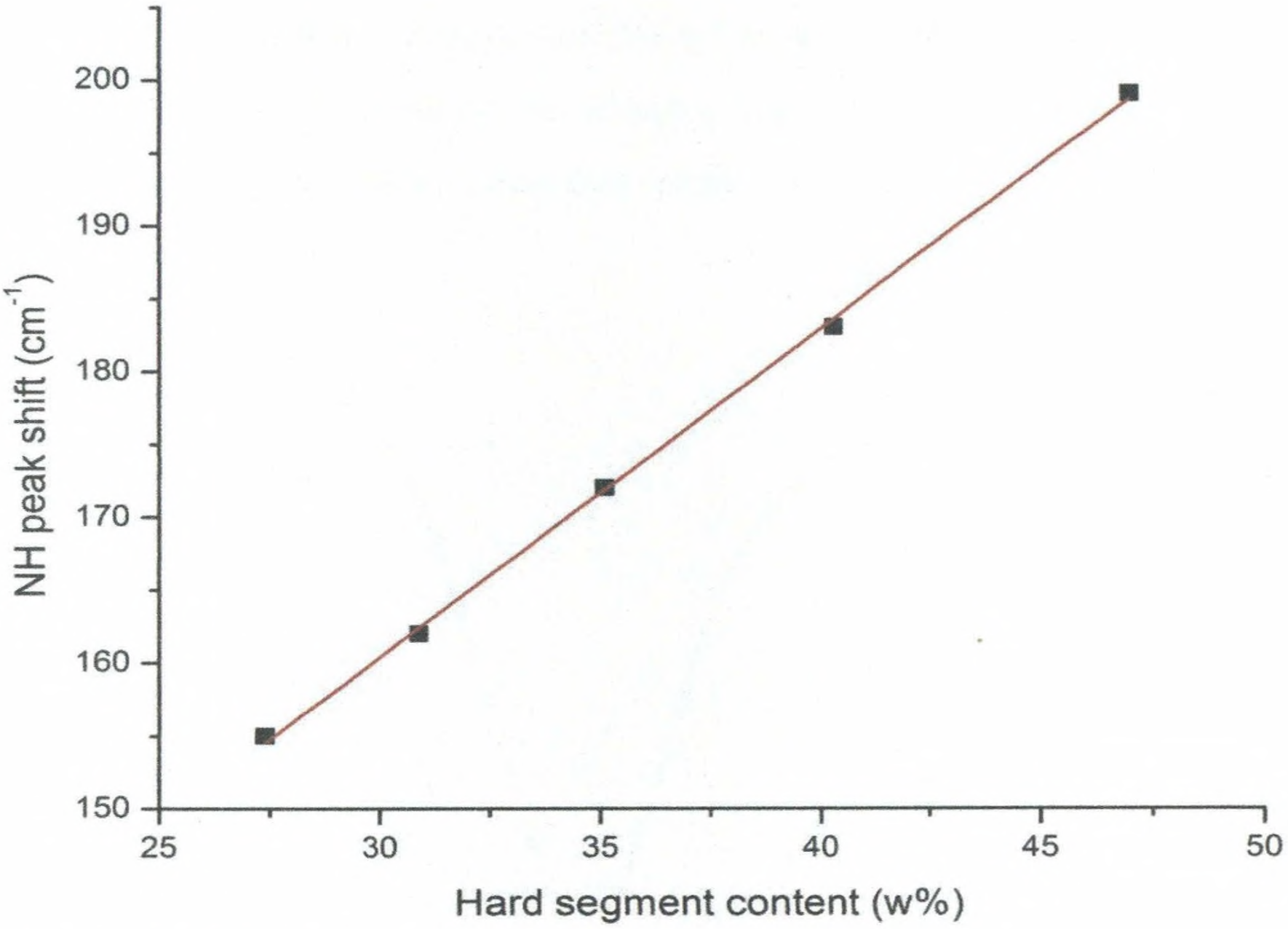

Figure 18: The relationship between NH peak shift and hard segment content

The data points were fitted to a straight line having the following equation with a significantly high R-square value of 0.9991.

$$y = a + bx$$

Where a = 92.94925 and b = 2.24822.

The increase in NH peak shift with the increase in hard segment content implies that hydrogen bond strength become stronger when hard segment content is increased. As a result, a growth in hard segment crystallinity is observed.

4.4.2.2 Film from polyurethane prepolymer (PUP-3 film)

The absence of crystalline hard segment bundles which are formed via hydrogen bonds at urethane linkages was able to confirm by the FT-IR spectra of the PUP-3 film. As there was no indication of hydrogen bonded NH groups or carbonyl groups in FT-IR spectra (Figure 19, Figure 20) it is fair enough to assume that crystalline hard segment bundles are not available in the polyurethane prepolymer films.

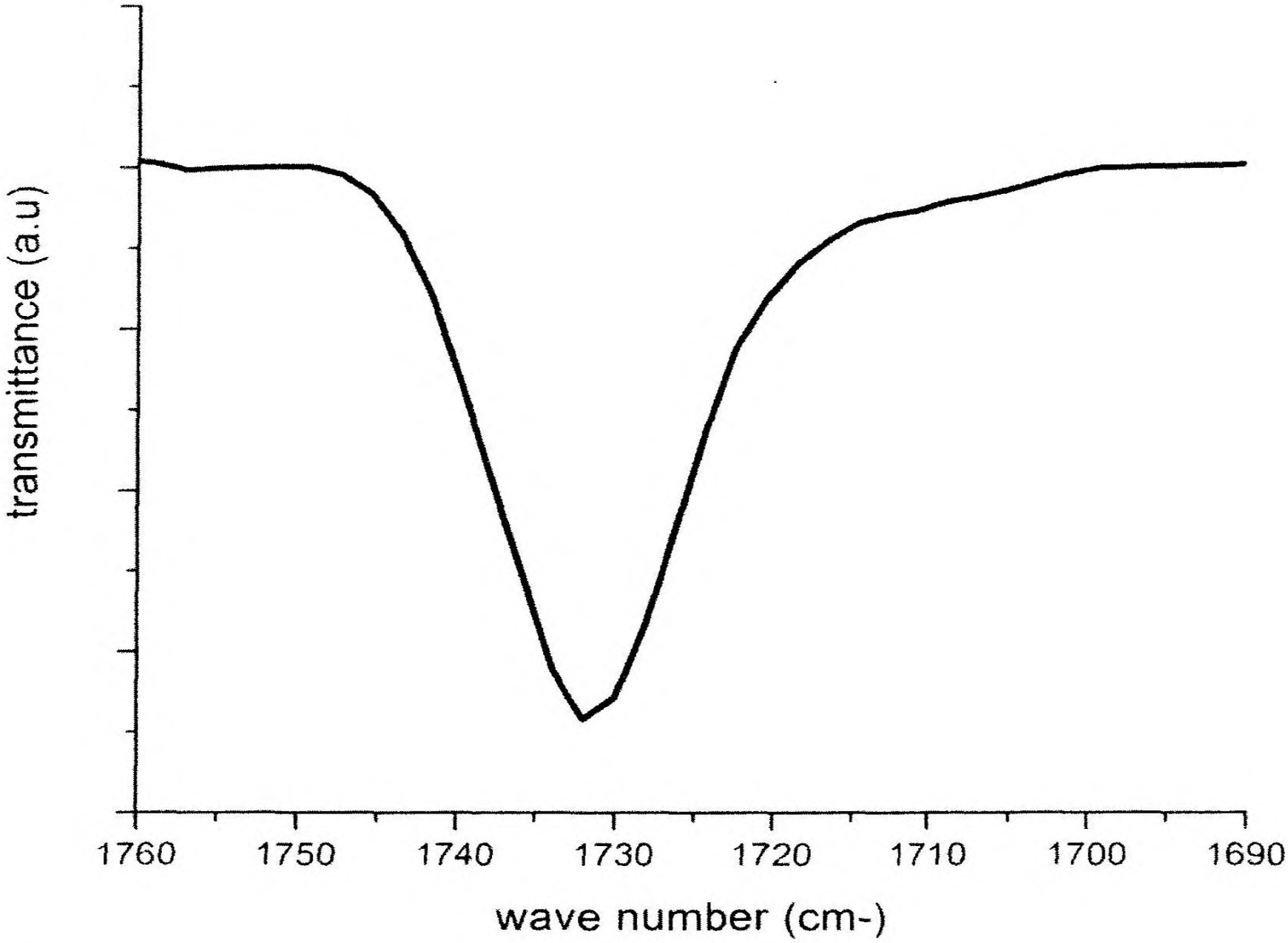

Figure 19: The C=O region of the FT-IR spectrum of PUP-3

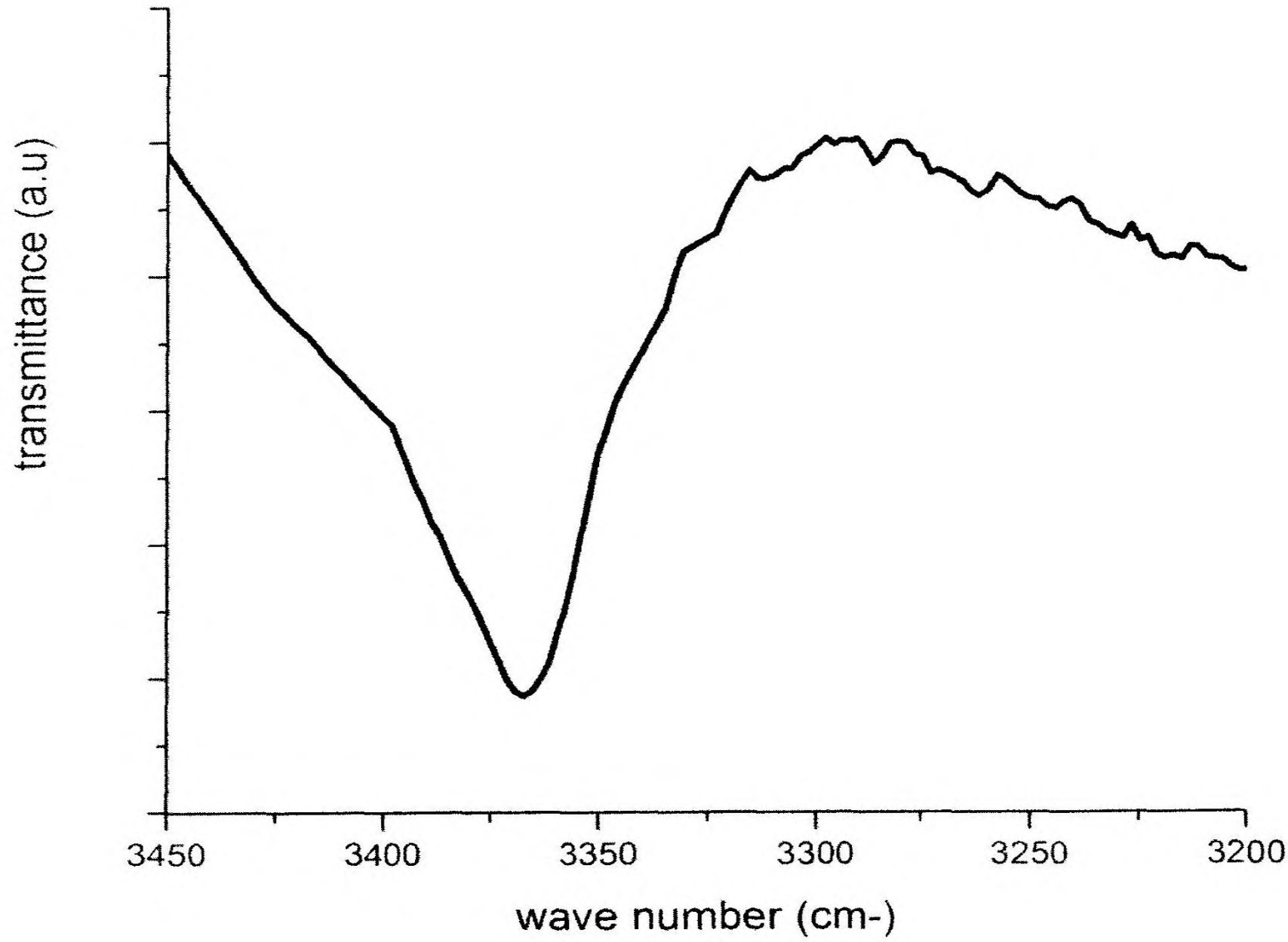

Figure 20: The N-H region of the FT-IR spectrum of PUP-3

4.4.3 Thermal properties of polyurethane films; DSC

4.4.3.1 Films from polyurethane dispersions (PUD films)

Thermal properties were analyzed using the DSC results. The thermal behavior of PUD films and the effect of the ionic group percentage on thermal properties were analyzed. The first heating cycle, cooling cycle and second heating cycle of the DSC thermograms are shown in below (Figure 21, Figure 23 & Figure 24).

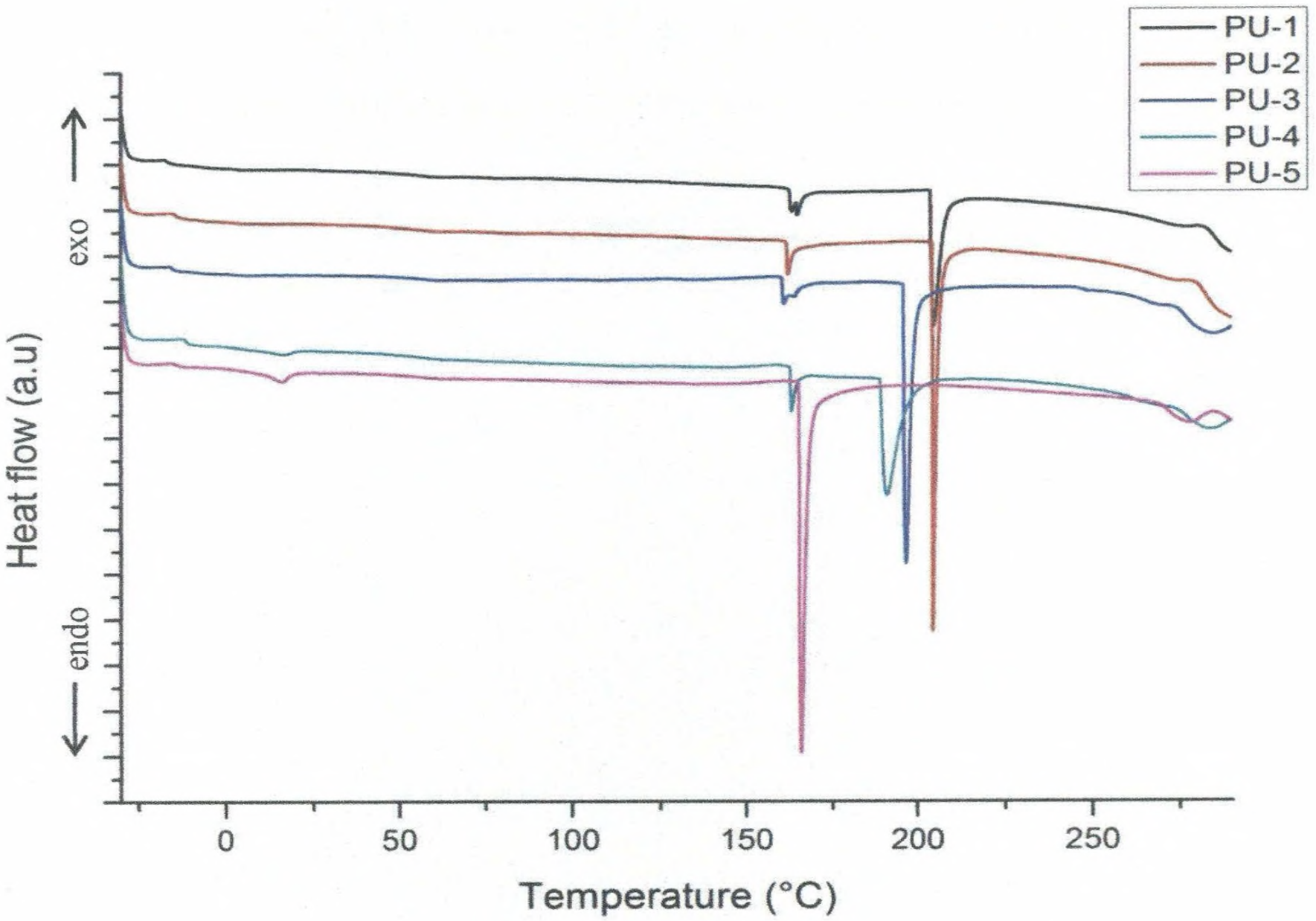

Figure 21: The first heating cycle of the polyurethane films obtained from dispersions

During the first heating cycle, all the five films had melting peaks at higher temperatures, in the range of 150 ^{0}C to 225 ^{0}C. This can be attributed to hard segment melting. The melting peaks around 180 ^{0}C has been assigned to MDI based crystalline hard segment melting as suggested by Mishra and coworkers. (84) The appearance of this hard segment melting peak in the first heating cycle depicts that when films from polyurethane dispersions were formed through solvent evaporation via oven drying, it leads to a micro structure of polyurethanes having crystalline hard segments. This could have been imparted by the presence of COO^- which can form columbic forces to bring hard segments much closer compared to that of non-ionic prepolymer. The other noticeable observation is the variation of the melting temperature with the hard segment

content. Hard segment content was varied by varying the polyol/ionomer molar ratio. As shown in Figure 22 the melting temperature increased as the hard segment content is increased.

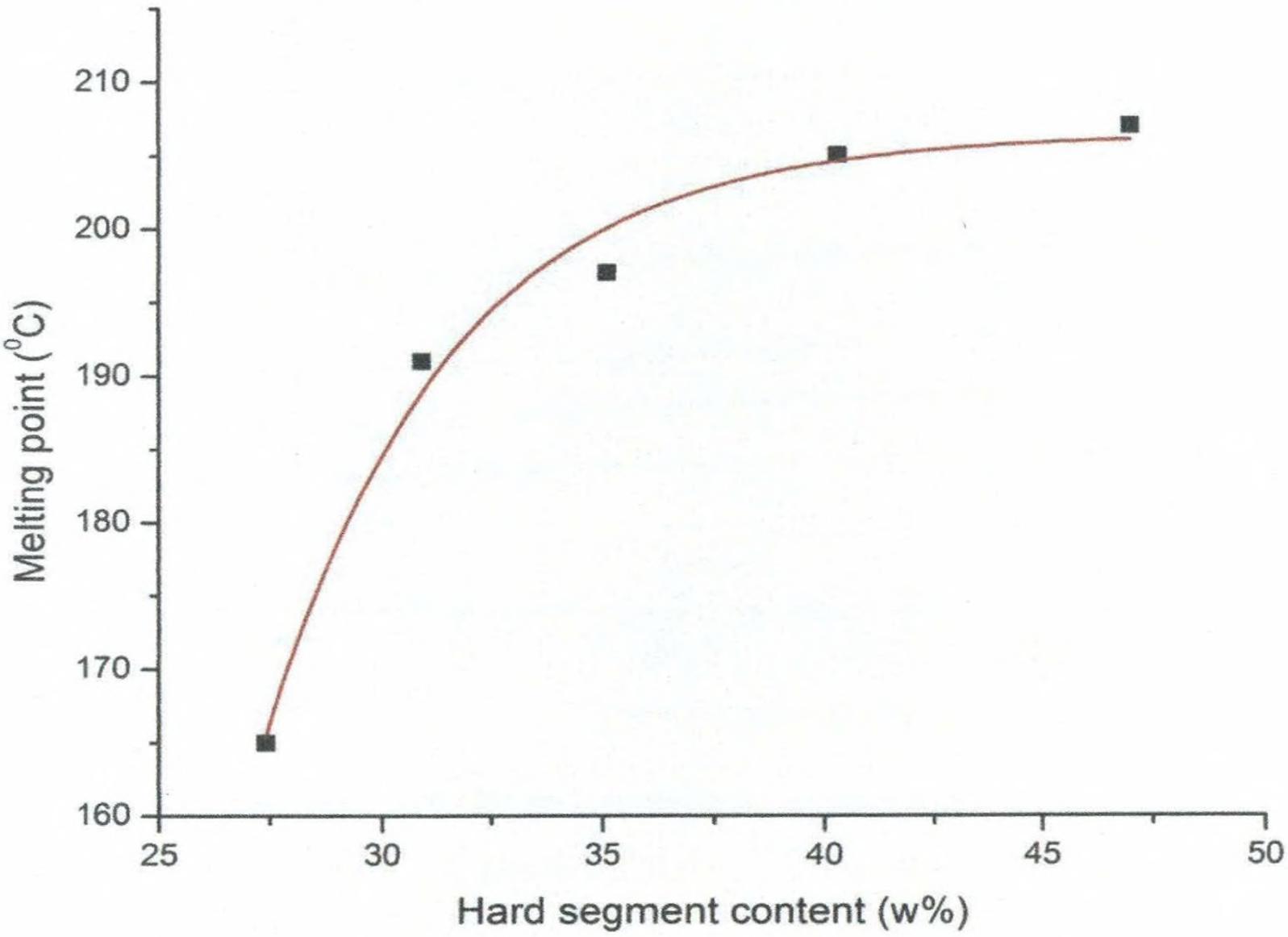

Figure 22: Variation in melting temperature compared to the hard segment content

The melting points were fitted very well to an exponential curve having the following equation with a significantly high R-square value of 0.9734.

$$y = A_1 e^{-x/t_1} + Y_0$$

Where A_1= -30742.71542, t_1 = 4.13792 and y_0 =206.40504.

The increase in hard segment content has led to an increase in melting temperature. As explained in the above section, with the increase of hard segment content there was an

increase in crystallinity. This increase in crystallinity has consequently resulted in higher melting temperatures.

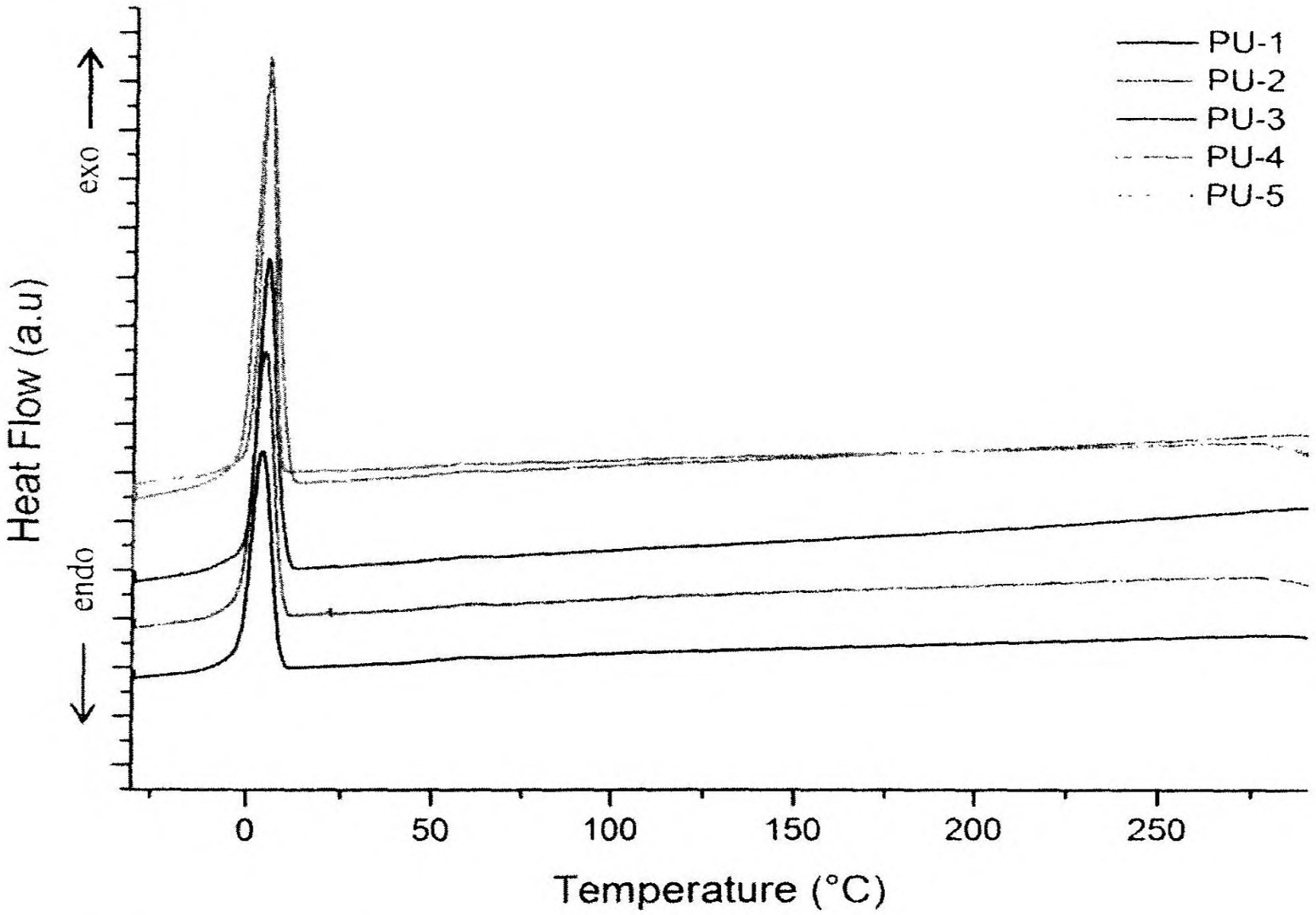

Figure 23: The cooling cycle of polyurethane films obtained from dispersions

During the slow cooling at a rate of 5 ^{0}C min^{-1}, PU samples produced a crystallization peak around 0 ^{0}C. Crystallization temperatures are almost the same. If the melted hard segments regained their crystallinity the crystallization peak should be at a higher temperature. Hence, this crystallization is definitely not related to the hard segment.

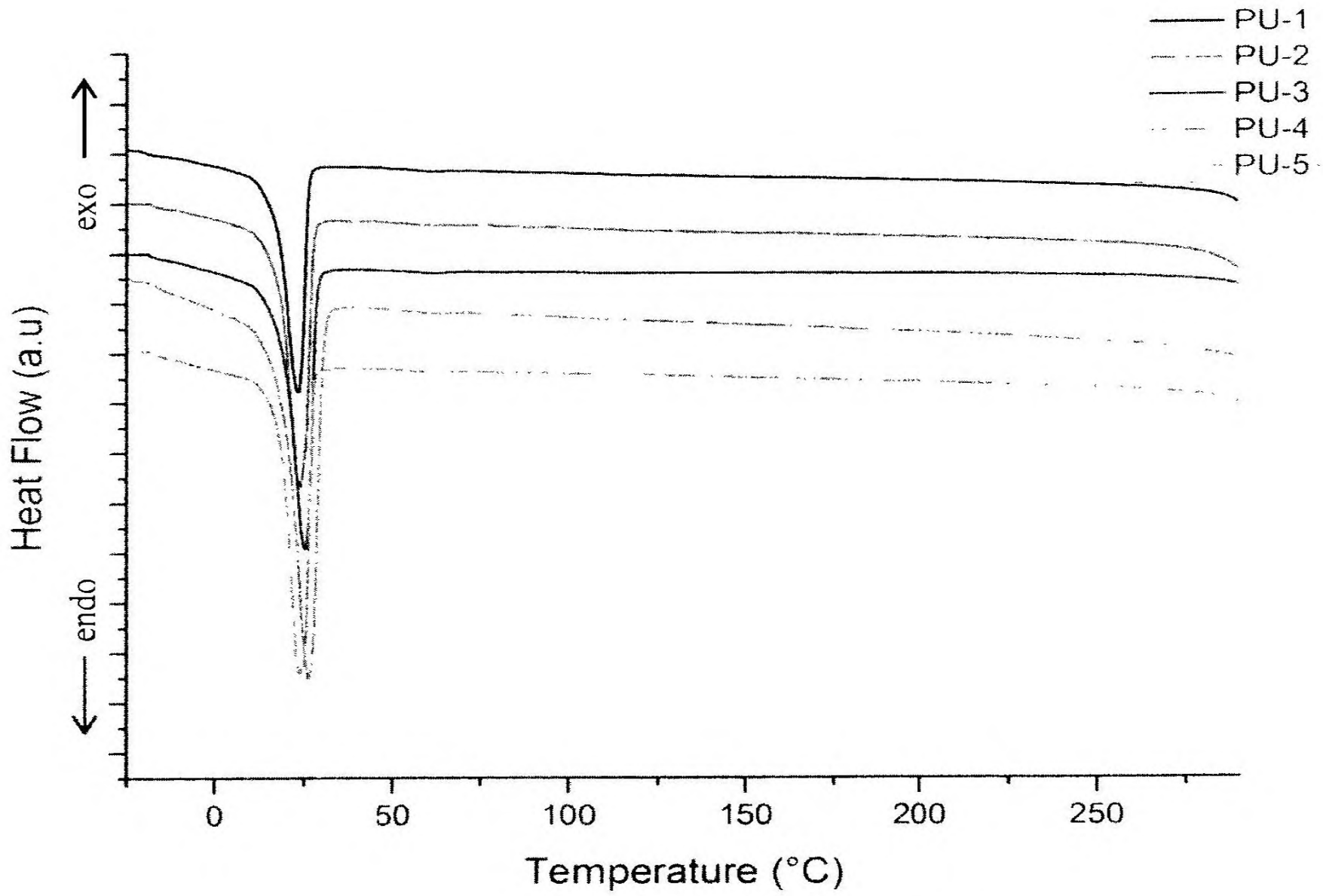

Figure 24: The second heating cycle of polyurethane films obtained from dispersions

In the second heating cycle, the peak corresponding to hard segment melting is absent. Instead there is a distinct melting peak around 25 ^{0}C. This is due to the melting of the soft segment consisting of PTHF. In the second heating cycle of MDI and PTHF based polyurethane, the disappearance of hard segment melting and appearance of soft segment melting has been observed by Mishra and coworkers too and the melting at 25 ^{0}C has been assigned to PTHF melting. (84) Hence, slow cooling of molten polyurethane at 5 ^{0}C /min leads to a micro structure of polyurethanes which is having crystalline soft segments instead of crystalline hard segments. It says that, there is an exchange in micro-structural arrangement from hard segment crystallinity to soft

segment crystallinity via the melting and re-crystallizing processes through a slow heat/cool route. In the PUD series studied in this study, it could be the fact that increase of temperature above 200^{0}C could have evaporated the counter-ion for COO^- groups presences. According to the MSDS provided by Sigma Aldrich, the DEA which acts as the counter ion has a vaporization temperature of 55 ^{0}C. In the molecular docking study carried out by Kua and co-workers, they have shown that when the positive charged ligand is replaced by a neutral ligand, the catalytic effect is reduced due to the weakening of binding. (86)

FT-IR technique can be used to collect the evidences to show these micro structural changes associated with heating/cooling processes during DSC thermogram.

The Figure 25 and Figure 26 show the CO region and NH region of the FT-IR spectra taken from the films which were obtained from the solvent evaporation after subjected to a gradual increase in temperature until it reaches to 220 ^{0}C via a DSC heating cycle which leads to hard segment melting followed by slow cooling process up to -30 ^{0}C via a DSC cooling cycle which leads to soft segment crystallization and re-heating up to 10 ^{0}C using another heating cycle. The temperature 10 ^{0}C was selected as the best suitable temperature, before crystallized soft segments start to melt, to open the DSC sample compartment.

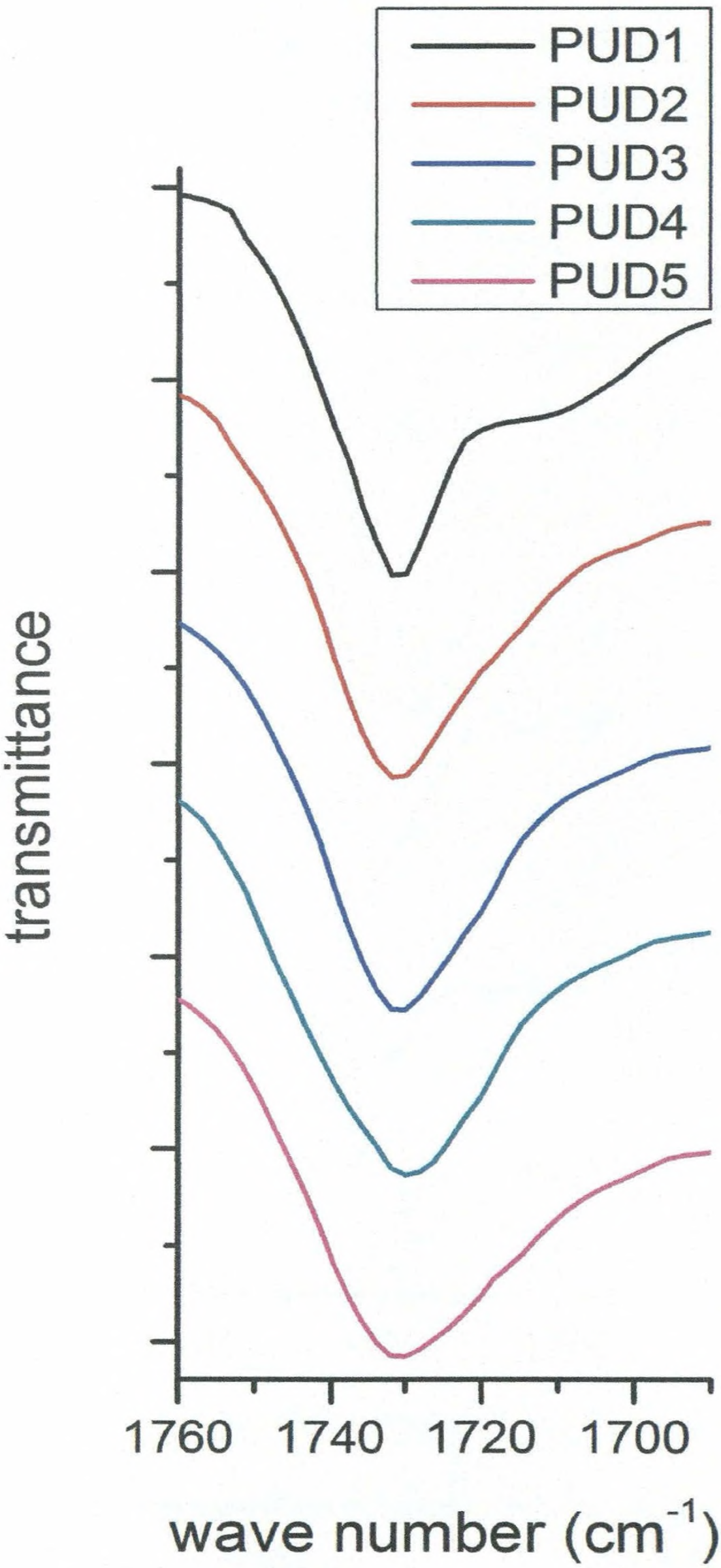

Figure 25: The C=O region of the FT-IR spectra of PUD films after the DSC profiling

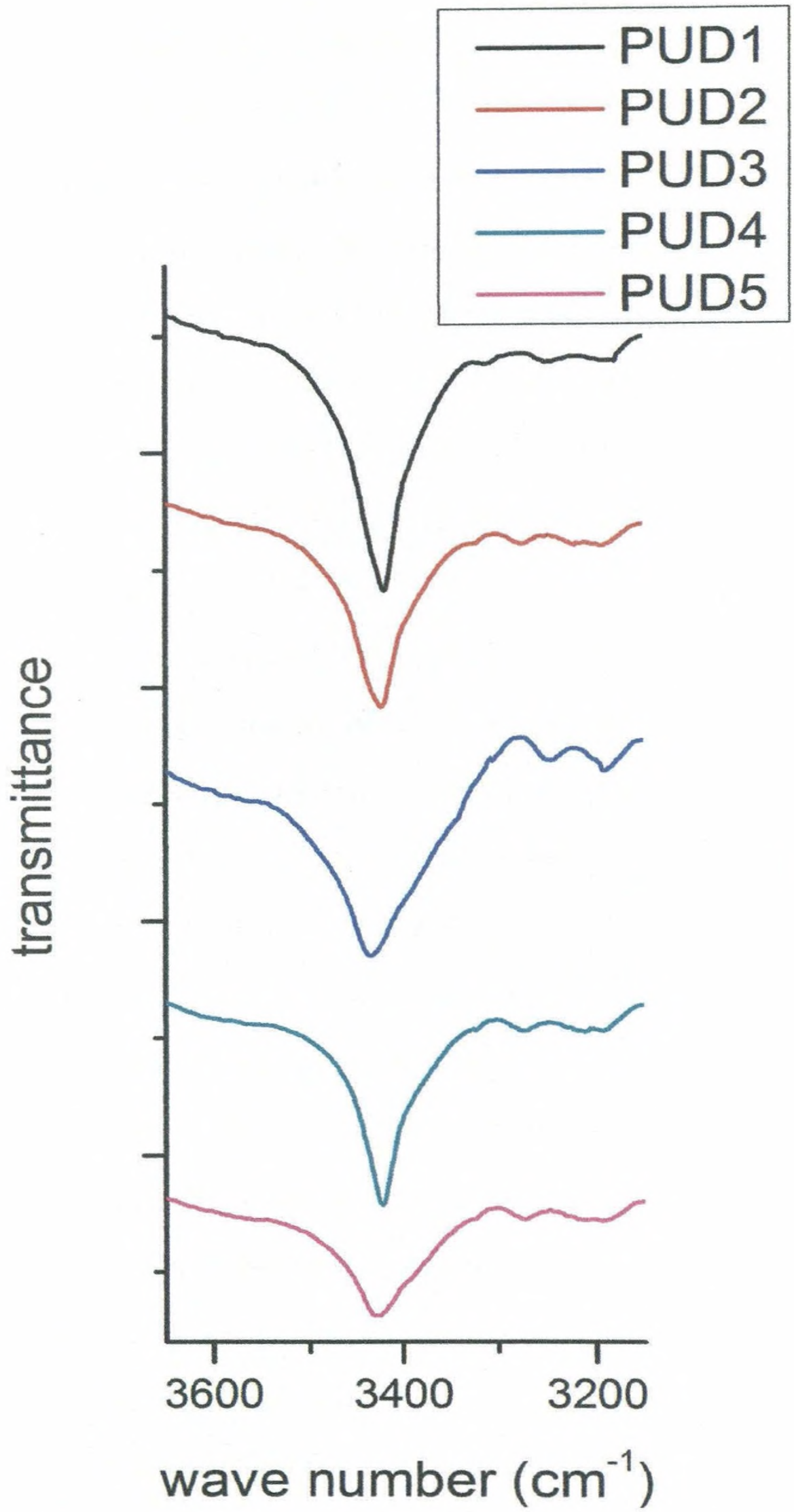

Figure 26: The N-H region of the FT-IR spectra of PUD films after the DSC profiling

When comparing those spectra (Figure 25 and Figure 26) with the spectra of the films obtained via solvent evaporation (Figure 15 and Figure 16), there is a disappearance of the hydrogen bonded NH and carbonyl peaks with an increase of the intensity of free NH and carbonyl peaks. The replacement of hard segment crystallinity by soft segment crystallinity after the slow heating/cooling process occurring during the DSC recording, can be well explained through this diminishment in the H bonded peaks and the growth in the free peaks of both carbonyl and NH bonds. When microstructure converts to soft segment crystallinity those hydrogen bonds are destroyed and hence H bonded peaks are diminished.

Therefore, the required microstructure of polyurethane solid can be achieved by the method of preparation of PUD films. If the crystalline hard segment based polyurethanes are needed, it can be obtained by evaporating the solvent. If the crystalline soft segment based polyurethanes are required, by melting the former and slow back cooling, they can be converted to crystalline soft segment based polyurethane.

4.4.3.2 Film from polyurethane prepolymer (PUP-3 film)

Thermal properties of the polyurethane prepolymer film were analyzed using DSC thermograms. Both heating cycles (first heating cycle and second heating cycle) showed a single melting peak at comparatively low temperatures. In both case the melting peak is located around 25 ^{0}C. The DSC thermograms of first and second heating cycles are shown in Figure 27 and Figure 28, respectively. During the cooling cycle which proceeded in between these two heating cycles, a crystallization peak was observed at a temperature somewhat lower than the melting temperature. As shown in Figure 29, it was around 10 ^{0}C. The appearance of this crystallization peak closure to the melting

peak and at lower temperature compared to the melting temperature suggests that it corresponds to the crystallization of the species which melted during the first heating cycle. It was proven by the re-appearance of the melting peak in the second heating cycle around 25 ^{0}C which was similar to first heating cycle melting peak. It implies that the component which is melted in first heating cycle, re-crystallized during the cooling cycle and it melted again during the second heating cycle.

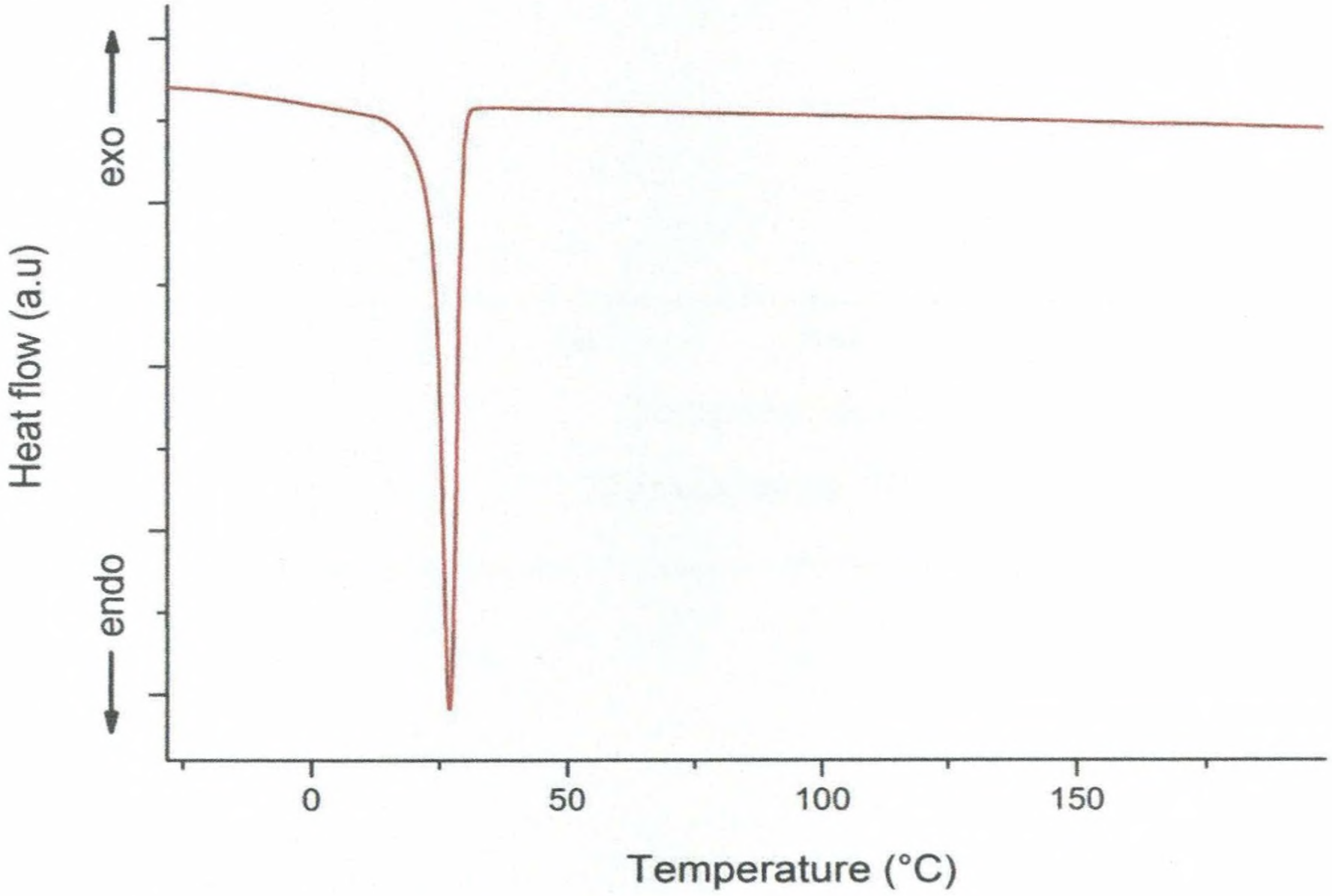

Figure 27: The first heating cycle of the polyurethane prepolymer (PUP-3) film

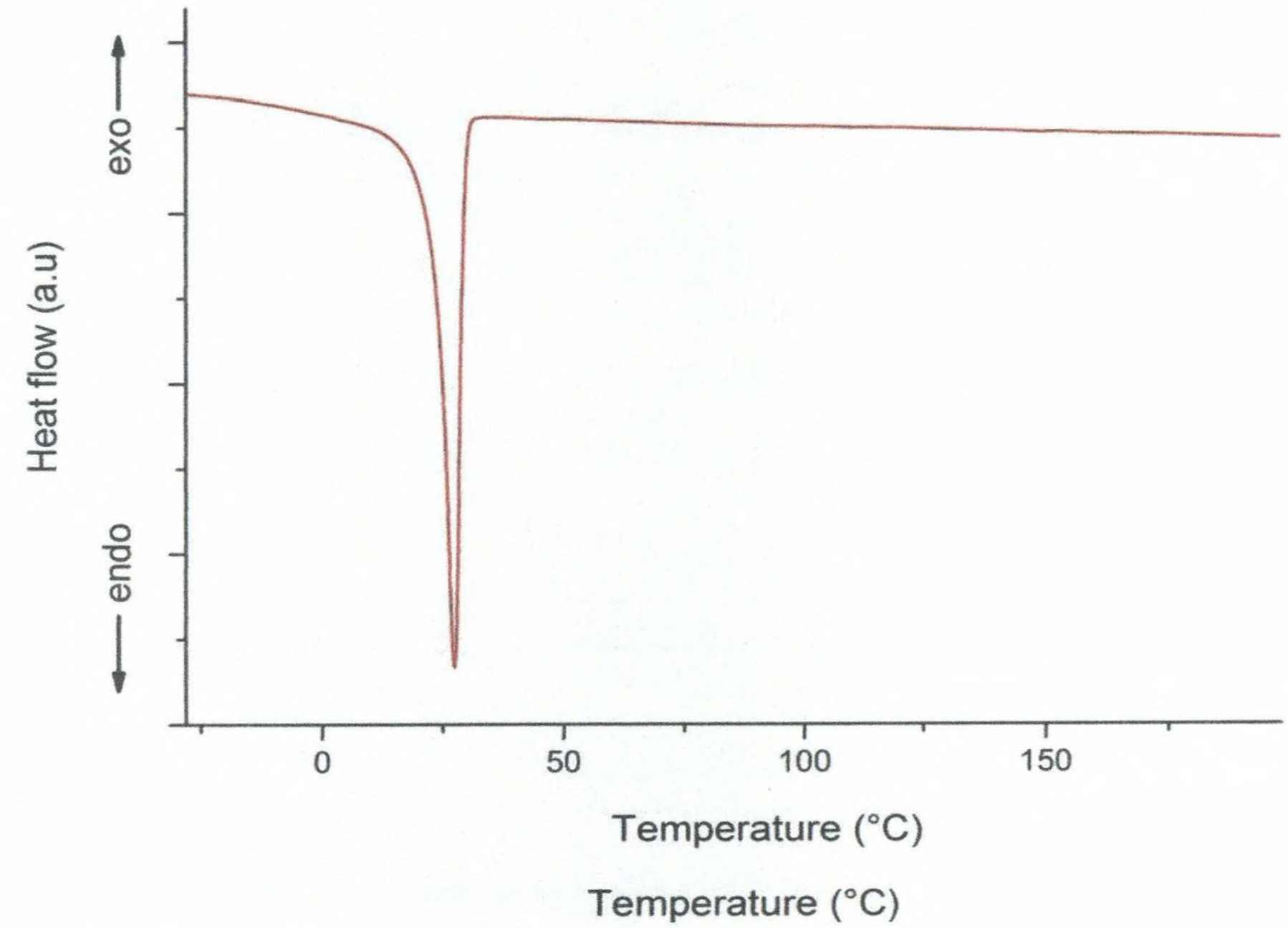

Figure 28: The second heating cycle of polyurethane prepolymer (PUP-3) film

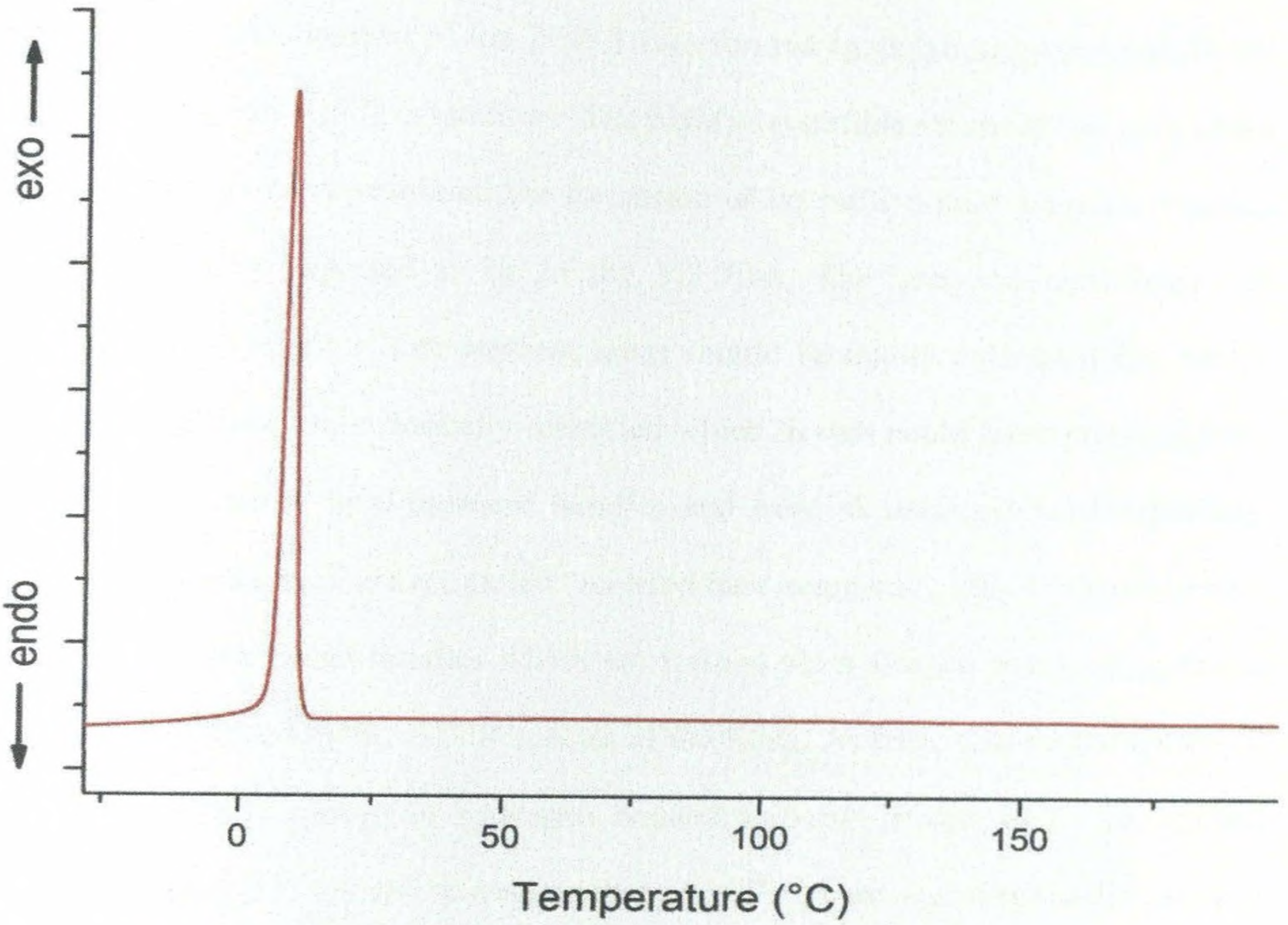

Figure 29: The cooling cycle of the polyurethane prepolymer (PUP-3) film

The DSC analysis of the polyurethane prepolymer film showed that the PUP-3 film had a crystalline melting peak around 25 ^{0}C. The absence of an exothermic peak (T_c) before the melting endotherm (T_m) showed that the material had reached the highest possible crystallinity. As crystalline melting of PU hard segments generally occurs above 150 ^{0}C, this cannot be due to hard segment melting. According to literature, melting of PTHF components in polyurethanes can be observed around 25 ^{0}C. (84,95) Hence, the melting endotherm of the DSC can be assigned to the crystalline melting of soft segment which consists of polytetrahydrofuran. The XRD results which were discussed in the section 4.4.1.2 also showed the presence of crystalline soft segments in the PUP-3 film. The long chain polytetrahydrofuran occupies a large volume in the polymer and would produce highly crystalline areas. The absence of a glass transition in the thermogram

confirms that the soft segment of the PUP-3 film formed by polytetrahydrofuran is not randomly oriented but highly crystalline. The highly crystalline nature of the long chain soft segments might have restricted the formation of crystalline hard segment bundles which are generally expected to be in the PU film. The unbound hard segments embedded in the crystalline soft segment areas should be highly entangled and hence hydrogen bond formation is sterically restricted which in turn could have prevented the formation of crystalline hard segment bundles and exist as unbound hard segments. These unbound hard segments are called "isolated hard segments". (96,97) The absence of crystalline hard segment bundles which are formed via hydrogen bonds at urethane linkages was confirmed by the FT-IR spectra of the films. As there was no indication of hydrogen bonded NH groups or hydrogen bonded carbonyl groups in FT-IR spectra (Figure 19 & Figure 20) it is fair to assume that crystalline hard segment bundles are not available in the polyurethane prepolymer film. According to these observations, PUP-3 film has a microstructure consisting of randomly trapped isolated hard segments with in the highly crystalline soft segment matrix.

4.4.4 UV absorbance properties of polyurethane films

4.4.4.1 Films from polyurethane dispersions (PUD films)

To deal with optical properties of polyurethanes, it is important to know their absorption ranges in the UV- visible light and the absorption maximum (λ_{max}). To get a better understanding about the UV absorbance behavior of PUD films, their absorption spectra were recorded. Overlay of the absorption spectra of five PUD films is shown in the Figure 30.

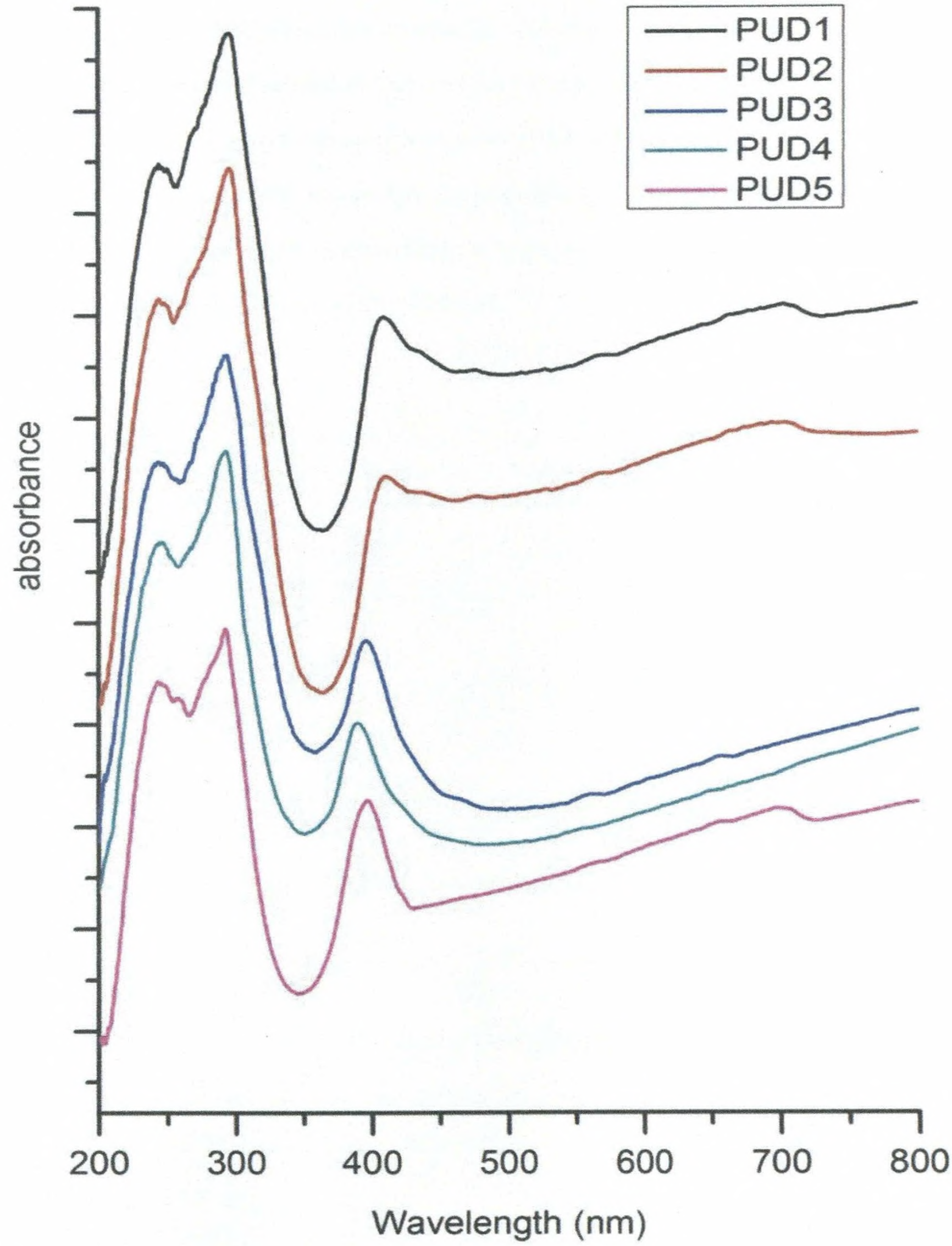

Figure 30: The UV absorption spectra of PUD films

According to the UV absorption spectra, it was able to conclude that the strongest absorbance is observed around 293 nm and the 293 nm was considered as λ_{max}.

4.4.4.2 Film from polyurethane prepolymer (PUP-3 film)

In order to determine the wavelength corresponding to absorption maximum (λ_{max}), absorption spectrum of the polyurethane prepolymer PUP-3 film was obtained. The absorption spectrum is shown in the Figure 31.

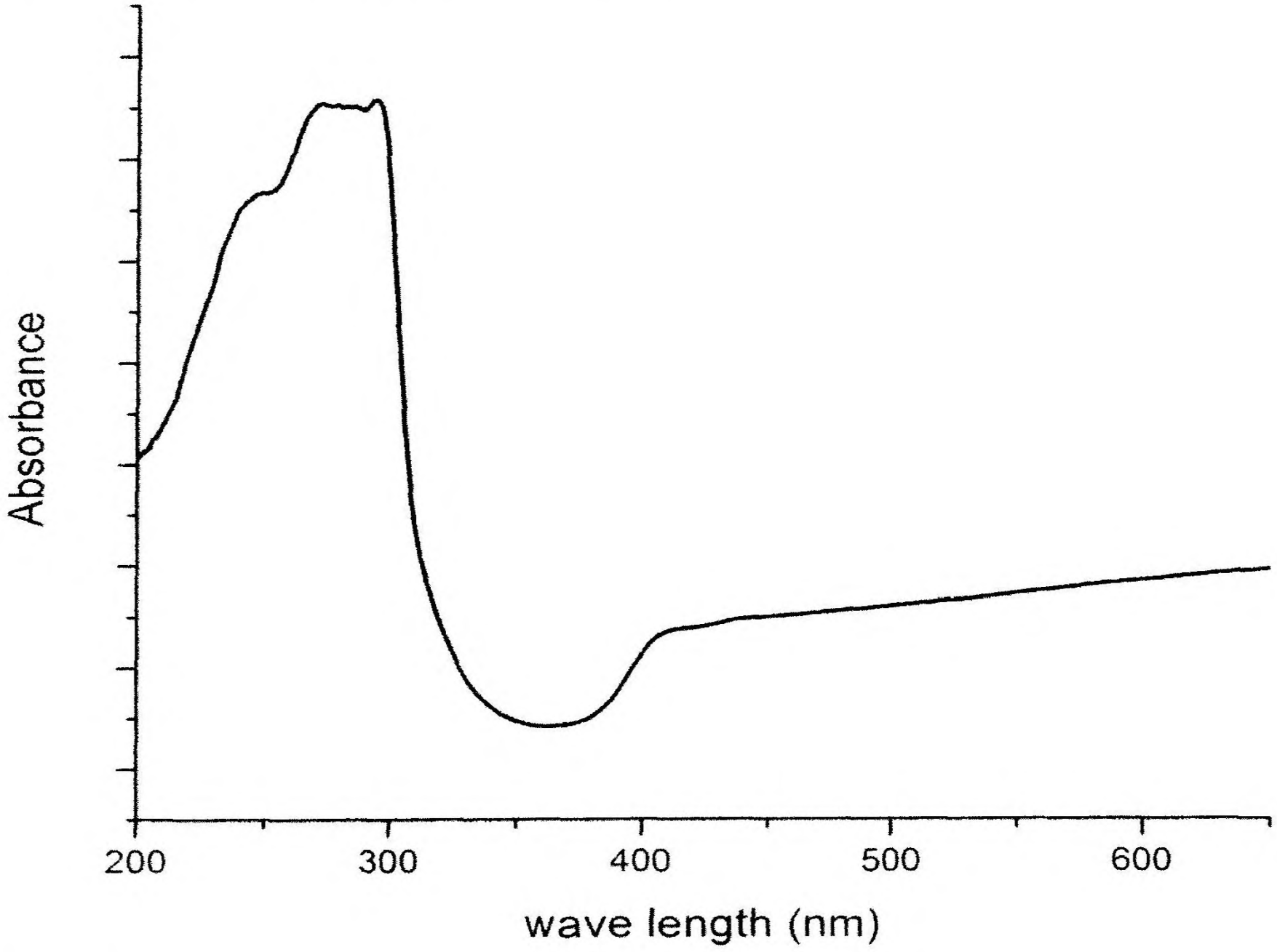

Figure 31: The UV absorption spectrum of the polyurethane prepolymer PUP-3 film

It was shown that PUP-3 film has an absorption maximum in the UV range and λ_{max} is located close to 293 nm.

4.4.5 Photo properties of polyurethane films; Fluorescence

Emission spectra of the polyurethanes were recorded while exciting the samples at 293 nm. The excitation wavelength was decided according to the UV- absorption spectra of the polyurethanes. Absorption maximum for both PUP-3 and PUD films was located around a single wavelength. The wavelength corresponding to absorption maximum was 293 nm, and hence it was selected as the excitation wavelength.

Initial emission spectra

Films from polyurethane dispersions (PUD films)

The initial emission spectra of five PUD films showed two peaks around 356 nm and around 423 nm. Both peaks were considerably broad however second peak was broader than first peak. The initial emission spectra of five PUD films are shown in Figure 32.

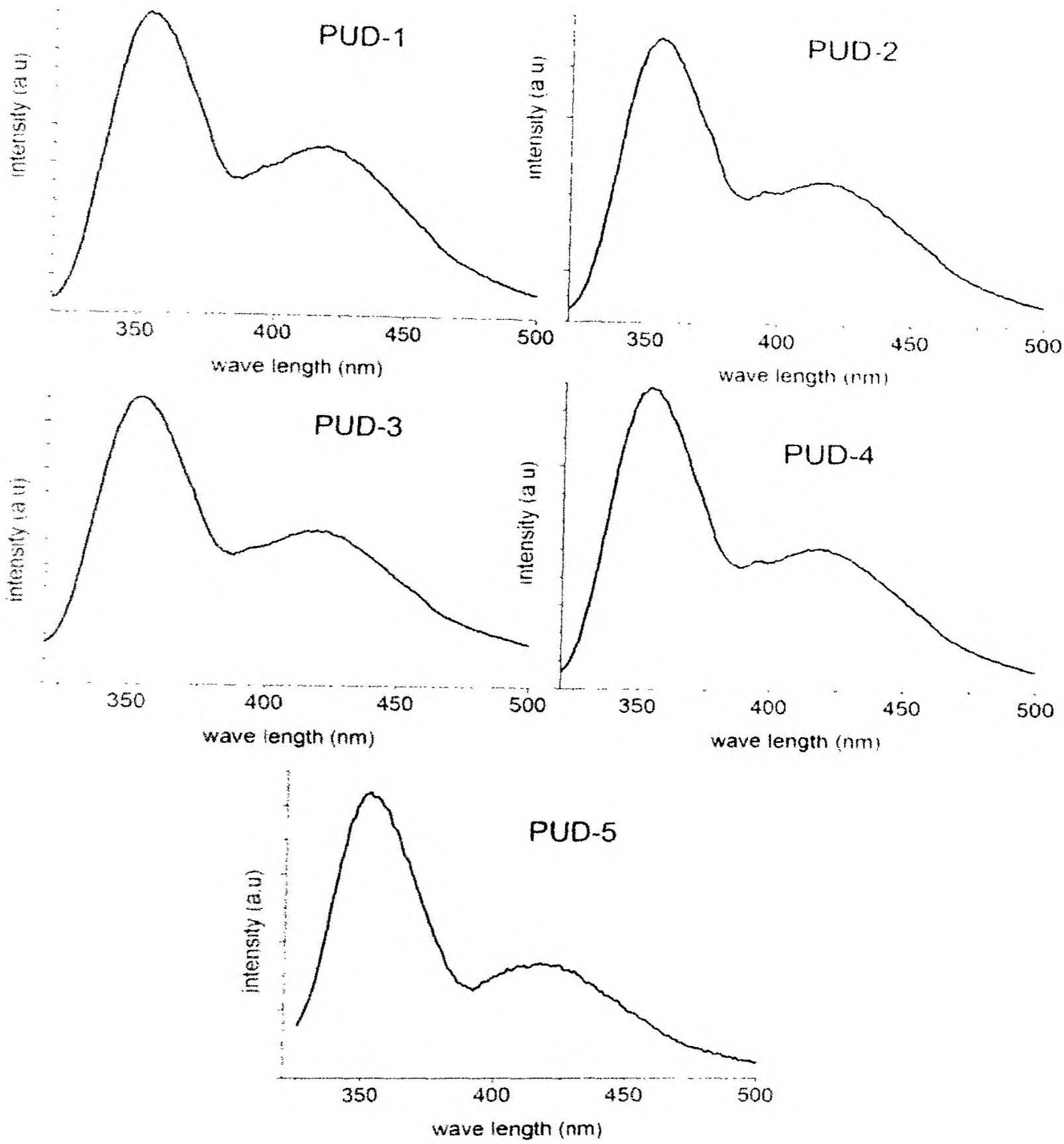

Figure 32: Initial fluorescence emission spectra of the five PUD films

Even though the patterns are similar, relative intensities of the peaks were varied with the hard segment content. The relative intensity of second peak compared to the first peak was calculated via the second peak intensity/first peak intensity ratio. As shown in Figure 33, the second peak intensity/first peak intensity ratio was increased with increased hard segment content.

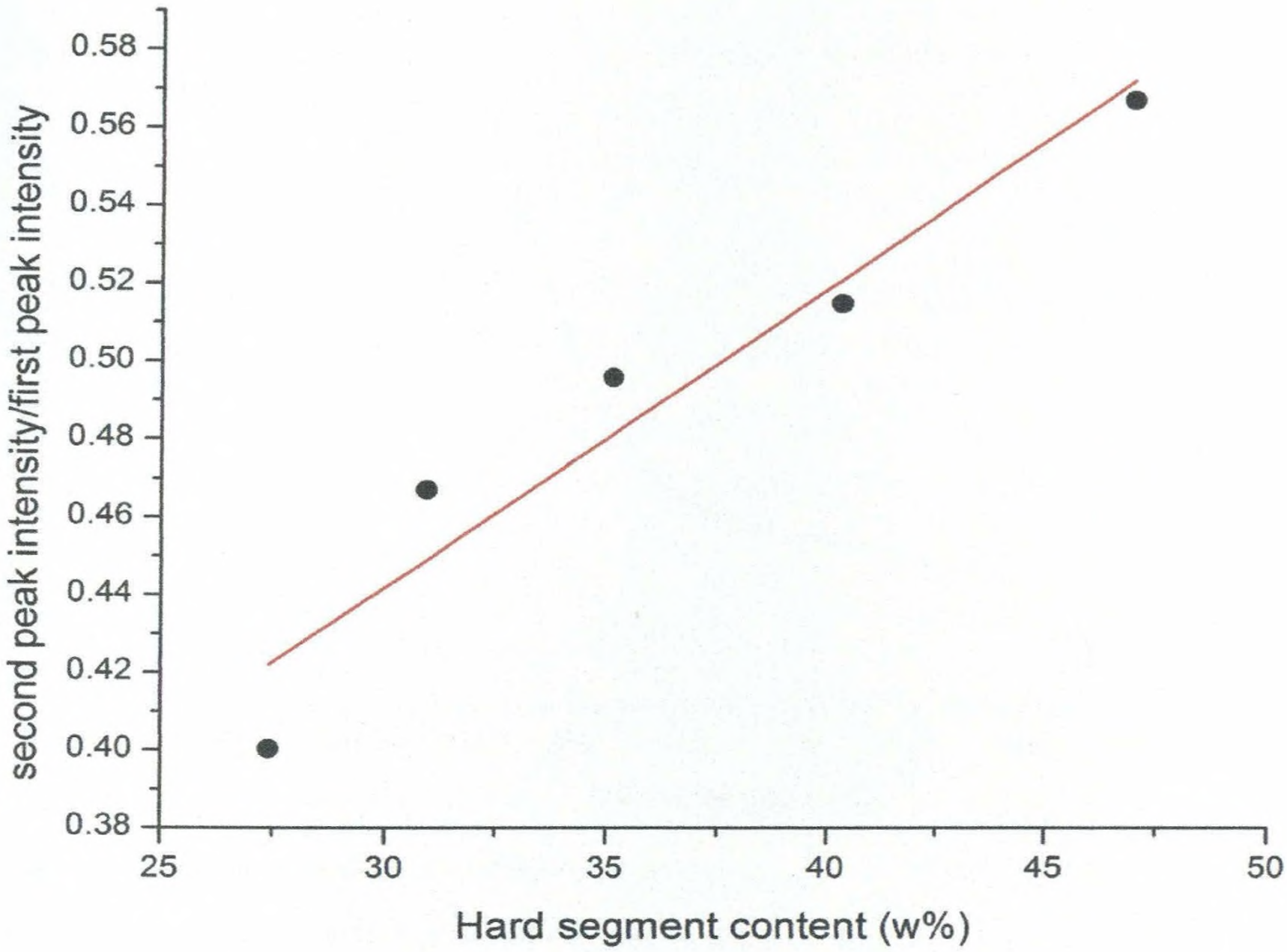

Figure 33: The variation in second peak/ first peak intensity ratio with respect to hard segment content

The data points were fitted to a straight line having the following equation with a significantly high R-square value of 0.9053.

$$y = a + bx$$

Where a = 0.21243 and b = 0.00765.

Film from polyurethane prepolymer (PUP-3 film)

Initial emission spectrum of PUP-3 film was differed from the emission spectra of PUD films. Instead of two peaks there was only a single peak in the initial emission spectrum of PUP-3 film. It was also a somewhat broad peak which is located at 356 nm (Figure 34). This peak was fit on to the lower wavelength peak among the two peaks observed for PUD films.

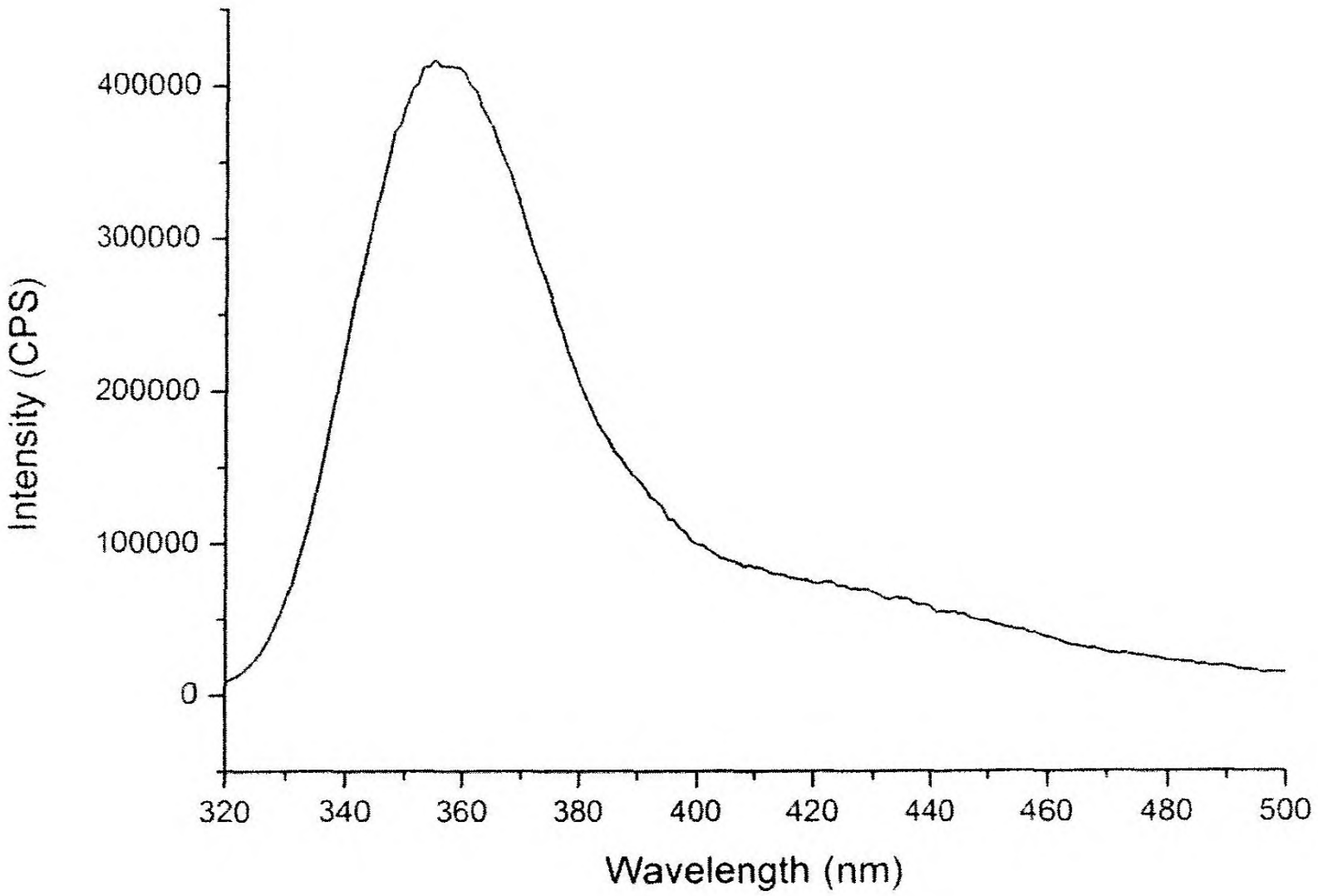

Figure 34: The initial emission spectrum of the PUP-3 film

Comparison, discussion & interpretations

Among the observed results two main observations can be highlighted. First one is PUP-3 does not show the second peak which was observed in PUD spectra. Secondly the relative intensity of second peak was increased with hard segment content. When the microstructures of PUP-3 and PUD films were considered, there was a significant difference. In the PUP-3 film there was a highly crystalline soft segment matrix which does not allow to hard segments to form crystalline hard segment bundles. In other words crystalline hard segment bundles were not available in PUP-3 film. In contrast to PUP-3 film, all the PUD films had a crystalline hard segment bundles. PUP-3 film which does not have crystalline hard segment bundles does not show the second peak around 423 nm while all the PUD films which have crystalline hard segment bundles have a second peak around 423 nm. Hence, it can be assumed that the second peak is generating due to crystalline hard segment bundles. The weight of this assumption is

enhanced by the secondly highlighted observation. It was shown in an afore section that the extent of hard segment crystallinity is increased with the increase of the hard segment content. According to that, it is clear that the relative intensity of the second peak is increased with the increase of crystalline hard segment bundles. Hence, it can be concluded that the second peak is most probably from crystalline hard segment bundles. Now it is important to investigate about the peak at 356 nm and to understand about the fluorophores.

Even though there is a possibility of the appearance of the fluorophore only after the polymerization, most probably it can be originated from a fraction of the structures of reactants which were used during the polymerization. In order to get an idea about the origin of the fluorophores, fluorescence spectra of reactants were recorded. The emission spectra of reactants DMAc, DABCO, PTHF, and MDI are shown below.

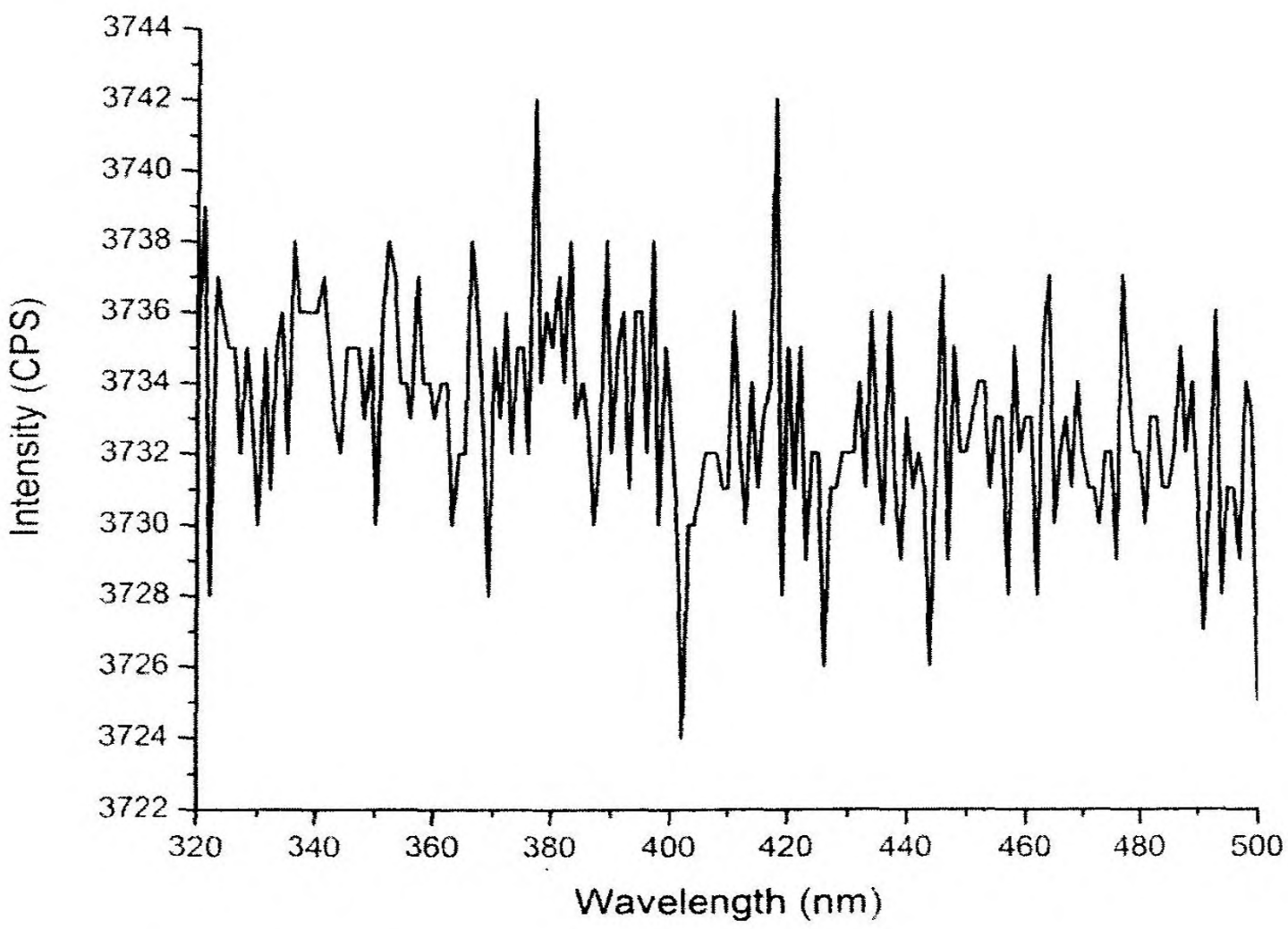

Figure 35: The emission spectrum of DMAc

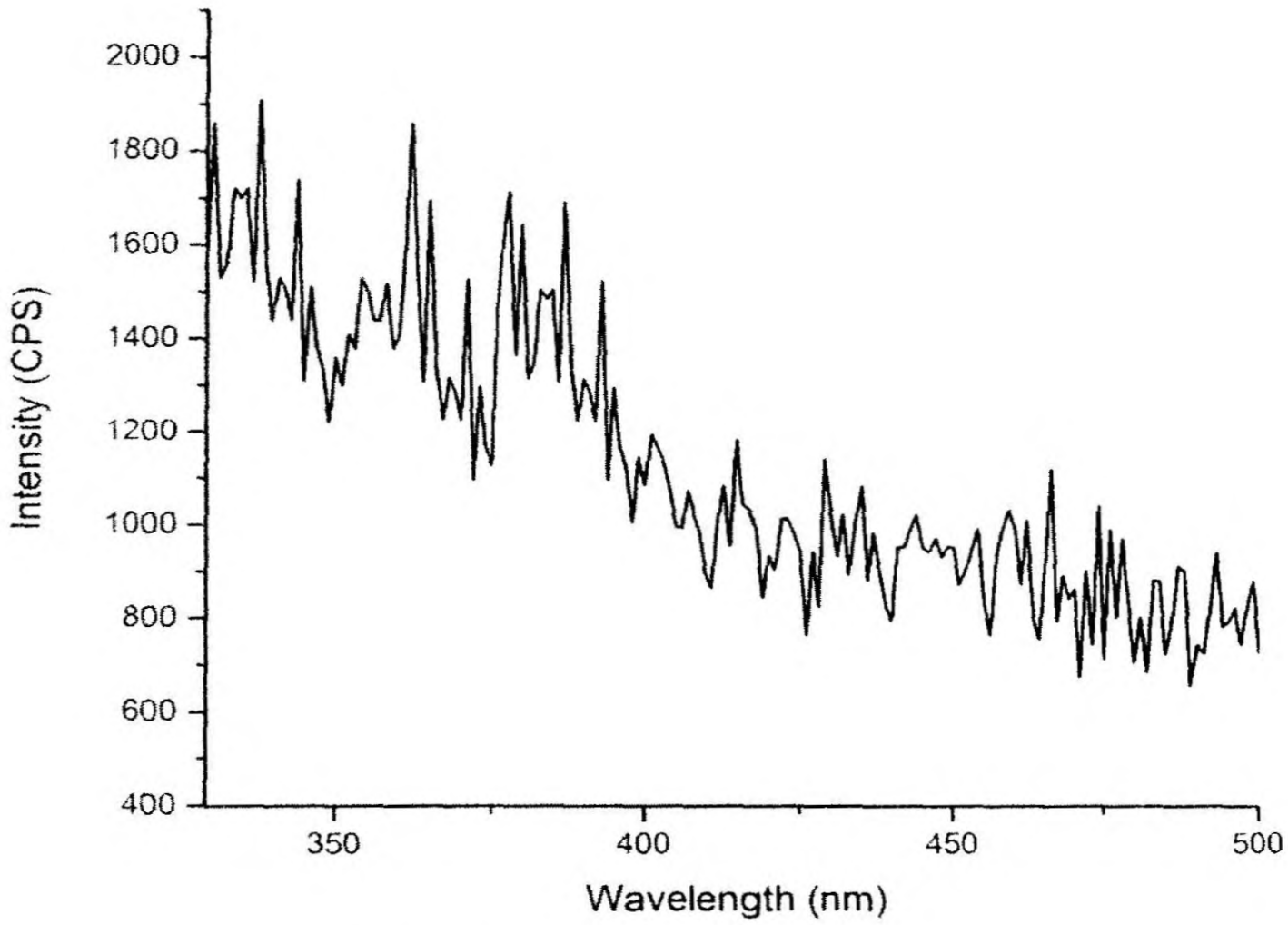

Figure 36: The emission spectrum of DABCO

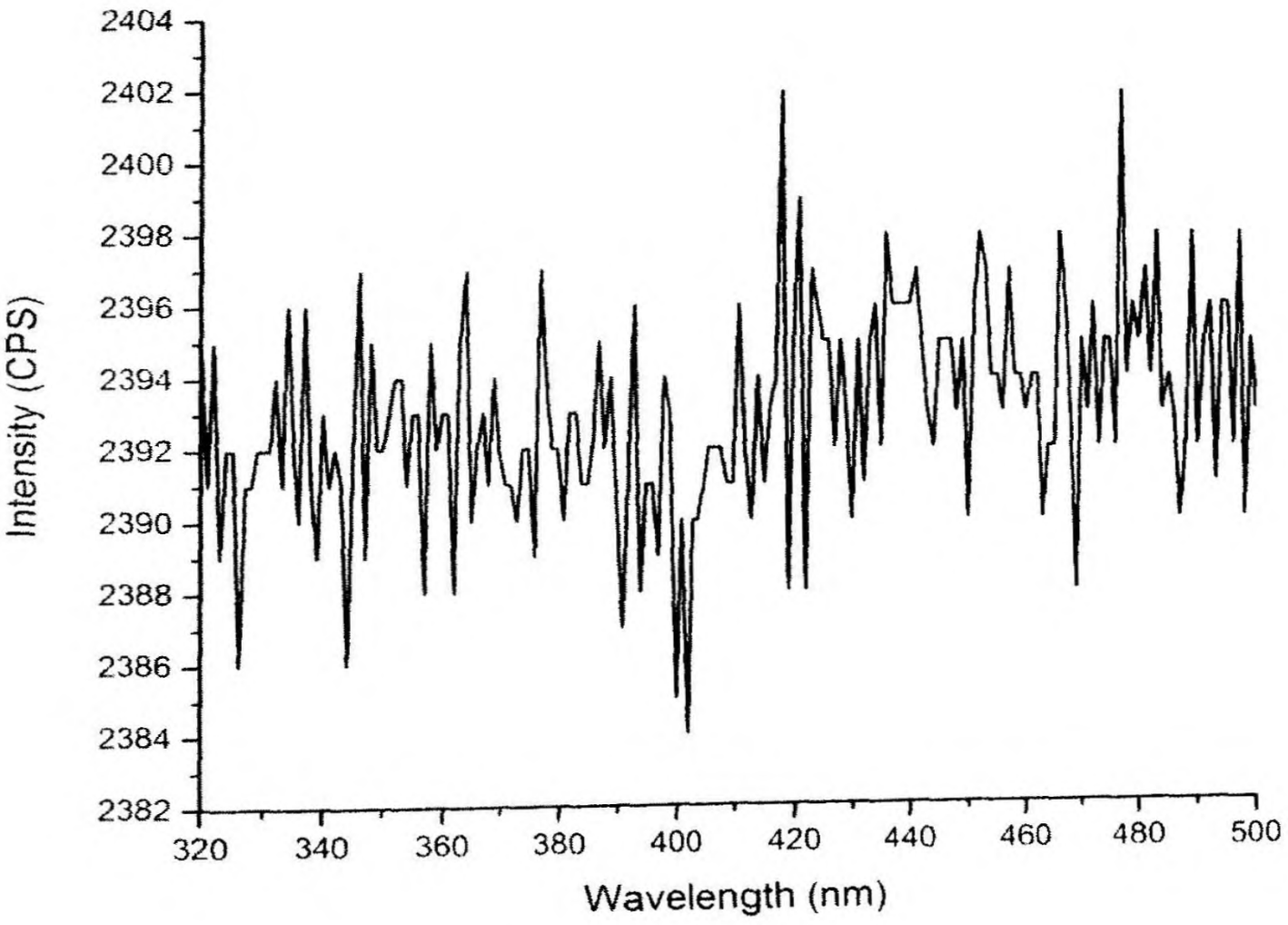

Figure 37: The emission spectrum of PTHF

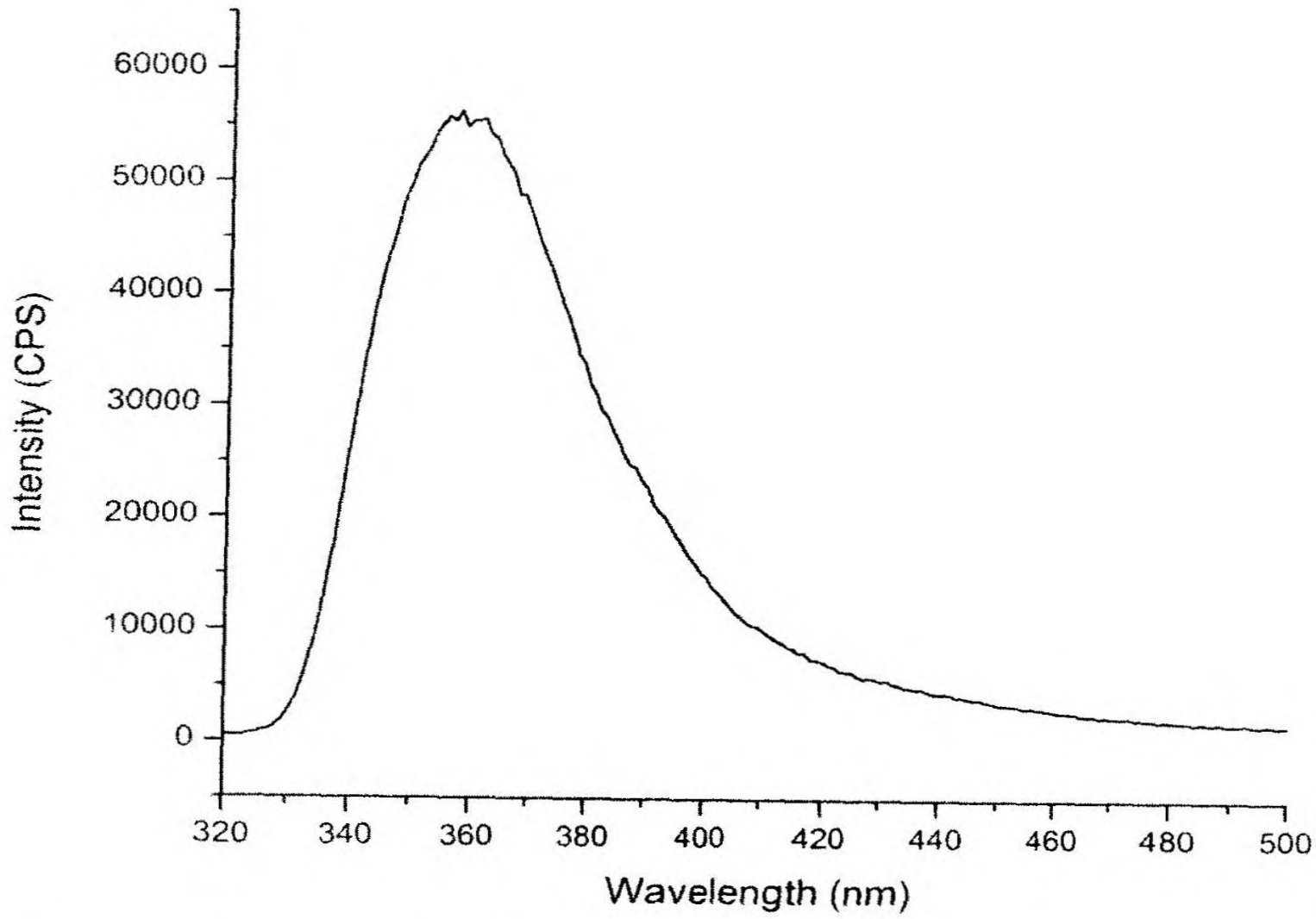

Figure 38: The emission spectrum of MDI

It was clear that a component in the structure of MDI is responsible for the 356 nm emission and none of other reactants contribute to the emissions. There is a possibility that the observed fluorescence is due the unreacted MDI in the PU films. In PUP-3, MDI was the limiting agent. As MDI:PTHF molar ratio in the prepolymer PUP-3 is 1:2 and MDI is highly reactive, it is reasonable to assume that unreacted MDI in the solvent based system would be remote. As the 356 nm peak is observed in this PUP-3 film as well, the 356 nm emitters are most probably occupied in the MDI components in the polyurethane chains. According to the design of the polyurethane chains, the MDI component is occupied in the hard segment section. As explained in the section of the crystallinity of polyurethanes, PUP-3 only consists of isolated hard segments in such a way crystalline hard segments are absent. As PUP-3 shows the 356 nm emission and MDI structure within the PUP-3 is only available as isolated hard segments, it can be concluded that 356 nm emitters are from isolated hard segments. In addition to

crystalline hard segment bundles, isolated hard segments are also available in PUD films. It was explained in the above with the help of FT-IR data. Hence, the appearance of 356 nm peak which are emanated from isolated hard segments in PUD films is also feasible. In addition to the theoretical requirement; the highly reactive limiting agent MDI must not be available in the system, extended analysis of fluorescence behavior of polyurethane films and MDI experimentally proved that the 356 nm peak observed in polyurethanes is not due to unreacted MDI. The variation of emission spectra with the continuous exposure to 293 nm wavelength was studied.

Variation of emission spectra with the continuous exposure to 293 nm

Films from polyurethane dispersions (PUD films)

When the emission spectrum of each PUD film was continuously and repeatedly recorded, there was a variation in the intensities of two peaks. The 356 nm peak intensity was reduced while that of the 423 nm peak was increased. The variation in spectra of five PUD systems with number of repeats is shown in the Figure 39.

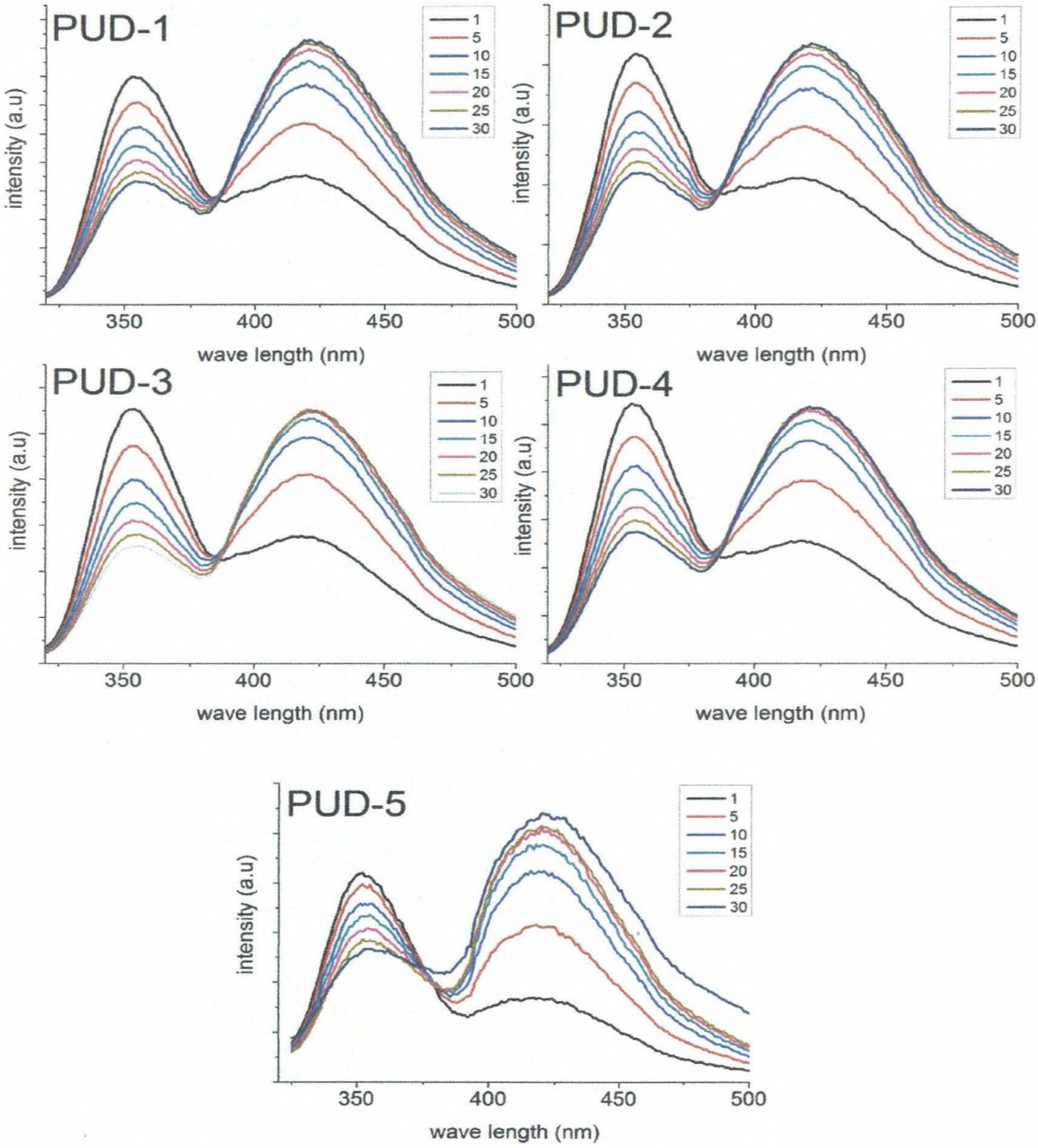

Figure 39: Spectral variation of five PUD films with exposure time (number of repeats)

How it happens will be explained after addressing the behavior of PUP-3 and MDI emission spectra with respect to repeated recordings.

Film from polyurethane prepolymer (PUP-3 film)

Similar to the PUD films, it was observed that with the repeated recordings there were changes in spectrum of from PUP-3 film. There was a reduction in intensity of the initially observed peak at 356 nm and the appearance of a new peak and growth of its intensity with continuous repeats. It is important to notice that the new peak was appeared at 423 nm on the same position where the second peak (higher wavelength peak) of PUD films was located. The variation in spectrums with number of repeats is shown below.

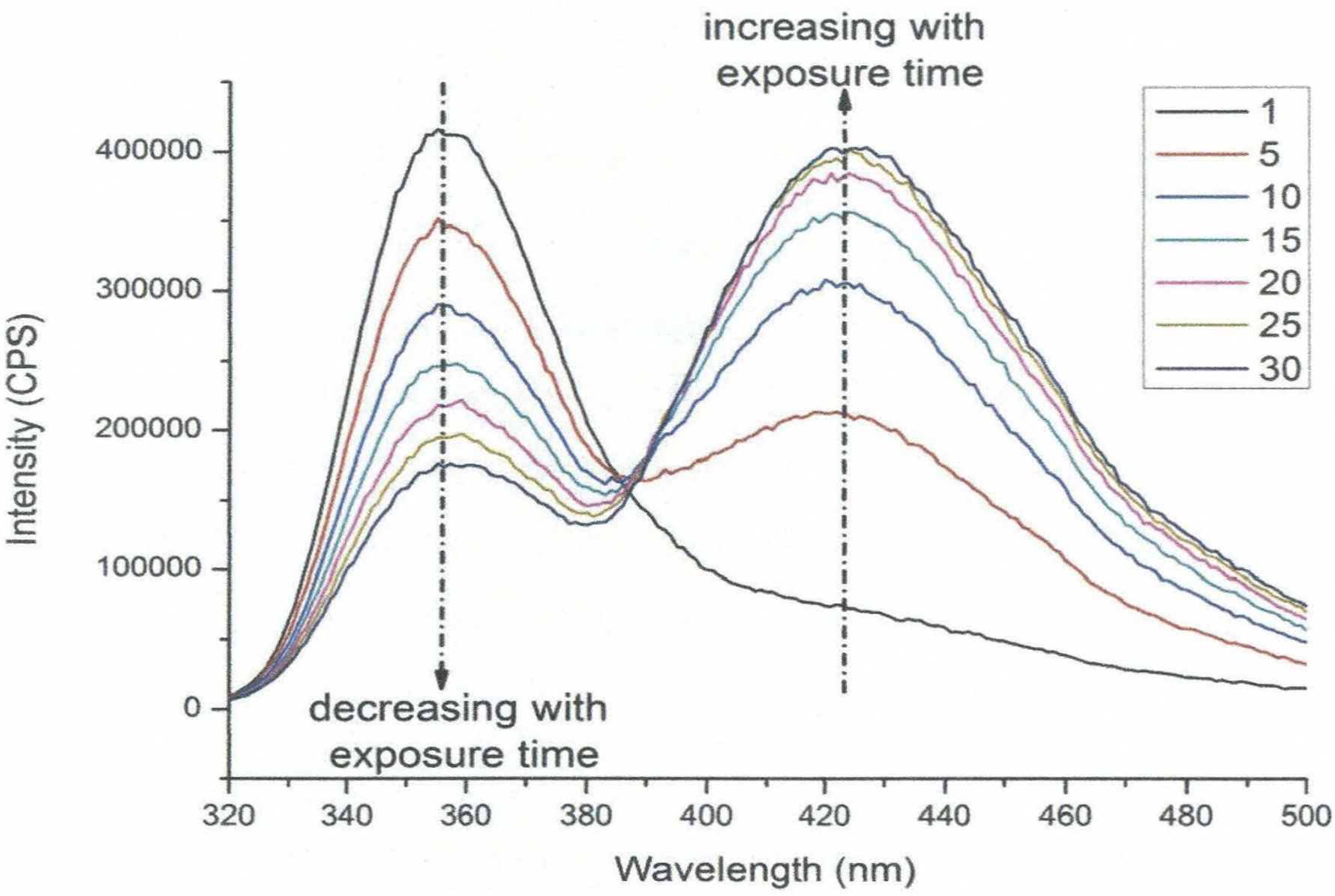

Figure 40: Variation of emission spectrum of the PUP-3 film with number of repeats

It was shown that the first peak which was at 356 nm was reduced with the number of repeats and a second peak was appeared at 423 nm whose intensity increased parallel to the decrease in the intensity of the first peak. Variation of the intensities in the two peaks is shown in the Figure 41.

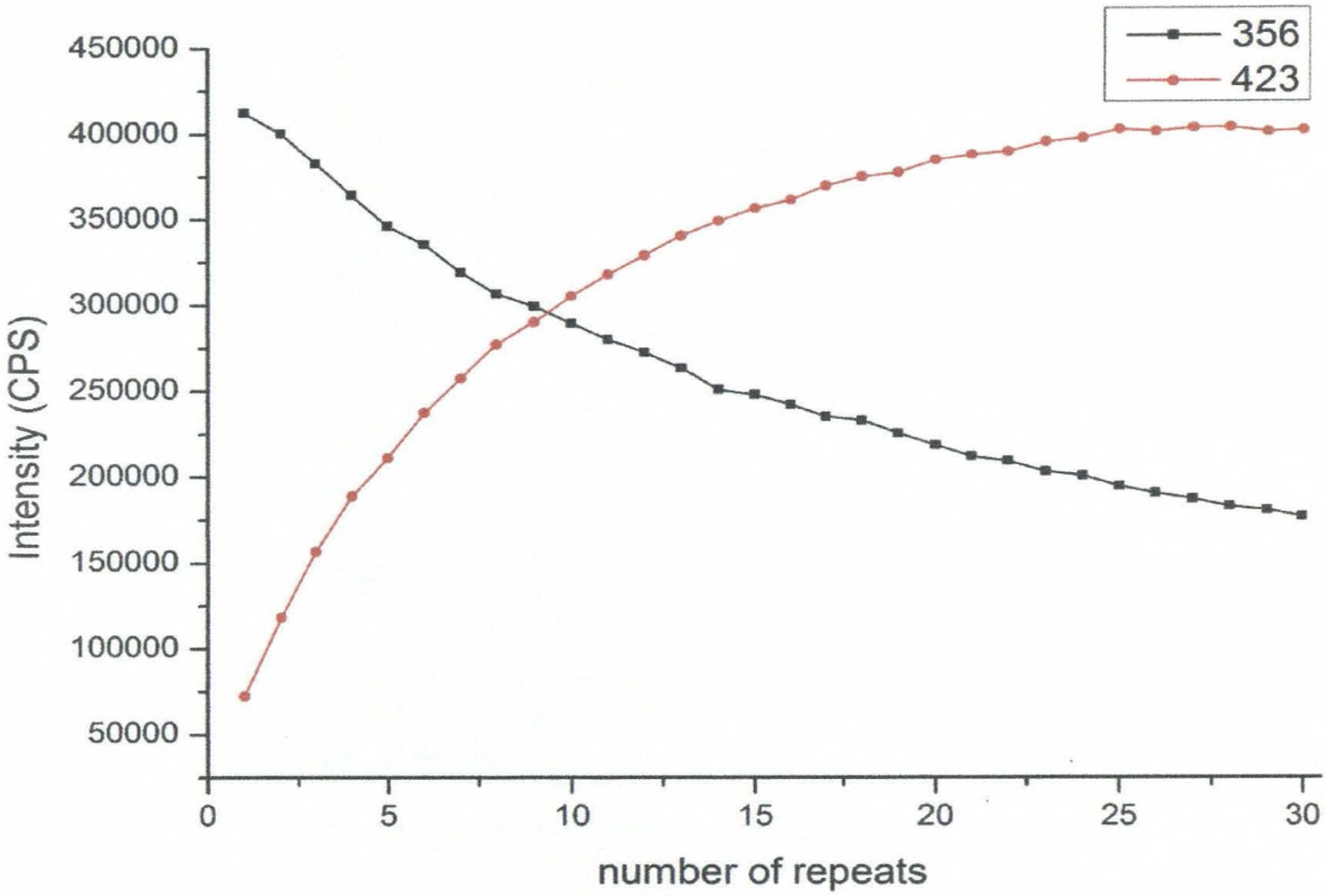

Figure 41: Variation of two peak intensities of PUP-3 film

Figure 41 indicates that, the intensity of the peak at 356 nm is reduced while that of the peak at 423 nm is increased. The extent of the reduction and the increase was reduced as the number of repeats increased. At initial repeats differences in intensities were high and at the later repeats the difference was very low.

MDI

In contrast to polyurethane films, MDI emission signal did not show any change in the shape of the spectrum with repeated recordings. The comparison of emission spectra of MDI in the first and tenth repeat is shown in Figure 42.

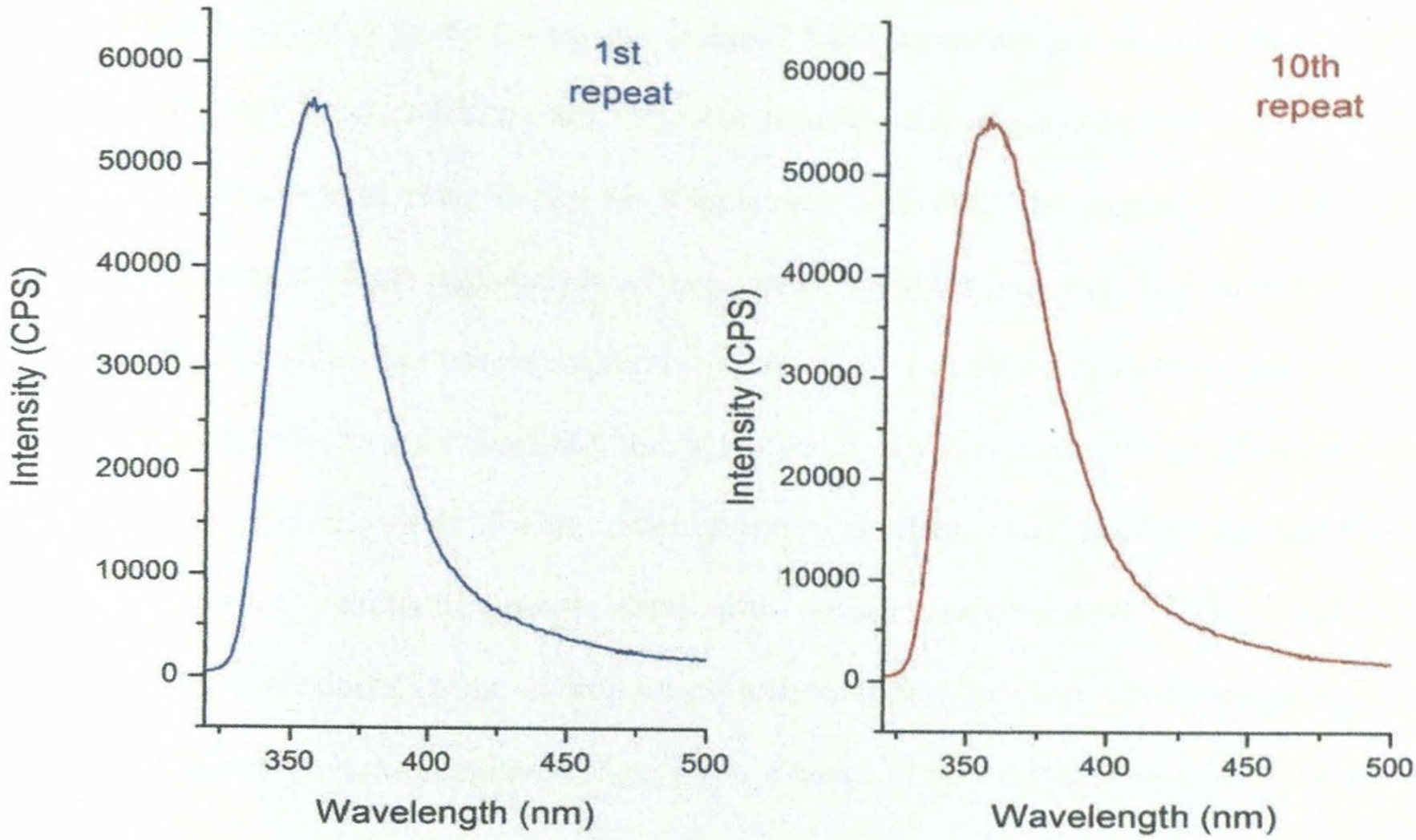

Figure 42: The comparison of emission spectra of MDI

Comparison, discussion & interpretations

With the number of repeats, only the exposure time to the 293 nm wavelength is varied which becomes higher with number of repeats. Each scan can be accounted as a 30 s exposure to the 293 nm wave length.

A smooth decrease of intensity of the 356 nm emission with increasing exposure to 293 nm and a simultaneous increase of the intensity of the peak at the 423 nm was observed in both PUD films and PUP-3 film. However, the exposure of MDI to 293 nm light did not produce a significant change in the emission at 356 nm compared to changes observed in the spectra for PU films. By comparing the fluorescence behaviors shown by MDI and polyurethane films, it could be able to experimentally prove that the 356 nm peak had emanated from the hard segments of the polyurethane which contained the fluorophores originating from MDI but not from the free MDI.

As explained earlier it is clear that the isolated hard segments are responsible for the 356 nm peak while crystalline hard segment bundles are responsible for the 423 nm peak. In accordance to that, it can be simply say that with the exposure to 293 nm wavelength isolated hard segments has been joined together and has formed crystalline hard segment bundles. In order to explain it in details, it is necessary to have understood how a reaction is occurred. Generally, reactions occur when molecules are close enough to interact with each other, thereby; the effective reaction rates depend on the local concentration of reactants rather than the global concentration. This can be mathematically modeled using an imaginary sphere drawn around a reactant molecule which is called the reaction sphere (Figure 43). Once a reactant meets the other member of the reaction within its reaction sphere, eventually the reaction occurs.

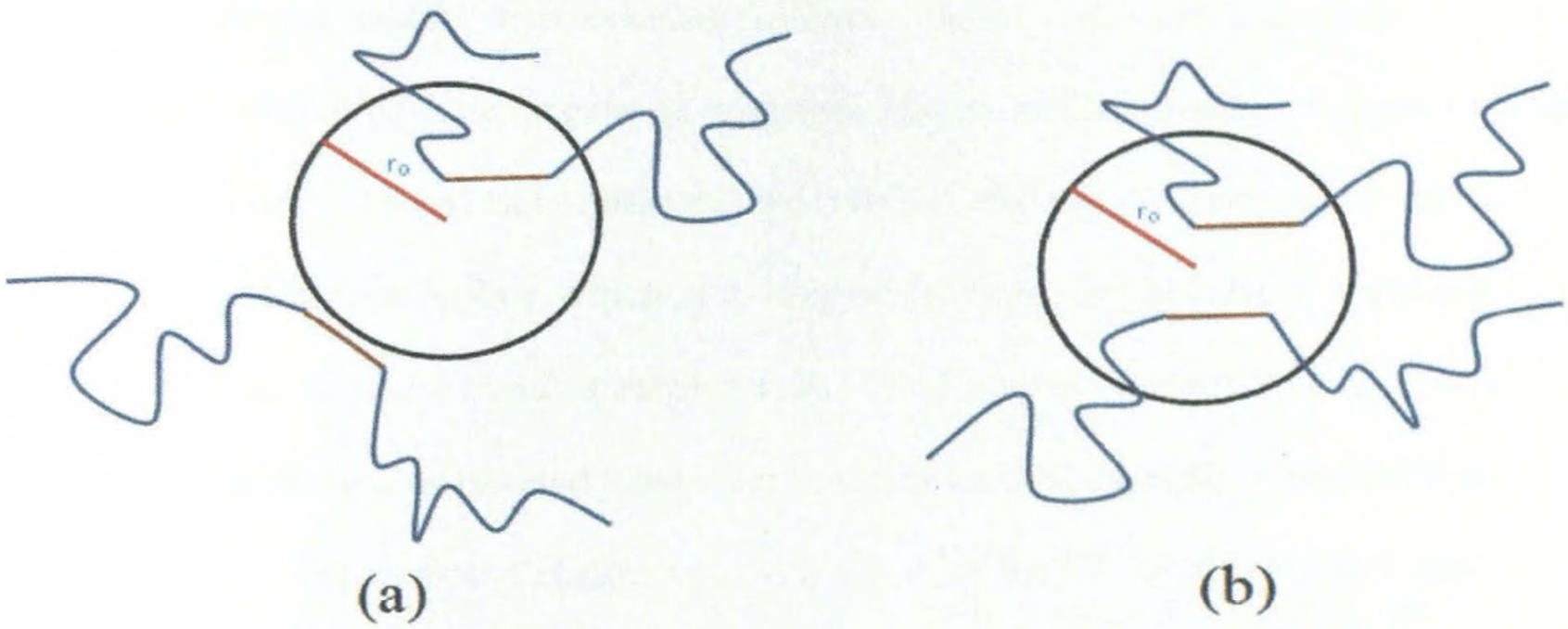

Figure 43: The reaction spheres; the brown color lines indicate the hard segments of polyurethanes while blue color lines for soft segments (a) the situation where hard segments cannot bond together (b) the situation where the hard segments can bond together as they met each other within the reaction sphere

Based on the statistics from the Cambridge Structural Database, Testa et al. have reported in their book that when NH is hydrogen bonded with a carbonyl oxygen, the optimal N-O distance is typically in between 2.8 and 3.2 A°. (98) Therefore in order to

form hydrogen bonds between two isolated hard segments they should come inside of a reaction sphere having a radius around 3 A°.

In the case of PUD films, some of the hard segments are trapped in soft segment matrix while almost all the hard segments in PUP-3 film are trapped as isolated hard segments. With the exposure to the 293 nm radiation, the localized melting of polyurethane films starts and the localized melting increases with exposure time. The isolated hard segments which are trapped in soft segment matrix can start to move to close to each other due to the localized melting in polyurethane films which is resulted owing to the UV exposure. Soft segments get melted and randomly oriented while allowing the hard segments to move. This facilitates the diffusion of isolated hard segments which were trapped in the polytetrahydrofuran matrix in such a way that the isolated hard segments can join together within their reaction spheres. Hence, with the exposure time, the amount of crystalline hard segments becomes higher while amount of isolated hard segments becomes lower. Subsequently, the 356 nm intensity become lesser while 423 nm intensity become higher which are originated from isolated hard segments and crystalline hard segment bundles respectively. The increase in crystalline hard segment bundles and decrease of isolated hard segments were experimentally observed from the FT-IR spectra. The carbonyl region and NH region of the FT-IR spectra recorded after the continuous exposure to 293 nm radiation is shown in Figure 44 & Figure 45 respectively.

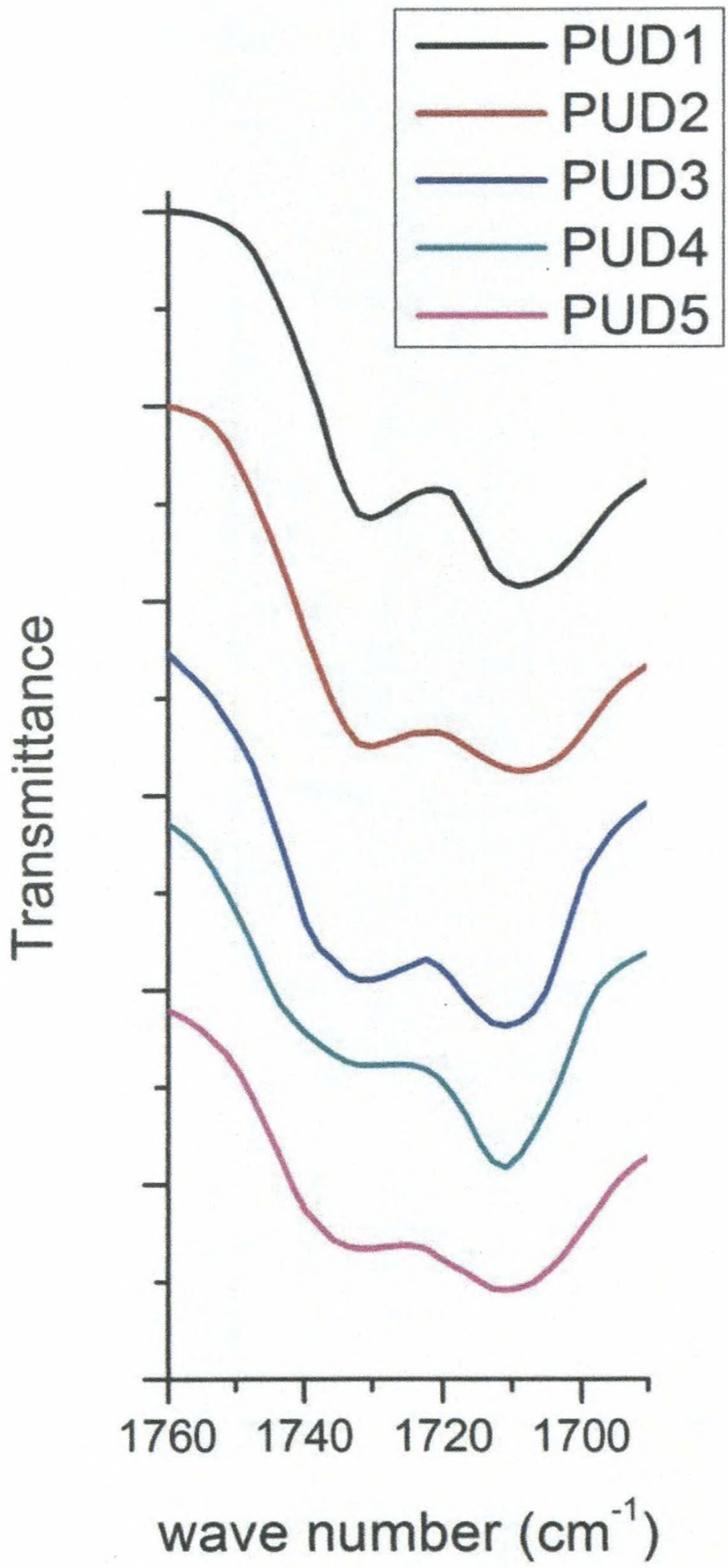

Figure 44: The carbonyl region of the FT-IR spectra of PUD films after the UV exposure

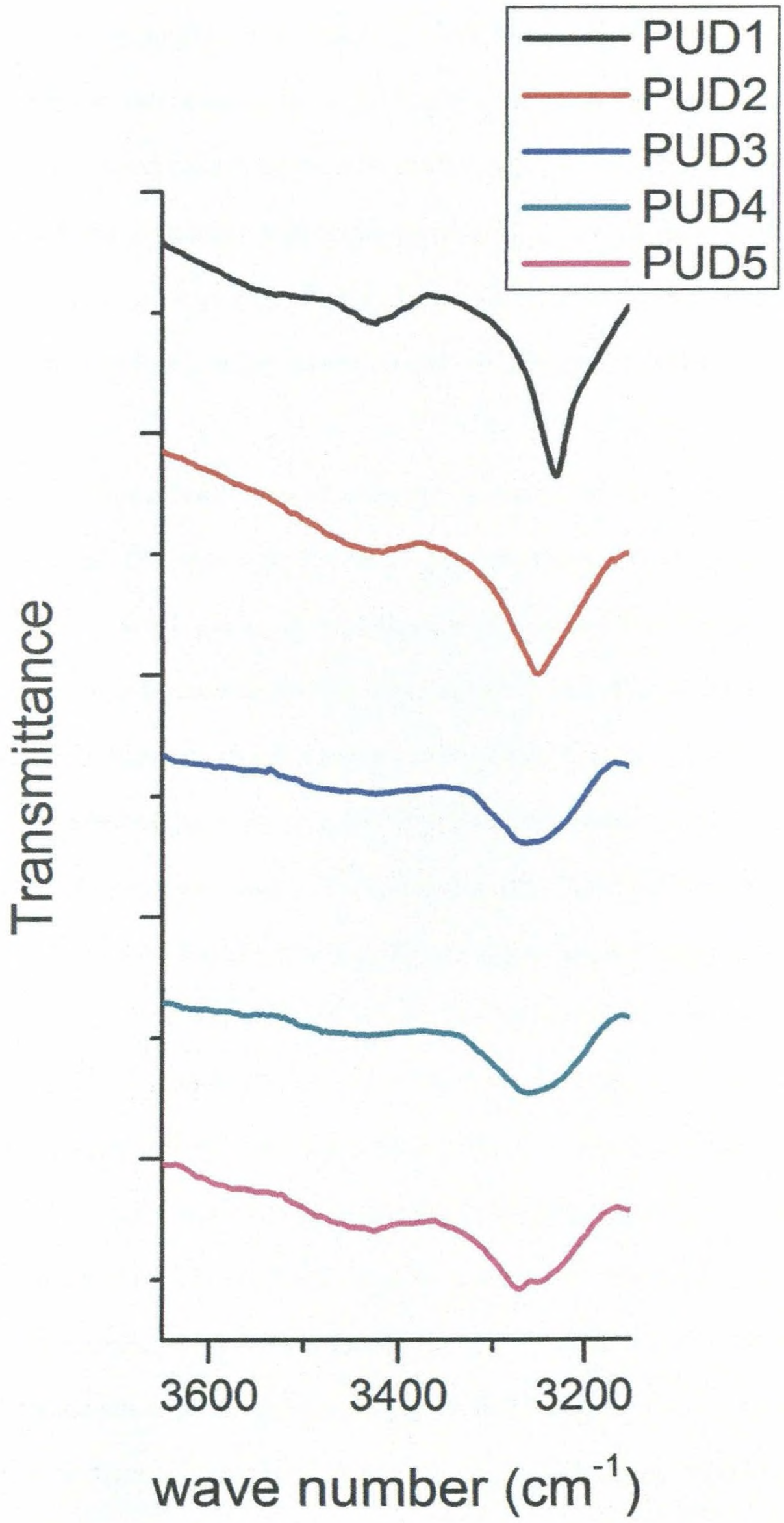

Figure 45: The NH region of the FT-IR spectra of PUD films after the UV exposure

By comparing the Figure 44 with Figure 15 and Figure 45 with Figure 16, it can be clearly distinguish that intensities of hydrogen bonded peaks have increased while intensities of free peaks have reduced with the UV exposure. As hydrogen bonded peaks are originated from crystalline hard segment bundles and free peaks are from isolated hard segments, with the observed intensity variation, it can be concluded that amount of crystalline hard segment bundles has increased and amount of isolated hard segments has decreased.

When we discuss about the fluorescence emission spectra, if we do not consider about the excitation of the fluorophores then the discussion is incomplete. Always fluorophores excite at a lower wavelength and emits at higher wavelength. The samples were excited at 293 nm wavelength which was selected from the UV absorption spectra. The isolated hard segments which are responsible for the 356 nm emission signal which is located at comparatively lower wave length should be excited by the energy supplied by the instrument via the irradiation of the sample using the filtered radiation of 293 nm. However, there are two possibilities to excite the crystalline hard segments which emit at 423 nm. One is direct excitation of crystalline hard segment bundles with 293 nm light and the second is excitation of crystalline hard segment bundles via the energy transfer from excited isolated hard segments to a ground state crystalline hard segment bundles. Energy transfer process was ruled out by the detailed analysis of emission and absorption spectra of the polyurethane films. In order to an energy transfer to take place, the ground state species must absorb the energy emits by the excited species. This can happen only if the emission of the excited species and the absorption of the ground state species are overlapped. When the PUD-1 film is considered, both isolated hard segments and crystalline hard segment bundles are available. Hence the emission

spectrum of PUD-1 film has the 356 nm peak while absorption spectrum of PUD-1 film is a combination of the absorption of isolated hard segments and crystalline hard segments bundles. The overlap of emission and absorption spectra of PUD-1 film in the attentive range is shown in Figure 46.

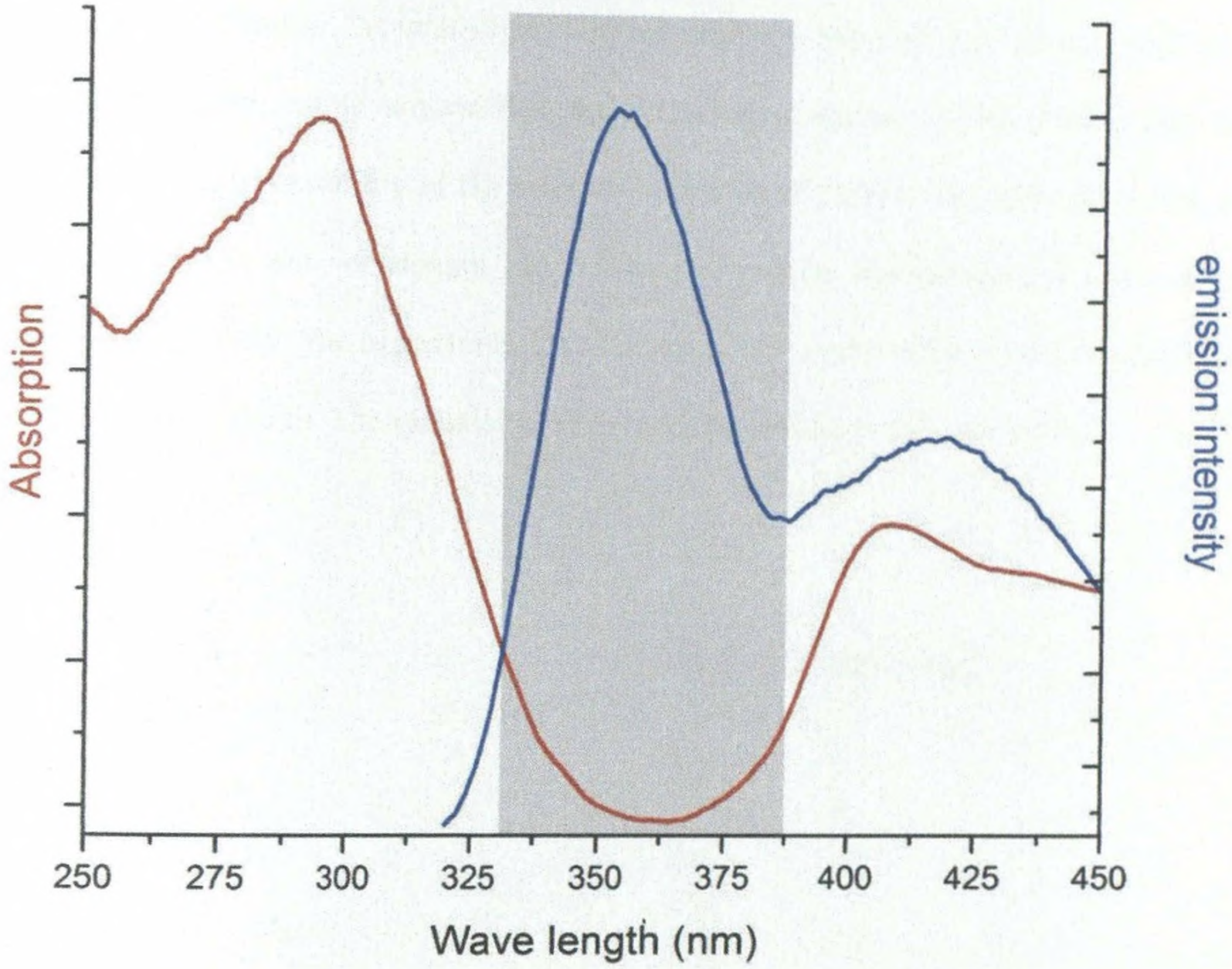

Figure 46: The overlap of absorption spectrum and emission spectrum of PUD-1 film; the 356 emission signal is highlighted

According to the Figure 46, there is a valley in the absorption spectrum in the range of the peak corresponding to 356 nm emission of PUD-1 film. It implies that the possibility of absorbing the energy released from excited isolated hard segments by the crystalline hard segments is negligible. Therefore, it is fair enough to rule out the energy transfer process. Therefore, crystalline hard segments should also be excited by absorbing the energy of the 293 nm wavelength which was used to irradiate the samples.

Reversibility of fluorescence

There is another observation during the extended analysis of fluorescence behavior of PUP-3 film. When the UV exposed PUP-3 film was kept out of light for three days, the peak at 356 nm re-increased and the peak at 423 nm re-decreased. Again with continuous recordings, the intensity of 356 nm peak was reduced and 423 nm peak was increased. These results suggest that the fluorescent behavior of the PUP-3 film is reversible. The reversibility of the intensity variation of PUP-3 film after the cease of exposure to 293 nm wavelength can be used to explain microstructural changes in polyurethane films. The exposure to UV – cease of UV cyclic process was repeated for three complete cycles. The variations of two peak intensities are shown below.

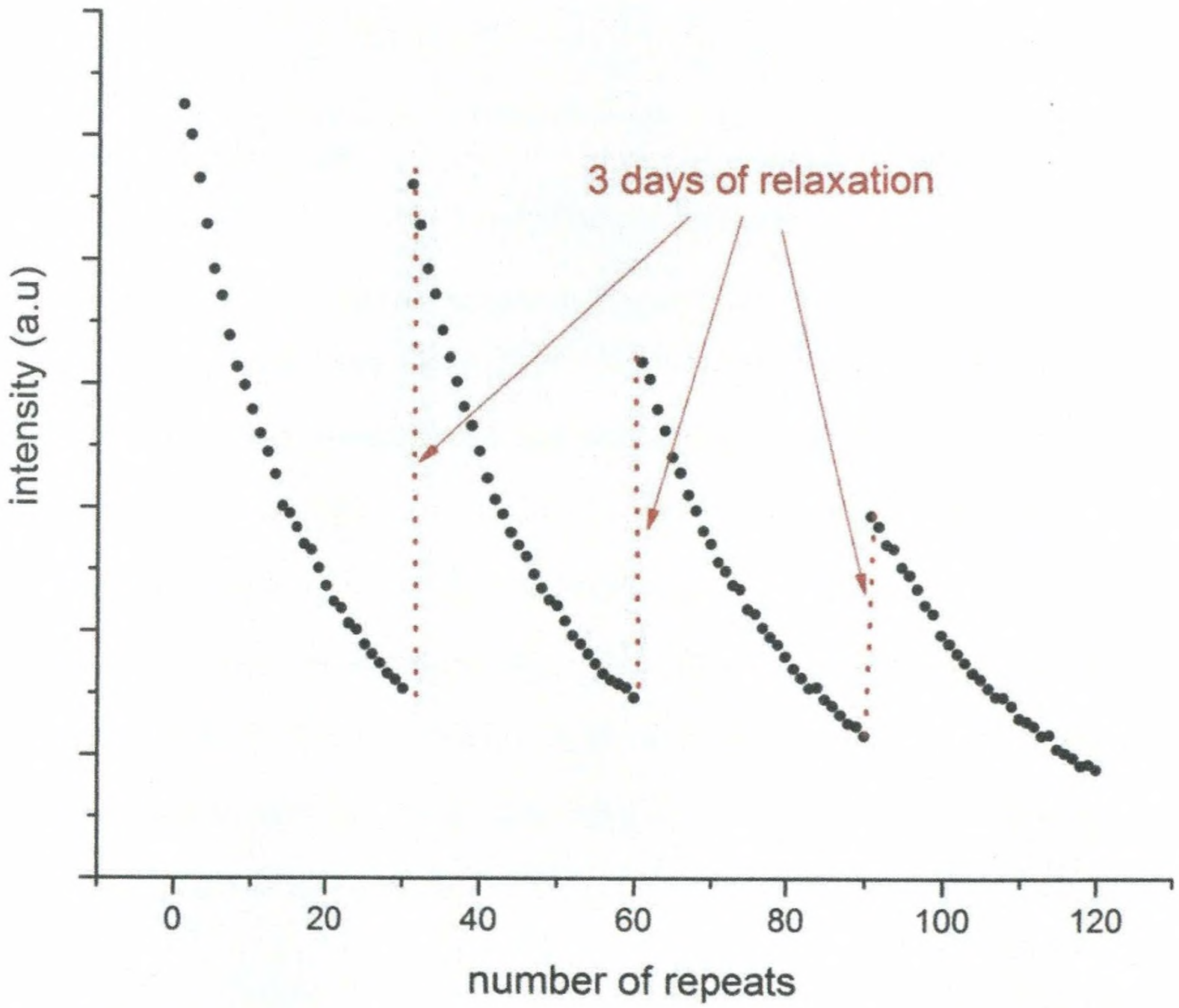

Figure 47: The variation in 356 nm peak intensity with UV exposure and relaxation

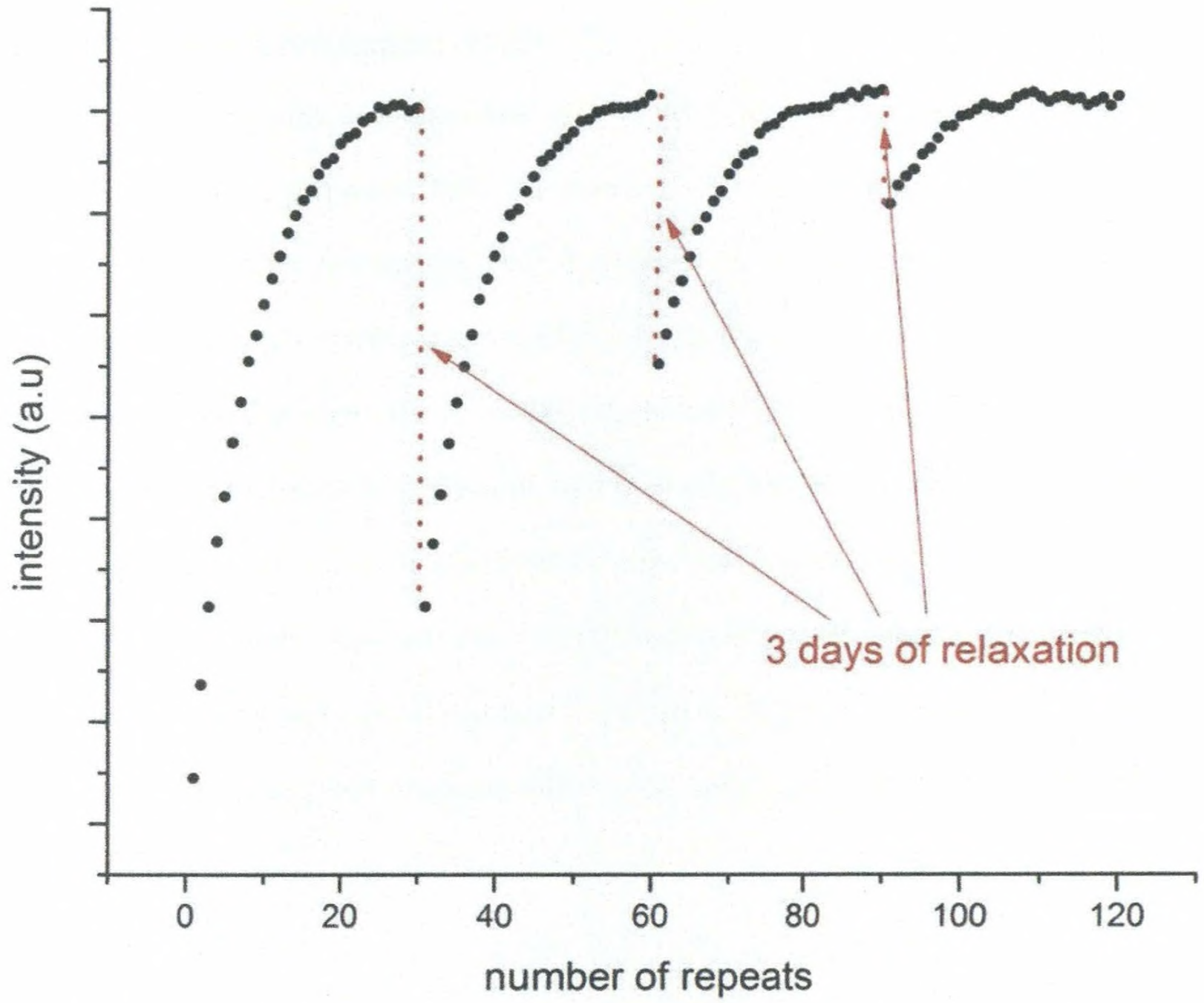

Figure 48: The variation in 423 nm peak intensity with UV exposure and relaxation

Exponential type decay was shown by the 356 nm emission intensity with respect to irradiation time while an exponential type growth was shown by the 423 nm emission intensity. When re-excited after 3 days of relaxation, the 356 nm emission intensity was increased while the 423 nm intensity was decreased.

As this reversibility is an important factor which helps to determine the actual process happening inside the PUP-3 film during the UV cease time, study was expanded in such a way to analyze the effect of different variables on the reversibility shown in the polyurethane fluorescence behavior.

Effect of relaxation time on fluorescence

In the above study, the relaxation time (UV cease time) after the continuous exposure was three days. In this case 100% reversibility was not achieved. In order to check whether the complete reversibility can be achieved by varying the relaxation time, the percentage reversibility with respect to different relaxation times was measured.

In each case of relaxation time, a similar fluorescence behavior was observed. In other words, initially there was a single peak, and then with continuous exposure there was a reduction in the first peak intensity while appearing a new peak and observing an increase in the second peak intensity, with the relaxation, there was a partial upsurge in first peak intensity and a parallel reduction in the second peak intensity. The intensity variation of two peaks with respect to different relaxation times is shown in Figure 49.

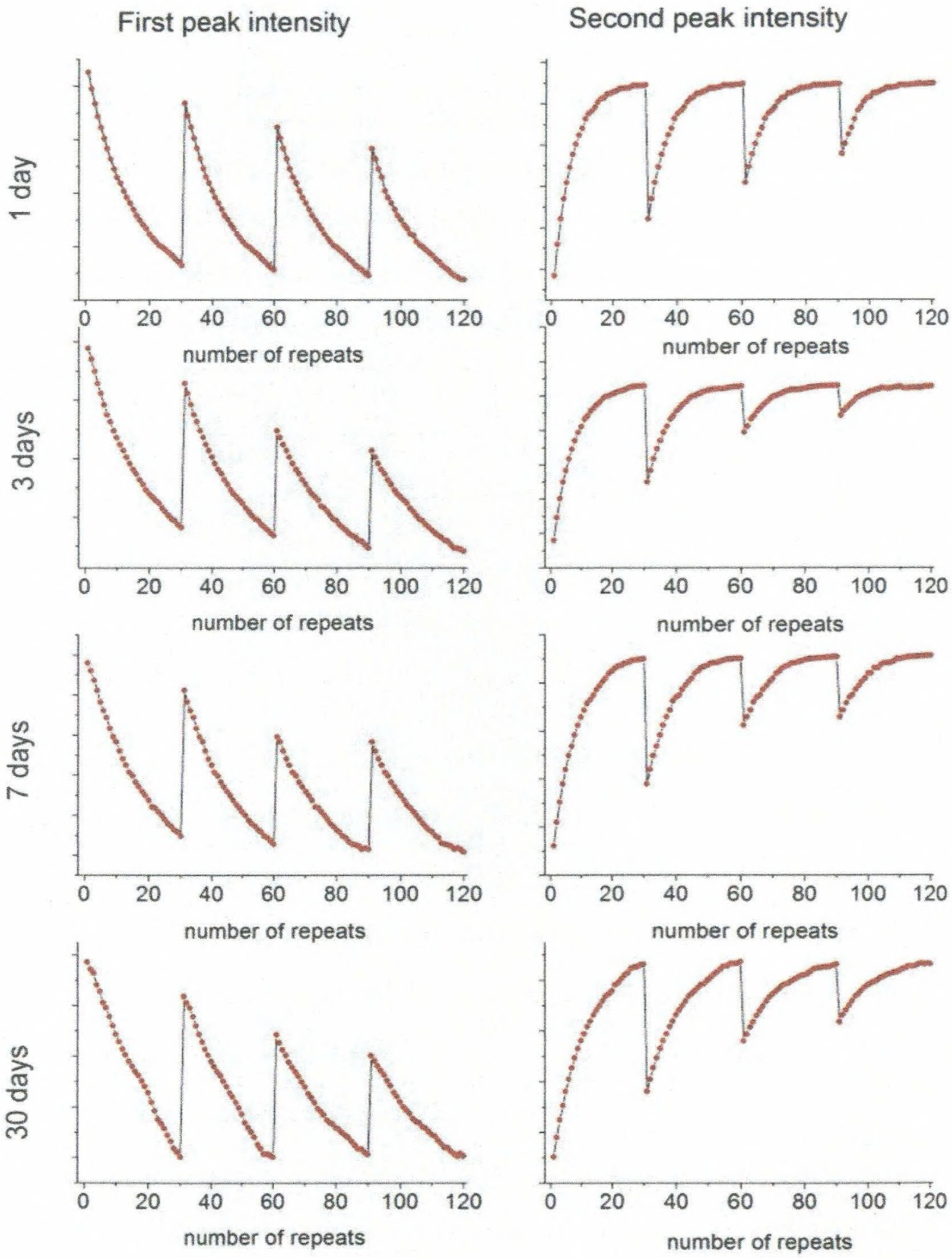

Figure 49: The intensity variation with relaxation time

The percentage reversibility was calculated according to the following equation (Equation 2).

$$\textbf{percentage recovery} = \frac{\boldsymbol{intensity\ of\ the\ 1st\ peak\ in\ the\ first\ repeat\ of\ second\ day}}{\boldsymbol{intensity\ of\ the\ 1st\ peak\ in\ the\ first\ repeat\ of\ first\ day}}$$

Equation 2: The equation which is used to calculate the percentage recovery

The effect of the relaxation times on percentage reversibility is tabled below (Table 4)

Table 4: Percentage reversibility with respect to different relaxation times

Relaxation time	Percentage recovery
1 day	90.6
3 days	89.8
7 days	92.1
30 days (1 month)	91.3

As shown in Table 4, the percentage recovery after one day is greater than three days. However, it is smaller than that of seven days. Hence, it was found that there was no correlation between the percentage reversibility and relaxation times. Even after one month it was not possible to achieve 100% reversibility. Hence, it can be assumed that only a partial reversibility is achievable even after infinite relaxation. In other words, 100% reversibility cannot be obtained

Effect of exposure time on fluorescence

The exposure time is also one such factor which can be varied to check whether there is an effect on percentage reversibility. As each scan amounting to 30 s of UV irradiation at 293 nm wavelength, the exposure time was varied by changing the number of repeats per one continuous recording cycle.

By calculating the percentage reversibility according to Equation 2, the percentage reversibility with respect to exposure time is tabled below (Table 5).

Table 5: The percentage reversibility w.r.t different exposure times

Number of repeats per cycle	Exposure time (min)	Percentage recovery (%)
20	10	92.2
30	15	86.8
40	20	89.8
50	25	89.7
60	30	89.8

According to the tabulated results, with the increase of exposure time there is a random variation in percentage recovery instead of smooth increase or decrease in percentage recovery. Therefore, it was concluded that the exposure time too does not have a correlation to the percentage reversibility.

Effect of degree of polymerization on fluorescence

By varying the degree of polymerization, three polyurethane systems having three different chain lengths were obtained. In other words, the average number of monomers per polymer chain was varied. Using these three systems, the effect of chain length on the fluorescence behavior was analyzed. It was clear that once the same precursors are used, even though the chain lengths were varied through the variation of degree of polymerization, a similar fluorescence behavior was shown by all three systems. In other words, all three systems showed a single peak at initially and with the exposure time there was a generation and growth of a second peak at a higher wave length with a

reduction the first peak intensity. In addition, a partial reversibility of the fluorescence intensity was also observed in all three systems.

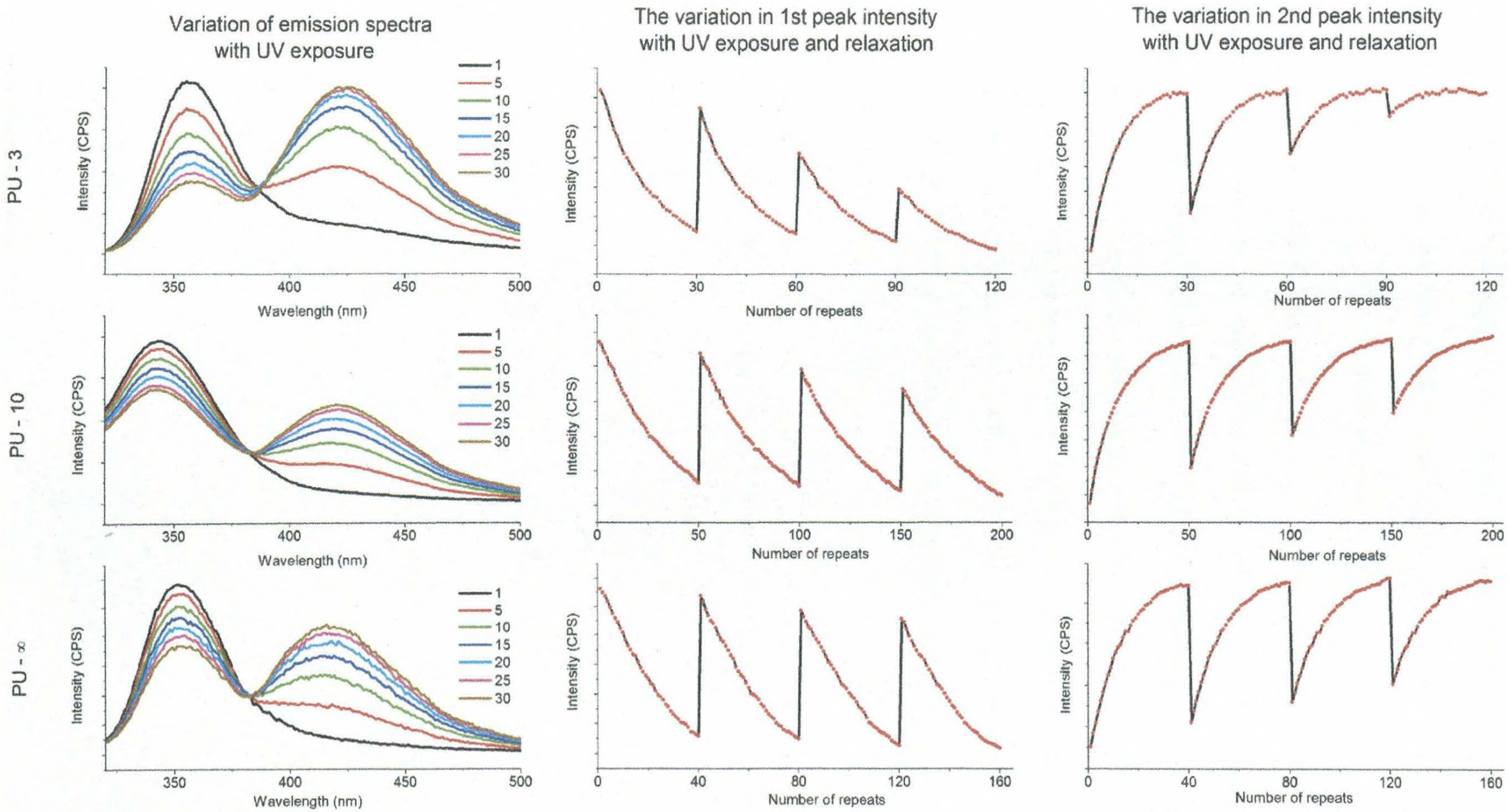

Figure 50: The fluorescence behavior of three polyurethane prepolymers

Hence, it was clear that this partially reversible florescence behavior was observed in polyurethanes prepared using MDI and PTHF irrespective of the exposure time, relaxation time and the polymer chain length.

Effect of solvent on fluorescence

In order to investigate the effect of solvent, a new polyurethane system was prepared using a similar composition to the PUP-3 system but in a different medium. Instead of DMAc, DMF was used as the solvent here and was labeled as PUP-3$_{_DMF}$. Similar to the PUP-3 system, initially there was a single peak and the appearance and growth of a second peak with a reduction of the first peak was observed with continuous exposure. Figure 51 shows the initial emission spectrum and how the fluorescence spectra varied with UV exposure.

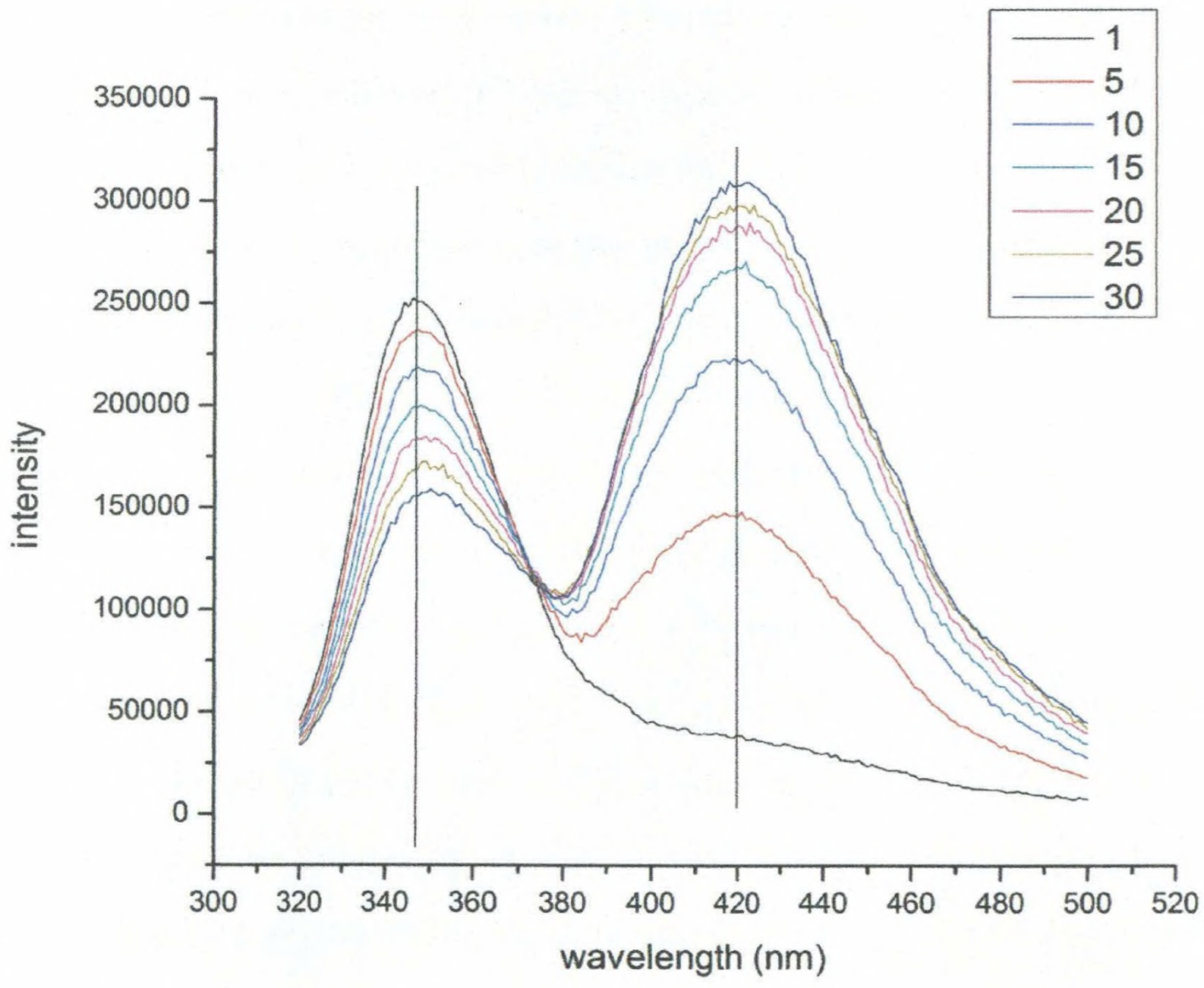

Figure 51: The spectra overlay of PUP-3$_{_DMF}$

However, in contrast to PUP-3 system, PUP-3_DMF did not show reversibility in the fluorescence behavior. After 3 days of relaxation, the fluorescence signal was similar to the emission spectrum obtained in the last repeat of the first day.

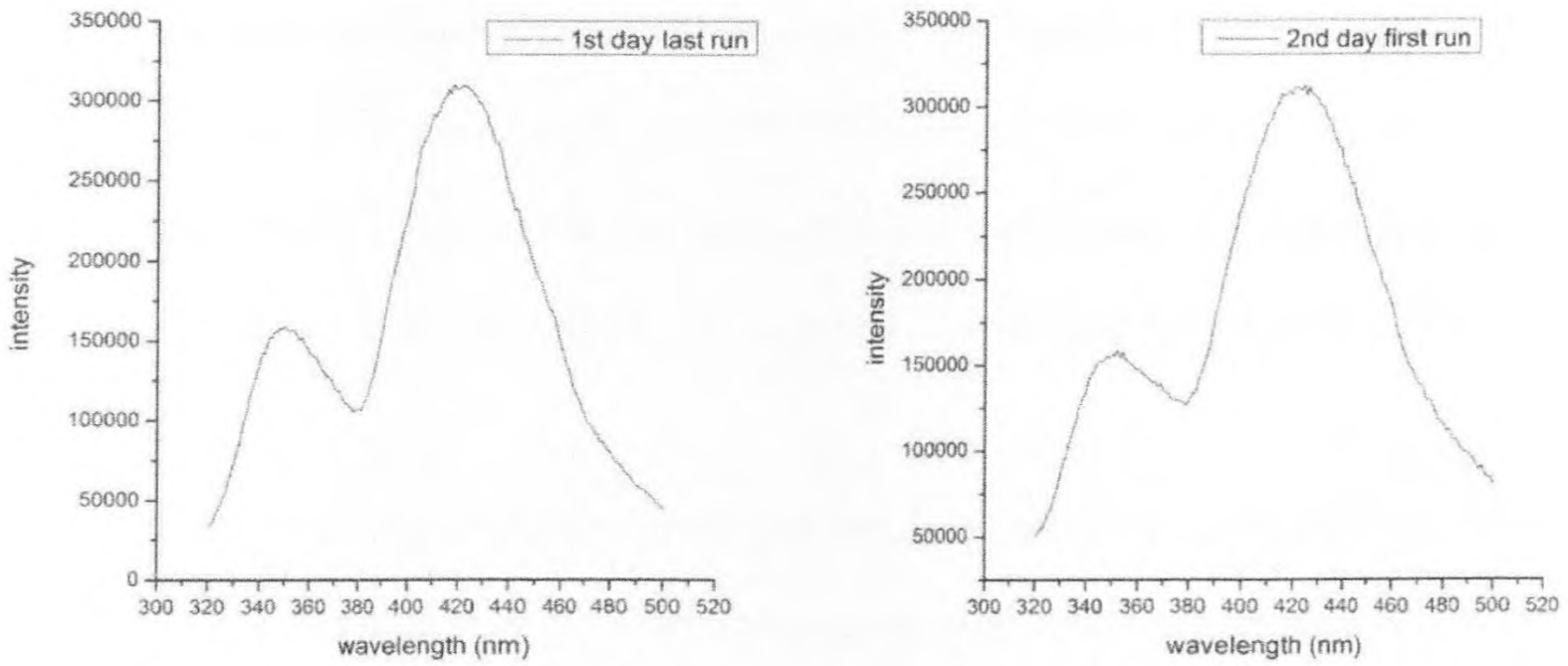

Figure 52: The non-reversibility of fluorescence behavior of PUP-3_DMF

Hence, it is clear that there is a solvent effect on the fluorescence behavior of the polyurethanes. After explaining that how the reversibility occurs, the way that solvent affects the fluorescence behavior will be discussed.

The peak at 356 nm re-increases and the peak at 423 nm re-decreases when UV irradiation is blocked for a considerable time period. However, both peaks do not come back to their original intensity even after UV cease time of one month. And also once the UV cease times were varied and percentage reversibility was calculated, it does not show that increase in that parameter effects on the percentage. This allows us to assume that 100% reversibility cannot be achieved even after infinite UV cease period.

The reversible nature of the fluorescence behavior can be explained using the micro structural changes in polymer system. When kept out of UV radiation, the melted polymer began to solidify reducing the entropy of molecules. This process re-crystallizes soft segments back to highly crystalline areas which in turn create tensile

forces on the hard segments. These tensile forces are capable of separating the crystalline hard segment bundles to re-produce isolated hard segments back. This reduction of crystalline hard segment bundles density can be attributed to reduction of 423 nm emission with simultaneous increase in 356 nm emission during the UV cease time. As the tensile forces cannot bring all the molecules back to the original spatial arrangement, some of the H-bonded hard segments will remain as crystalline hard segment bundles. This will result in a partial reversibility instead of complete reversibility.

It can be observed that the initial intensity of the peak at 423 nm increases while the initial intensity of the peak at 356 nm reduces with each cycle. It indicates that with each cycle of irradiation the density of crystalline hard segment bundles increases. Photo degradation could cleave some of the polymer molecules during the prolonged UV irradiation which in turn can reduce the tensile forces on H-bonded hard segments (crystalline hard segment bundles). Hence, the ground state crystalline hard segment bundles density increases with the number of excitation cycles.

It was revealed that when the solvent is changed from DMAc to DMF the reversibility of the fluorescence behavior disappeared. The two possibilities which are postulated here for this blocking of reversibility originate from the steric effect. When DMAc and DMF molecules are considered, in the DMAc molecule the formyl hydrogen of DMF is replaced by a methyl group which is arranged in a tetrahedral geometry while occupying a large volume of space. Hence, DMF is sterically less hindered compared to DMAc. Thus its ability to be embedded inside the polymer matrix is greater. In the films obtained by solvent casting method, the residual solvent molecules can remain in the film. Residual DMF molecules can be more easily embedded inside the polymer

matrix compared to DMAc. The two possibilities which blocked the reversibility are; firstly, the embedded DMF molecules retard the tensile forces which the hard segment bundles were subject to. Therefore, the isolated hard segments and hard segment bundles remains as they are. This effect is somewhat similar to the role of plasticizers. In literature there are some articles explaining that residual solvent molecules act as plasticizers; the action of residual chloroform as a plasticizer to the polylactide (PLA) films has been reported. (99,100) The second possibility is, there is not any effect to the explained mechanism in such a way when UV cease the polymer molecules re-arranged as explained but, DMF molecules which embedded in to the polymer matrix during the localized melting step comes and joins with isolated hard segments to form MA type complex instead of crystalline hard segment bundles which also emits at 423 nm. There are several possibilities for the hydrogen bond formation between urethane group and DMF molecules. (101) DMF and urethane linkages are joined together via two pair of hydrogen bonds. (101) This suggests that the MA type complex formation between DMF and isolated hard segments is feasible. This ability of complex formation enhances the reliability of the second possibility. There is a third possibility which is least probable; when DMF is present they could induce a photo degradation product which emits at 423 nm.

PUD films also did not show this reversibility. As PUD films are obtained from polyurethane solutions in DMF-water medium, presence of the residual DMF molecules in PUD films is feasible. As explained in the above section DMF may be responsible to the blocking of reversibility in PUD films.

After this complete analysis, it was able to explain the fluorescence behavior associated with MDI based polyurethanes and the way that the microstructure of films affects to

the emission signals. Microstructural rearrangements associated with UV exposure and UV cease was also able to explain using the fluorescence technique. Finally, overall fluorescence behavior of MDI based polyurethanes was able to explain using a set of photo chemical reactions. It was able to propose a mechanism based on the polyurethane micro-structure to explain what kind of photo chemical and physical processes are happened in the polyurethane film during the UV exposure. The proposed mechanism is shown below. In that mechanism; H_I stands for ground state isolated hard segments while H_C for ground state crystalline hard segment bundles. H_I^* and H_C^* stands for their excited species respectively.

i. $H_I + h\nu_{293} \longrightarrow H_I^*$ (excitation of isolated hard segments)

ii. $H_I^* \longrightarrow H_I + h\nu_{356}$ (relaxation of isolated hard segments)

iii. $H_C + h\nu_{293} \longrightarrow H_C^*$ (excitation of crystalline hard segment bundles)

iv. $H_C^* \longrightarrow H_C + h\nu_{423}$ (relaxation of crystalline hard segment bundles)

v. $nH_I \xrightarrow{\text{UV exposure}} H_C$ (formation of crystalline hard segment bundles)

vi. $H_C \xrightarrow{\text{UV cease}} nH_I$ (dissociation of crystalline hard segment bundles)

Figure 53: Set of photo chemical processes occurred in MDI based polyurethanes

The proposed mechanism consists of 6 basic steps. Firstly, isolated hard segments of the polyurethanes which contained the fluorophores originating from MDI get excited by 293 nm wavelength (i) and relaxed back to their ground state by emitting the 356 nm wavelength (ii). Crystalline hard segment bundles also get excited by absorbing the 293 nm energy (iii) and relaxed back to its ground state by emitting the 423 nm wavelength (iv). In addition to excitation of the two fluorophores, UV exposure leads to the formation of crystalline hard segment bundles due to the localized melting (v). In addition to these photo chemical processes there is another process which is responsible

to reversibility. It is the dissociation of the formed crystalline hard segment bundles due to the tensile forces (vi).

As we were able to explore the fluorescence behavior of MDI based polyurethanes, there are possibilities of using this novel phenomena in various applications such as sensor based applications.

CHAPTER 5 - CONCLUSION

MDI based stable polyurethane dispersions (in 30% DMF-water) were obtained. There stability was achieved by the introduction of DMPA which helps to increase the hydrophilicity of the polymer. With the increase of DMPA percentage, the stability of the dispersions was increased while reducing the size of the dispersed particle.

Films obtained from polyurethane dispersions had a microstructure consisting of crystalline hard segment bundles while prepolymer films had a microstructure consisting of isolated hard segments embedded in a crystalline soft segment matrix. Hard segment crystallinity of the PUD films was increased with the increase of DMPA percentage.

MDI based polyurethanes were fluoresced and showed two broad peaks at 356 nm and 423 nm due to the isolated hard segments and crystalline hard segments, respectively. With the UV exposure 356 nm peak intensity was reduced and 423 nm peak intensity was increased due to the formation of more crystalline hard segment bundles via approach of isolated hard segments to each other due to the localized melting in the matrix. This intensity variation was reversible because during the UV cease the melted polymer recrystallized back to reduce the entropy while separating some crystalline hard segment bundles in to isolated hard segments using the tensile forces. However, some solvents were capable to remove this reversibility effect. To explain the picture of overall fluorescence behavior a set of photochemical reactions were proposed.

REFERENCES

1. Chattopadhyay DK, Raju KVSN. Structural engineering of polyurethane coatings for high performance applications. Progress in polymer Science. 2007; 32: p. 352-418.

2. Raghu AV, Jeong HM, Kim JH, Lee YR, Cho YB, Sirsalmat K. Synthesis and characterization of novel polyurethanes based on 4-((4-Hydroxyphenyl)iminomethyl)phenol. Macromolecular research. 2008; 16(3): p. 194-199.

3. Takami K, Matsuno R, Ishihara K. Synthesis of polyurethanes by polyaddition using diol compounds with methacrylate-derived functional groups. Polymer. 2011; 52: p. 5445-5451.

4. Nagle DJ, Celina M, Rintoul L, Fredericks PM. Infrared microspectroscopic study of the thermo-oxidativedegradation of hydroxy-terminated polybutadiene/isophorone diisocyanate polyurethane rubber. Polymer Degradation and Stability. 2007; 92: p. 1446-1454.

5. Clemitson IR. Castable polyurethane elastomers. New York: CRC press,Taylor and Francis Group; 2008.

6. Raftopoulos KN, Janowski B, Apekis L, Pielichowski K, Pissis P. Molecular mobility and crystallinity in polytetramethylene ether glycol in the bulk and as soft component in polyurethanes. European Polymer Journal. 2011; 47: p. 2120–2133.

7. Subramani S, Park YJ, Lee YS, Kim JH. New development of polyurethane dispersion derived from blocked aromatic diisocyanate. Progress in Organic Coatings. 2003; 48: p. 71-79.

8. Ashida K. Polyurethane and related foams: chemistry and technology.New York: CRC Press, Taylor & Francis Group; 2007.

9. Krol P. Synthesis methods, chemical structures and phase structures of linear polyurethanes. Properties and applications of linear polyurethanes in polyurethane elastomers, copolymers and ionomers. Progress in Materials Science. 2007; 52: p. 915–1015.

10. Odian G. Principles of Polymerization. 4th ed. New York: John Wiley & Sons, Inc; 2004.

11. Billiet L, Fournier D, Prez FD. Step-growth polymerization and 'click' chemistry: The oldest polymers rejuvenated. Polymer. 2009; 50: p. 3877–3886.

12. Szycher M. Szycher's Handbook of Polyurethanes. 2nd ed. New York: CRC press, Taylor and Francis group; 2013.

13. Houghton RP, Mulvaney W. Mechanism of tin (IV) - catalysed urethane formation. Journal of Organometallic Chemistry. 1996; 518: p. 21-27.

14. Silva AL, Bordado JC. Recent Developments in Polyurethane Catalysis:Catalytic Mechanisms Review. Catalysis Reviews: Science and Engineering. 2004; 46(1): p. 31–51.

15. Gabriel LP, Zavaglia CAC, Jardini AL, Dias CG, Filho RM. Isocyanates as precursors to biomedical polyurethanes. Chemical Engineering Transactions. 2014; 38: p. 253-258.

16. Madra H, Ersolmaz SBT, Guner FS. Monitoring of oil-based polyurethane synthesis by FTIR-ATR. Polymer Testing. 2009; 28: p. 773–779.

17. Rosu D, Rosu L, Cascaval CN. IR-change and yellowing of polyurethane as a

result of UV irradiation. Polymer Degradation and Stability. 2009; 94: p. 591–596.

18. Yilgor E, Burgaz E, Yurtsever E, Yilgor I. Comparison of hydrogen bonding in polydimethylsiloxane and polyether based urethane and urea copolymers. Polymer. 2000; 41: p. 849–857.

19. Tanaka T, Yokoyama T, Yamaguchi Y. Quantitative study on hydrogen bonding between urethane compound and ethers by infrared spectroscopy. Journal of polymer science: part A-1. 1968; 6: p. 2137-2152.

20. Yilgor E, Yilgor I, Yurtsever E. Hydrogen bonding and polyurethane morphology. I. Quantum mechanical calculations of hydrogen bond energies and vibrational spectroscopy of model compounds. Polymer. 2002; 43: p. 6551–6559.

21. Hwang HD, Park CH, Moon JI, Kim HJ, Masubuchi T. UV-curing behavior and physical properties of waterborne UV-curable polycarbonate-based polyurethane dispersion. Progress in Organic Coatings. 2011; 72: p. 663–675.

22. Bai CY, Zhang XY, Dai JB, Li WH. A new UV curable waterborne polyurethane:Effect of C=C content on the film properties. Progress in Organic Coatings. 2006; 55: p. 291–295.

23. Lukas K, LeMaire PK. Differential Scanning Calorimetry: Fundamental Overview. Connecticut State University, Department of Physics; 2009.

24. Murakami H, Nishiide R, Ohira S, Ogata A. Synthesis of MDI and PCL-diol-based polyurethanes containing [2] and [3]rotaxanes and their properties. Polymer. 2014; 55: p. 6239-6244.

25. Mohamed HA, Badran BM, Rabie AM, Morsi SMM. Synthesis and characterization of aqueous (polyurethane/aromatic polyamide sulfone) copolymer

dispersions from castor oil. Progress in Organic Coatings. 2014; 77: p. 965–974.

26. Pan J, Li G, Chen , Chen X, Zhu W, Xu. Alternative block polyurethanes based on poly(3-hydroxybutyrate-co-4-hydroxybutyrate) and poly(ethylene glycol). Biomaterials. 2009; 30: p. 2975–2984.

27. Kariduraganavar MY, Tambe SM, Tasaganva RG, Kittur AA, Kulkarni SS, Inamdar SR. Studies on nonlinear optical polyurethanes containing heterocyclic chromophores. Journal of Molecular Structure. 2011; 987: p. 158–165.

28. Tasaganva RG, Kariduraganavar MY, Inamdar SR. Synthesis and nonlinear optical properties of polyurethanes containing nitro-substituted 1,3,4-oxadiazole chromophores. Synthetic Metals. 2009; 159: p. 1812–1819.

29. Rodrigues JME, Pereira MR, Souza AGD, Carvalho ML, Neto AAD, Dantas TNC, et al. DSC monitoring of the cure kinetics of a castor oil-based polyurethane. Thermochimica Acta. 2005; 427: p. 31–36.

30. Simas ER, Akcelrud L. Fluorescent aggregates in naphthalene containing poly(urethane–urea)s. Journal of Luminescence. 2003; 105: p. 69–79.

31. Buruiana EC, Buruiana T, Strat G, Strat. Synthesis and fluorescence of polyurethane cationomers N-modified with a stilbene chromophore. Journal of Photochemistry and Photobiology A: Chemistry. 2004; 162: p. 23–31.

32. Buruiana EC, Buruiana T, Strat G, Strat M. Synthesis and optical properties of new polyurethane cationomers with anchored stilbene chromophores. Journal of Polymer Science: Part A: Polymer Chemistry. 2002; 40: p. 1918–1928.

33. Peinado C, Allen NS, Salvador F, Corrales T, Catalina. Chemiluminescence and fluorescence for monitoring the photooxidation of an UV-cured aliphatic

polyurethane-acrylate based adhesive. Polymer Degradation and Stability. 2002; 77: p. 523–529.

34. Chen XD, Wang Z, Liao ZF, Mai YL, Zhang MQ. Roles of anatase and rutile TiO2 nanoparticles in photooxidation of polyurethane. Polymer Testing. 2007; 26: p. 202–208.

35. Hoyle C, Kim KJ. Photolysis of Aromatic Diisocyanate-Based Polyurethanes in Solution. Journal of Polymer Science: Part A: Polymer Chemistry. 1986; 24: p. 1879-1894.

36. Hoyle CE, Kim KJ, No YG, Nelson GL. Photolysis of Segmented Polyurethanes.The Role of Hard-Segment Content and Hydrogen Bonding. Journal of Applied Polymer Science. 1987; 34: p. 763-774.

37. Hoyle CE, Kim KJ. Effect of Crystallinity and Flexibility on the Photodegradation of Polyurethanes. Journal of Polymer Science: Part A: Polymer Chemistry. 1987; 25: p. 2631-2642.

38. Bosch P, Almudena F, Salvador EF, Corrales T, Catalina F, Peinado C. Polyurethane-acrylate based films as humidity sensors. Polymer. 2005; 46: p. 12200–12209.

39. Buruiana C, Buruiana T, Olaru M, Zamfir M, Pohoata V. Fluorescent polymers for sensor applications. SCIENTIFIC STUDY & RESEARCH. 2006; VII (1): p. 141-150.

40. Palacios MA, Pohl R, Zyryanov , Anzenbacher. Anion Sensors in Polyurethane Matrices: Synergy Between Matrix and Sensor Materials Improves Selectivity of the Sensing Process. Polymeric Materials: Science and Engineering. 2007; 96: p.

595-596.

41. Buruiana EC, Olaru M, Simionescu BC. Photochemical aspects in anthracene-containing cationic polyurethanes. European Polymer Journal. 2007; 43: p. 1359–1371.

42. Mohaghegh SMS, Barikani M, Entezami AA. The effect of grafted poly(ethylene glycol monomethyl ether) on particle size and viscosity of aqueous polyurethane dispersions. Colloids and Surfaces A: Physicochem. Eng. Aspects. 2006; 276: p. 95–99.

43. Liminana MAP, Ais A, Palau MT, Barcelo ACO, Martınez JMM. Characterization of waterborne polyurethane adhesives containing different amounts of ionic groups. International Journal of Adhesion & Adhesives. 2005; 25: p. 507–517.

44. Mequanint K, Sanderson R. Hydrolytic stability of nano-particle polyurethane dispersions: Implications to their long-term use. European Polymer Journal. 2006; 42: p. 1145–1153.

45. Pacios VG, Iwata Y, Colera M, Martinez JMM. Influence of the solids content on the properties of waterborne polyurethane dispersions obtained with polycarbonate of hexanediol. International Journal of Adhesion & Adhesives. 2011; 31: p. 787–794.

46. Ramos BGZ, Senna E, Cramail H, Cloutet E, Borsali R, Soldi V. The role of surfactant in the miniemulsion polymerization of biodegradable polyurethane nanoparticles. Materials Science and Engineering C. 2008; 28: p. 526–531.

47. Lee SK, Kim BK. High solid and high stability waterborne polyurethanes via ionic groups in soft segments and chain termini. Journal of Colloid and Interface

Science. 2009; 336: p. 208–214.

48. Zhu X, Jiang X, Zhang Z, Kong XZ. Influence of ingredients in water-based polyurethane–acrylic hybrid latexes on latex properties. Progress in Organic Coatings. 2008; 62: p. 251–257.

49. Hoyle E, Kim KJ. Excimer formation of a naphthalene diisocyanate based polyurethane in solution. Macromolecules. 1988; 21: p. 2100-2106.

50. Hu XH, Zhang Y, Dai JB, Liu J. Synthesis and fluorescent investigations of VBL-based waterborne polyurethane dye. Journal of Luminescence. 2011; 131: p. 2160–2165.

51. Hu X, Zhang X, Dai B. Synthesis and characterization of a novel waterborne stilbene-based polyurethane fluorescent brightener. Chinese Chemical Letters. 2011; 22: p. 997–1000.

52. Hu XH, Zhang XY, Dai JB. Synthesis and fluorescence enhancement behavior of a novel fluorescent aqueous polyurethane emulsion DDAQ-TDI-PU. Chinese Chemical Letters. 2012; 23: p. 855–858.

53. Buruiana EC, Buruiana T, Strat G, Strat M. Synthesis of Ionic Polyurethanes with Pyrene Rings:Spectral Properties and Fluorescence Quenching Study. Journal of Polymer Science: Part A: Polymer Chemistry. 2005; 43: p. 3945–3956.

54. Buruiana C, Buruiana , Pohoata V. Synthesis, properties and fluorescence quenching in a polycation based on polyetherurethane with pyrene fluorophore. Journal of Photochemistry and Photobiology A: Chemistry. 2006; 180: p. 150–156.

55. Nanda AK, Wicks DA. The influence of the ionic concentration, concentration of the polymer, degree of neutralization and chain extension on aqueous polyurethane

dispersions prepared by the acetone process. Polymer. 2006; 47: p. 1805-1811.

56. Jhon Y, Cheong I, Kim JH. Chain extension study of aqueous polyurethane dispersions. Colloids and Surfaces A: Physicochemical and Engineering Aspects. 2001; 179 : p. 71–78.

57. Lee HT, Wu S, Jeng J. Effects of sulfonated polyol on the properties of the resultant aqueous polyurethane dispersions. Colloids and Surfaces A: Physicochem. Eng. Aspects. 2006; 276: p. 176–185.

58. Lei L, Zhong L, Lin X, Li , Xia. Synthesis and characterization of waterborne polyurethane dispersions with different chain extenders for potential application in waterborne ink. Chemical Engineering Journal. 2014; 253: p. 518–525.

59. Pacios VG, Costa V, Colera M, Martinez JMM. Waterborne polyurethane dispersions obtained with polycarbonate of hexanediol intended for use as coatings. Progress in Organic Coatings. 2011; 71: p. 136–146.

60. Liu X, Xu K, Liu H, Cai , Su J, Fu Z, et al. Preparation and properties of waterborne polyurethanes with natural dimer fatty acids based polyester polyol as soft segment. Progress in Organic Coatings. 2011; 72: p. 612– 620.

61. Sardon H, Irusta L, Berridi MJF, Luna J, Lansalot M, Lami EB. Waterborne Polyurethane Dispersions Obtained by the Acetone Process: A Study of Colloidal Features. Journal of AppliedPolymer Science. 2011; 120: p. 2054–2062.

62. Najafi F, Manouchehri , Shaabanzadeh. Synthesis and Characterization of Anionic Polyester-Polyurethane Dispersion as Environmentally-Friendly Water Based Resins. Journal of Chemical Health Risks. 2011; 1(2): p. 23-26.

63. Nanda AK, Wicks DA, Madbouly SA, Otaigbe JU. Effect of ionic content, solid

content, degree of neutralization, and chain extension on aqueous polyurethane dispersions prepared by prepolymer method. Journal of applied polymer science. 2005; 98: p. 2514-2520.

64. Hwang HD, Kim HJ. UV-curable low surface energy fluorinated polycarbonate-based polyurethane dispersion. Journal of colloid and interface science. 2011; 362: p. 274-284.

65. Pan H, Chen. Preparation and characterization of waterborne polyurethane/attapulgite nano composites. European Polymer Journal. 2007; 43: p. 3766–3772.

66. Xin H, Shen Y, Li X. Novel cationic polyurethane-fluorinated acrylic hybrid latexes: synthesis, characterization and properties. Colloids and surfaces A: phisicochem. Eng. Aspects. 2011; 384: p. 205-211.

67. Daemi H, Rad RR, Barikani M, Adib M. Catalytic activity of aqueous cationic polyurethane dispersions:A novel feature of polyurethanes. Applied Catalysis A: General. 2013; 468: p. 10-17.

68. Pielichowska K, Król P, Król B, Pagacz. TOPEM DSC study of glass transition region of polyurethane cationomers. Thermochimica Acta. 2012; 545: p. 187–193.

69. Athawale VD, Kulkarni MA. Synthesis, characterization, and comparison of polyurethane dispersions based on highly versatile anionomer ATBS and conventional DMPA. J. Coat. Technol. Res. 2010; 7: p. 189-199.

70. Yang Z, Wicks DA, Hoyle CE, Pu H, Yuan J, Wan D, et al. Newly UV-curable polyurethane coatings prepared by multifunctional thiol- and ene-terminated polyurethane aqueous dispersions mixtures: Preparation and characterization.

Polymer. 2009; 50: p. 1717–1722.

71. Yang Z, Wicks DA, Yuan J, Pu H, Liu Y. Newly UV-curable polyurethane coatings prepared by multifunctional thiol- and ene-terminated polyurethane aqueous dispersions: Photopolymerization properties. Polymer. 2010; 51: p. 1572–1577.

72. Sadek PC. The HPLC solvent guide. 2nd ed. New York: A John Wiley and sons, Inc.; 2002.

73. Cakic SM, Stamenkovic JV, Djordjevic DM, Ristic IS. Synthesis and degradation profile of cast films of PPG-DMPA-IPDI aqueous polyurethane dispersions based on selective catalysts. Polymer Degradation and Stability. 2009; 94: p. 2015–2022.

74. Larsson M, Hill A, Duffy J. Suspension stability; Why particle size, zeta potential and rheology are important. Annual Transactions of the nordic rheology society. 2012; 20: p. 209-214.

75. Sample dispersion & refractive index guide England: Malvern Instruments Ltd.; 1997.

76. El-Dossoki FI. Refractive Index and Density Measurements for Selected Binary Protic-Protic, Aprotic-Aprotic, and Aprotic-Protic Systems at Temperatures from 298.15 K to 308.15 K. Journal of the Chinese Chemical Society. 2007; 54: p. 1129-1137.

77. Garcia JMB, Lopez AG, Torres AC, Baltazar EA, Silva GAI. Densities and Viscosities of (N,N-Dimethylformamide + Water) at Atmospheric Pressure from (283.15 to 353.15) K. J. Chem. Eng. Data. 2008; 53: p. 1024–1027.

78. Sengwa RJ, Khatri V, Sankhla S. Structure and hydrogen bonding in binary

mixtures of N,N-dimethylformamide with some dipolar aprotic and protic solvents by dielectric characterization. Indian Journal of Chemistry. 2009; 48: p. 512-519.

79. KIM BK, LEE JC. Waterborne Polyurethanes and Their Properties. Journal of Polymer Science: Part A Polymer Chemistry. 1996; 34: p. 1095-1104.

80. Jang JY, Jhon YK, Cheong IW, Kim JH. Effect of process variables on molecular weight and mechanical properties of water-based polyurethane dispersion. Colloids and Surfaces A: Physicochemical and Engineering Aspects. 2002; 196: p. 135–143.

81. Son SH, Lee HJ, Kim JH. Effects of carboxyl groups dissociation and dielectric constant on particle size of polyurethane dispersions. Colloids and Surfaces A: Physicochemical and Engineering Aspects. 1998 ; 133: p. 295-301.

82. MARTIN DJ, MEIJS GF, GUNATILLAKE PA, YOZGHATLIAN SP, RENWICK GM. The Influence of Composition Ratio on the Morphology of Biomedical Polyurethanes. Journal of Applied Polymer Science. 1999; 71: p. 937–952.

83. Paul D, Paul S, Roohpour N, Wilks M, Vadgama P. Antimicrobial, Mechanical and Thermal Studies of Silver Particle-Loaded Polyurethane. Journal of Functional Biomaterials. 2013; 4: p. 358-375.

84. Mishra A, Maiti P. Aromatic polyurethanes: the effect of hard segment and chain structure on their properties. Journal of Polymer Engineering. 2011; 31: p. 253–259.

85. Asif A, Shi. UV curable waterborne polyurethane acrylate dispersions based on hyperbranched aliphatic polyester: effect of molecular structure on physical and

thermal properties. Polymers for advanced technologies. 2004; 15: p. 669–675.

86. Kua J, Zhang , McCammon J. Studying Enzyme Binding Specificity in Acetylcholinesterase Using a Combined Molecular Dynamics and Multiple Docking Approach. J. AM. CHEM. SOC.. 2002; 124: p. 8260-8267.

87. LIU LZ, CHU B. Crystalline Structure and Morphology of Microphases in Compatible Mixtures of Poly(tetrahydrofuran-methylmethacrylate) Diblock Copolymer and Polytetrahydrofuran. Journal of Polymer Science: Part B: Polymer Physics. 1999; 37: p. 779 –792.

88. Motokucho S, Furukawa M, Kawashima M, Kojio K, Yoshinaga K. Physical properties of poly(tetrahydrofuran)-block-poly(2-ethyl-2-oxazoline) triblock copolymer. Polymer Journal. 2013; 45: p. 1115–1119.

89. Hutten PFv, Mangnus RM, Gaymans. Segmented copolymers with polyesteramide units of uniform length: structure analysis. POLYMER. 1993; 34: p. 4193-4202.

90. Fernandez A, Lozano , Gonzalez , Rodriguez. Hydrogen Bonding in Copoly(ether-urea)s and Its Relationship with the Physical Properties. Macromolecules. 1997; 30: p. 3584-3592.

91. Yilgor E, Yilgor I, Yurtsever E. Hydrogen bonding and polyurethane morphology. I. Quantum mechanical calculations of hydrogen bond energies and vibrational spectroscopy of model compounds. Polymer. 2002; 43: p. 6551–6559.

92. Huang SL, Lai JY. Structure- tensile properties of polyurethanes. Eur. Polym. J. 1997; 33: p. 1563-1567.

93. Joseph J, Jemmis ED. Red-, Blue-, or No-Shift in Hydrogen Bonds: A Unified Explanation. Journal of american chemical society. 2007; 129: p. 4620-4632.

94. Brunette CM, Hsu SL, MacKnight WJ. Hydrogen-Bonding Properties of Hard-Segment Model Compounds in Polyurethane Block Copolymers. Macromolecules. 1982; 15: p. 71-77.

95. Wang CH, Shieh YT, Guo G, Nutt S. Effects of Organophilic-Modified Attapulgite Nanorods on Thermal and Mechanical Behavior of Segmented Polyurethane Elastomers. polymer composites. 2010; 31(11): p. 1890-1898.

96. Pielichowski K, Njuguna. Thermal Degradation of Polymeric Materials Crewe, UK: Smithers Rapra Technology; 2005.

97. Petrovic ZS, Ferguson J. Polyurethane elastomers. Progress in Polymer Science. 1991; 16: p. 695-836.

98. Testa B, Waterbeemd HVd, Folkers G, Guy R. Pharmacokinetic optimization in drug research switzerland: Verlag Helvetica Chimica Acta; 2001.

99. Rhim JW, Mohanty AK, Singh SP, Ng PKW. Effect of the Processing Methods on the Performance of Polylactide Films: Thermocompression Versus Solvent Casting. Journal of Applied Polymer Science. 2006; 101: p. 3736 –3742.

100. Pinto AM, Cabral J, Tanaka DP, Mendes AM, Magalhaes FD. Effect of incorporation of graphene oxide and graphene nanoplatelets on mechanical and gas permeability properties of poly(lactic acid) films. Polymer International. 2013; 62(1): p. 33-40.

101. Zhang C, Ren Z, Yin Z, Jiang L, Fang S. Experimental FTIR and simulation studies on H-bonds of model polyurethane in solutions. I: In dimethylformamide (DMF). Spectrochimica Acta Part A. 2011; 81: p. 598– 603.

Appendix – 1

List of Publications

Journal articles

Senevirathna SR, Amarasinghe S, Karunaratne V, koneshwaran M, Karunanayake L. The effect of change of ionomer/polyol molar ratio on dispersion stability and crystalline structure of films produced from hydrophilic polyurethanes. J. Appl. Polym. Sci. 2017; 134.
DOI: 10.1002/app.44475

Conference proceedings

Pathmakumari MVL, Senevirathna S, Karunanayake L, Karunaratne V, Amarasinghe S. Investigation of the potential to fabricate a conductivity sensor based on fluorescence properties of polyurethane. In Proceedings of the international symposium on polymer science and technology 2015 in collaboration with industries institutions and universities; 2015; Colombo


25 OCT 2016

National Digitization Project

National Science Foundation

Institute : National Science Foundation

1. Place of Scanning : Sanje (Private) Ltd. Hokandara

2. Date Scanned : .....2017/04/03.....

3. Name of Digitizing Company : Sanje (Private) Ltd. No 435/16. Kottawa Rd.
Hokandara North. Arangala. Hokandara

4. Scanning Officer

Name : ....Angelo Melvin.....

Signature : .....A.M.....

Certification of Scanning

I hereby certify that the scanning of this document was carried out under my supervision, according to the norms and standards of digital scanning accurately, also keeping with the originality of the original document to be accepted in a court of law.

Certifying Officer

Designation : Information Officer

Name : Renuka Sugathadasa

Signature : .....

Date : .....

"This document/publication was digitized under National Digitization Project of the National Science Foundation, Sri Lanka"